



UNIVERSITAT
POLITÈCNICA
DE VALÈNCIA

PhD Thesis:

Transcriptional Insights for Spinal Cord Injury and Neural
Precursor Cell Therapy: Toward a Novel Optogenetics-
Based Treatment for cAMP Neuronal Induction

PhD candidate:

Beatriz Martínez Rojas

Supervisors:

Victoria Moreno Manzano

Esther Giraldo Reboloso

~ Valencia, December, 2023 ~

“Todo hombre puede ser, si se lo propone, escultor de su propio cerebro”

-Santiago Ramón y Cajal

AGRADECIMIENTOS

Llevar a cabo este doctorado ha sido un viaje desafiante y transformativo que no hubiera podido completar sin el apoyo de las personas que me han acompañado a lo largo de este camino.

En primer lugar, quiero agradecer a mis supervisoras de tesis, las doctoras Victoria Moreno y Esther Giraldo. Vuestro apoyo constante, asesoramiento y entusiasmo incansable me han empujado a través de las complejidades de la investigación. Por estar siempre disponibles para ayudarme, por fomentar el trabajo en equipo y al mismo tiempo favorecer nuestro crecimiento individual. Vuestra mentoría no solo me ha enriquecido a nivel académico si no también personal y profesional. Me siento tremendamente afortunada de haber tenido unas mentoras tan inspiradoras.

A mis padres y hermano, por vuestro cariño y confianza en mí, por considerar mis logros como propios y por sufrir mi mal humor con mis fracasos. Gracias por haberme enseñado el valor del esfuerzo y la perseverancia. A mis abuelos, titos y primos por no dejar escapar ninguna oportunidad de preguntarme “¿cómo va la tesis?”, por vuestro entusiasmo y vuestro apoyo.

Les debo también un gran agradecimiento a mis compañeros del laboratorio I44: Pablo, Marina, Ana, Mara, Sonia, MMar, María, Guillem, Anita. He aprendido tanto de cada uno de vosotros. Este grupo de personas irrepetible ha hecho que el I44 haya sido el ambiente ideal, con el equilibrio perfecto de complicidad y trabajo en equipo. Habéis conseguido que llegar cada mañana a trabajar sea un gusto ...incluso los lunes. Gracias a Ana y Mara, por ser maestras y confidentes, por vuestra generosidad, positividad y cariño, por vuestra capacidad de hacer que cada momento sea especial. Gracias a Pablo y a Marina, por acogerme y enseñarme los primeros pasos, por servirme de ejemplo a seguir. Gracias a María y Guillem, por ser fuente de inspiración en esta pasión compartida. Gracias a MMar por contagiarme de tu energía positiva y desenfadada por tantos momentos únicos dentro y fuera del laboratorio. Gracias a Sonia por haber compartido conmigo este camino, codo con codo, por endulzar los días largos de trabajo, por nuestros viajes inolvidables y los que están por venir. Gracias a todos por ser mucho más que compañeros de bancada. Os llevo en el corazón.

Gracias también a todas las personas que he tenido la suerte de conocer durante este camino, a las personas de este centro que trabajan para ayudar a los demás, al servicio de microscopía, informática, animalario y recepción, y por supuesto, a ese grupo tan excepcional de “jóvenes CIPF”. Especialmente gracias al I-05, a Teresa, Rosa, Paco, Carlos y Susana por dejarme tan buenos recuerdos. A Juan, por ser mi ojito izquierdo, por iluminar siempre los pasillos del CIPF, por tu sonrisa eterna.

A mis amigos Gloria, Cristina y Ezequiel, por estar siempre.

A Eric, el regalo más inesperado. Gracias por escucharme y apoyarme en cada reto. Por ser mi hogar y mi refugio. Por tu paciencia y positividad. Y a mi pequeña perrita por permanecer todo el rato a mis pies mientras redacto las siguientes páginas. A Iván, M^aCarmen y Juan por vuestra cálida acogida y vuestro apoyo.

Por último, gracias a los animales de experimentación, por dar su vida por el avance de la ciencia. Por que hagamos que vuestro sacrificio haya merecido la pena.

LIST OF ACRONYMS:

AC	Adenylate cyclase
ASIA	American Spinal Injury Association, impairment scale
BBB	Basso, Beattie and Bresnahan locomotor test
BDNF	Brain-derived neurotrophic factor
bPAC	Photoactivatable adenylyl cyclase from <i>beggiatoa sp.</i>
cAMP	3',5'-cyclic adenosine monophosphate
ChAT	Choline acetyltransferase
CNS	Central Nervous System
CPG	Central pattern generator
CST	Corticospinal tract
db-cAMP	dibutyryl-cyclic AMP
DEG	Differentially expressed genes
DHT	5,7-Dihydroxytryptamine
DRG	Dorsal root ganglia
EPAC2	exchange protein activated by cAMP
GFAP	Glial fibrillary acidic protein
Gs	Stimulating G-protein
LPGi	Lateral paragigantocellular nuclei
NPCs	Neural progenitor cells
P-CREB	Phosphorylated cAMP-Response Element Binding protein
PDE	Phosphodiesterase
PKA	Protein Kinase A
PnC	Pontine caudalis
PnO	Pontine oralis nuclei
qPCR	Quantitative polymerase chain reaction
RpST	Raphespinal tract
RST	Rubrospinal tract
RtST	Reticulospinal tract
SCI	Spinal cord injury
SD	Sprague Dawley
VGi or GiA	Gigantocellular ventral nuclei
VGlut1/2	Vesicular glutamate transporter 1/2
WGA	Wheat germ agglutinin

LIST OF CONTENTS

List of Figures

Figure 1: Principles of the anatomy of the spinal cord..	21
Figure 2: Descending motor pathways from the brain to the spinal cord..	23
Figure 3: Evolution of the CST in mammals.....	24
Figure 4: Outstanding methods for cAMP manipulation.....	35
Figure 5: Timeline of publications in PubMed under the search query 'spinal cord injury' (from 1900 up to September 2023)..	118

List of Tables

Table 1: Compilation of in vivo studies investigating the effects of pharmacological cAMP modulators as SCI treatment in rodents.....	34
--	----

INDEX

LIST OF ACRONYMS:.....	5
LIST OF CONTENTS.....	6
INDEX	7
SUMMARY	8
RESUMEN.....	10
RESUM.....	12
INTRODUCTION	16
Spinal cord injury:	16
Introduction to Spinal Cord Injury.....	16
Main causes of SCI.....	16
Pathophysiology of SCI: temporal stages	16
Clinical Management of SCI patients	18
Spinal cord injury Research	19
CNS anatomy and function	20
The process of walking	20
Principles on spinal cord anatomy	20
Spinal pathways: Ascending and Descending.....	21
CNS reorganization upon injury	26
Brain plasticity	27
Spinal cord plasticity	28
Maladaptive plasticity.....	29
Treatments for spinal cord injury: from basic to clinical research.....	30
Overview of the main therapeutical approaches	30
NPCs transplantation.....	31
cAMP as a master regulator of CNS repair	32
cAMP therapies in SCI.....	32
Novel tools for cAMP manipulations.....	35
HYPOTHESIS AND OBJETIVES	38
RESULTS	42
CHAPTER 1: NPC transplantation rescues sci-driven cAMP/EPAC2 alterations, leading to neuroprotection and microglial modulation.....	42
CHAPTER 2: Stimulation of corticospinal neurons by optogenetic cAMP inductions promotes motor recovery via raphespinal tract modulation	80
DISCUSSION	118
CONCLUSIONS	126

SUMMARY

Traumatic spinal cord injury (SCI) refers to a neurological condition in which a mechanic insult disrupts the proper communication of the impulses through the central nervous system (CNS), resulting on the loss of locomotor function below the injured area. The subsequent paralysis has devastating effects over the quality of life of the injured patients. Unfortunately, nowadays there is still no effective cure to completely restore the functionality of the spinal cord after the injury, although great advances are being made in recent years.

The search for an efficient treatment for SCI remains a daunting challenge in virtue of our still incomplete understanding of the myriad of biological processes triggered by the primary injury. Therapies to induce neuronal plasticity and regeneration after SCI include electrical stimulation, local growth factor delivery, extracellular matrix degraders or stem cell transplantation. Among them, cell therapy is the most recurring approach for SCI treatment. In the past decades several cell-based strategies have been explored, being one of the most promising the transplantation of neural progenitor cells (NPCs). Many pre-clinical studies have evidenced the potential of the NPCs transplantation to provide a substantial motor recovery in animal models, yet functional improvements in human patients receiving NPCs grafts have been limited and the feasibility for its translational application is a still ongoing research subject. Therefore, efforts still need to be made in disclosing the precise cascade of molecular processes along SCI pathophysiology as well as the NPCs underlying mechanism at the preclinical and clinical stages.

In that context, Chapter 1 of the present work aimed to provide a comprehensive characterization of the spinal transcriptional changes along the different temporal stages of rats suffering a severe contusive injury. Additionally, we have described the transcriptional impact of acute and subacute NPCs transplantation in injured animals. Interestingly we have shown that while SCI caused a strong dysregulation of several cAMP-signaling components (being EPAC2 the most downregulated gene), NPCs was able to restore SCI-derived alterations over this pathway with EPAC2 significant upregulation. In order to further explore EPAC2 role in NPCs-mediated therapeutical mechanism we performed a loss-of-function experiment by sustained EPAC2 inhibition via ESI-05 administration along with NPCs transplantation after SCI. Compared with only transplanted animals, NPCs+ESI-05 animals showed increased scar area, exacerbated microglia polarization into an inflammatory profile and widened gaps of preserved neurons across the lesion. Overall, these results suggest that NPC therapeutic

mechanisms in the context of SCI involve an EPAC2-dependent mechanism, reducing neuroinflammation and providing a neuro-permissive environment.

Based on our previous findings, Chapter 2 aimed to further explore cAMP potential for SCI regeneration. We designed a novel strategy for artificial cAMP inductions in corticospinal neurons via optogenetic activation of a photoinducible adenylyl cyclase (bPAC). Daily optogenetic cAMP stimulation in rats suffering a thoracic dorsal hemisection, which completely disrupt the dorsal aspect of the corticospinal tract (CST), promoted an early and sustained locomotor recovery compared to non-treated control animals. We have shown that bPAC stimulation increased the number of retrograde traced neurons from the lumbar segment both in the motor cortex and the raphe-reticular formation, but not in the red nuclei. Moreover, immunolabelling of the raphespinal tract by 5-HT showed that bPAC stimulation increased the ratio of descending serotonergic axons caudal to the injury which significantly correlated with improved functional parameters. Our results from corticobulbar projection study, WGA trans-synaptic tracing, and P-CREB analysis suggest that bPAC modulation of cortico-serotonergic pathway might occur at the brainstem level. Lastly, the serotonergic system depletion by 5,7-Dihydroxytryptamine administration suppressed bPAC-mediated recovery, confirming the implication of the serotonergic tract in the recovery of stimulated animals.

In summary, our research has provided new insights into the transcriptional changes that occur along SCI progression and after NPCs transplantation with a special emphasis on cAMP signaling. Optogenetic cAMP manipulation in corticospinal neurons after SCI has proven to be effective for functional recovery and allowed to unveil a cortical rerouting pathway through the serotonergic descending tract.

RESUMEN

La lesión medular traumática (LM) se refiere a una condición neurológica en la que un insulto mecánico interrumpe la adecuada comunicación de los impulsos nerviosos a través del sistema nervioso central (SNC), resultando en la pérdida de la función locomotora por debajo del área lesionada. La consiguiente parálisis tiene efectos devastadores en la calidad de vida de los pacientes lesionados. Lamentablemente, en la actualidad aún no existe una cura efectiva para restaurar completamente la funcionalidad de la médula espinal después de la lesión, aunque se han realizado grandes avances en los últimos años.

La búsqueda de un tratamiento eficiente para LM sigue siendo un gran desafío debido a nuestra aún incompleta comprensión de la multitud de procesos biológicos desencadenados por la lesión primaria. Las terapias dedicadas a inducir la plasticidad neuronal y la regeneración tras la LM incluyen la estimulación eléctrica, la administración local de factores de crecimiento, el uso de degradadores de la matriz extracelular y el trasplante de células madre. Entre ellos la terapia celular destaca como la aproximación más recurrente para el tratamiento de la LM. En las últimas décadas, se han explorado varias estrategias basadas en células, siendo una de las más prometedoras el trasplante de células progenitoras neurales (CPN). Muchos estudios preclínicos demostraron el potencial del trasplante de CPN para proporcionar una recuperación motora sustancial en modelos animales, sin embargo, las mejoras funcionales en pacientes humanos tratados han sido limitadas y su aplicabilidad para la translación clínica sigue siendo un tema de estudio. Por lo tanto, aún se deben realizar esfuerzos para descubrir la cascada precisa de procesos moleculares a lo largo de la fisiopatología de LM, así como el mecanismo subyacente de los CPN.

En ese contexto, el Capítulo 1 del presente trabajo tuvo como objetivo proporcionar una caracterización de los cambios en el perfil transcripcional medular a lo largo de las diferentes etapas temporales de las ratas que sufren una lesión severa contusiva. Además, hemos descrito el impacto transcripcional del trasplante agudo y subagudo de CPN en animales lesionados. Notablemente, hemos demostrado que mientras la LM conllevó una fuerte desregulación de varios componentes de señalización de AMPc (siendo EPAC2 el gen más regulado a la baja), el trasplante de CPN pudo restaurar las alteraciones derivadas de LM en esta vía, con sobreexpresión de EPAC2. Para explorar el papel de EPAC2 en el mecanismo terapéutico mediado por CPN, realizamos un experimento de pérdida de función mediante la inhibición sostenida de EPAC2 debido a la administración de ESI-05 junto con el trasplante de CPN en animales lesionados. En

comparación con los animales solo trasplantados, los animales CPN +ESI-05 mostraron un aumento en el área de cicatriz, una exacerbación de la polarización de la microglía hacia un perfil inflamatorio y una ampliación de la brecha de neuronas preservadas a lo largo de la lesión. En general, estos resultados sugieren que los mecanismos terapéuticos de CPN en el contexto de LM implican un mecanismo dependiente de EPAC2, reduciendo la neuroinflamación y proporcionando un entorno neuro-permisivo.

Basándonos en nuestros hallazgos anteriores, el Capítulo 2 explora el potencial del AMPc para la regeneración de la LM. Hemos diseñado una estrategia innovadora para inducir artificialmente el AMPc en las neuronas corticoespinales a través de la activación optogenética de un adenilato ciclasa foto-inducible (bPAC). La estimulación optogenética diaria de AMPc en ratas con una hemisección dorsal torácica (que daña completamente la parte dorsal del tracto corticoespinal), promovió una recuperación locomotora temprana y sostenida en comparación con los animales de control. Hemos demostrado que la estimulación de bPAC aumentó el número de neuronas marcadas retrógradamente desde el segmento lumbar tanto en la corteza motora como en la formación rafe-reticular, pero no en el núcleo rojo. Además, la inmunotinción del tracto rafeespinal por 5-HT mostró que la estimulación de bPAC aumentó el ratio de axones serotoninérgicos caudales a la lesión, lo que se correlacionó significativamente con una mejora de parámetros funcionales. Nuestros estudios de las proyecciones corticobulbares, trazado transináptico con WGA y análisis de P-CREB sugieren que la modulación de bPAC sobre la vía cortico-serotoninérgica podría ocurrir a nivel del tronco encefálico. Por último, la depleción del sistema serotoninérgico mediante la administración de 5,7-Dihydroxytryptamina suprimió la abolió la mejora mediada por bPAC, confirmando la implicación de la vía serotoninérgica en la recuperación de los animales estimulados.

En resumen, nuestra investigación ha proporcionado nuevos conocimientos sobre los cambios transcripcionales que ocurren a lo largo de la progresión de la LM y tras el trasplante de CPN, con un énfasis especial en la señalización de AMPc. La manipulación optogenética de AMPc en las neuronas corticoespinales después de la LM ha demostrado ser efectiva para la recuperación funcional y ha permitido descubrir una ruta cortical alternativa a través del tracto descendente serotoninérgico

RESUM

Lesió medul·lar traumàtica (LM) es refereix a una condició neurològica en la qual un traumatisme interromp la comunicació adequada dels impulsos a través del sistema nerviós central (SNC), amb el resultat de la pèrdua de la funció locomotora per baix de la zona lesionada. La subseqüent paràlisi té efectes devastadors sobre la qualitat de vida dels pacients lesionats. Lamentablement, en l'actualitat encara no hi ha una cura efectiva per a restaurar completament la funcionalitat de la medul·la espinal després de la lesió, tot i que s'estan fent grans avanços en els últims anys.

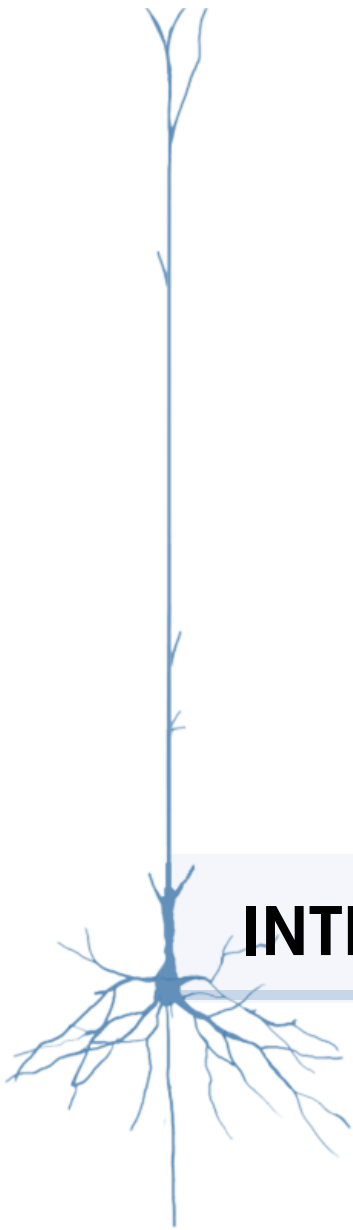
La recerca d'un tractament eficient per a la LM roman un repte complex a causa de la nostra comprensió encara incompleta de la gran quantitat de processos biològics desencadenats per la lesió primària. Les teràpies destinades a induir la plasticitat neuronal i la regeneració després de la LM inclouen l'estimulació elèctrica, l'administració local de factors de creixement, l'ús de degradadors de la matriu extracel·lular i el trasplantament de cèl·lules mare. D'entre ells, la teràpia cel·lular destaca com l'aproximació més recurrent per al tractament de la LM. En les dècades passades, s'ha explorat diverses estratègies basades en cèl·lules i una de les més prometedores és el trasplantament de cèl·lules progenitores neurals (CPN). Molts estudis preclínic han demostrat el potencial del trasplantament de CPN per proporcionar una recuperació motora substancial en models animals, no obstant això, les millores funcionals en pacients humans tractats són limitades i la seua aplicabilitat per a la translació clínica segueix sent un tema d'estudi. Per tant, encara s'han de fer esforços per a descobrir la cascada precisa de processos moleculars al llarg de la fisiopatologia de la LM, així com el mecanisme subjacent dels CPN.

En aquest context, el Capítol 1 del present treball va tindre com a objectiu proporcionar una caracterització dels canvis en el perfil transcripcional espinal al llarg de les diferents etapes temporals de les rates que pateixen una lesió contusiva. A més, s'ha descrit l'impacte transcripcional del trasplantament d'CPN aguts i subaguts en animals lesionats. Notablement, s'ha demostrat que mentre la LM va causar una forta desregulació de diversos components de senyalització de AMPc (sent EPAC2 el gen més regulat a la baixa), el trasplantament de CPN van ser capaç de restaurar les alteracions derivades de la LM en aquesta via, sent l'augment d'EPAC2 el canvi més destacable. Per a explorar el paper d'EPAC2 en el mecanisme terapèutic mediat per CPN, es va realitzar un experiment de pèrdua de funció mitjançant la inhibició sostinguda d'EPAC2 degut a l'administració d'ESI-05 juntament amb el trasplantament de CPN en animals lesionats. En comparació amb els animals només trasplantats, els animals

CPN+ESI-05 van mostrar un augment de l'àrea de cicatriu, una exacerbació de la polarització de les micròglies cap a un perfil inflamatori i una ampliació de la bretxa de neurones preservades a través de la lesió. En general, aquests resultats suggereixen que els mecanismes terapèutics de les CPN en el context de la LM involucren un mecanisme dependent d'EPAC2, reduint la neuroinflamació i proporcionant un entorn més neuropermissiu.

En base als resultats previs, el Capítol 2 va tindre com objectiu explotar el potencial de regeneració de AMPc dissenyant una nova estratègia per a les induccions artificials de AMPc en les neurones corticoespinals mitjançant l'activació optogenètica d'una adenilat ciclasa fotoinduïble (bPAC). L'estimulació optogenètica diària de AMPc en rates que pateixen una hemisècció dorsal toràcica va promoure una recuperació locomotora primerenca i sostinguda en comparació amb els animals control. S'ha demostrat que l'estimulació de bPAC va augmentar el nombre de neurones marcades retrògradament des del segment lumbar, tant a l'escorça motora com a la formació rafe-reticular, però no al nucli roig. A més, la immunotinció del tracte rafespinal per 5-HT va mostrar que l'estimulació de bPAC va augmentar la ràtio d'axons serotoninèrgic cabals a la lesió, cosa que es va correlacionar significativament amb una millora dels paràmetres funcionals. Els estudis de les projeccions corticobulbars, traçat transinàptic amb WGA i anàlisi de P-CREB del grup suggereixen que la modulació de bPAC sobre la via cortico-serotoninèrgica podria passar a nivell del tronc encefàlic. Finalment, la depleció del sistema serotoninèrgic mitjançant l'administració de 5,7-Dihydroxytryptamina va suprimir i va abolir la millora mediada per bPAC, confirmant la implicació de la via serotoninèrgica en la recuperació dels animals estimulats.

En resum, la investigació del grup ha proporcionat nous coneixements sobre els canvis transcripcionals que tenen lloc a la llarga de la progressió de la LM i després del trasplantament de CPN, amb un èmfasi especial en la senyalització d'AMPc. La manipulació optogenètica d'AMPc a les neurones corticoespinals després de la LM ha demostrat ser efectiva per a la recuperació funcional i ha permès descobrir una ruta cortical alternativa a través del tracte descendent serotoninèrgic



INTRODUCTION

INTRODUCTION

Spinal cord injury:

Introduction to Spinal Cord Injury

Spinal cord injury (SCI) is a life-changing neurological condition in which an insult to the spinal cord disrupts the proper communication of executive commands from the brain to the muscles that can lead to motor, sensory, respiratory, cardiac, bladder and sexual dysfunction. The degree of functional impairment after SCI depends on factors such as the severity of the injury and its location in the spinal cord. The most common injuries (50%) occur at the cervical level, leading to the impairment of all four limbs (tetraplegia), followed by injuries at the thoracic (35%) or lumbar (11%) levels, which result in paraplegia [1, 2].

In an attempt to classify human patients according to their severity and prognosis the American Spinal Cord Injury Association (ASIA) established a 5-grade scale (A-E, from more to less severe) with Grade A indicating complete sensory and motor loss, Grade B complete motor loss but preserved sensation, Grade C and D different degrees of motor function preservation and Grade E normal sensory and motor function [3].

Main causes of SCI

SCI can have many originating causes, but for the sake of simplicity, they can be categorized into traumatic or non-traumatic SCI. Traumatic SCI are defined as compressions, contusions, transections or shearing of the spinal cord [1] as a result of an external mechanical insult mostly caused by car crashes, falls, violent assaults, sports or diving incidents, among others [4]. Non-traumatic spinal cord injuries comprise a miscellaneous group of pathologies including congenital (i.e., spina bifida) or acquired disorders (i.e. infectious, vertebral column disorders, autoimmune, spinal tumors, vascular problems, among others). The present thesis is specially focused on the understanding and assessment of locomotor function after traumatic SCI.

Pathophysiology of SCI: temporal stages

SCI represents a heterogeneous and complex pathology involving a myriad of molecular pathways and dozens of cellular types. The temporal evolution of the pathophysiology of SCI can be divided into three stages: acute, subacute and chronic [5].

The acute phase comprises the first 48 hours after the primary insult and represents the temporal window of development of many pathological events directly triggered by the

injury [5]. In the first instance, primary trauma can result in the axotomy of ascending and descending spinal tracts which impedes neuronal transmission; according to that SCI are categorized in anatomical complete or anatomical incomplete depending in if all tracts have been axotomized or there are spare axons remaining. Moreover, the initial disruption of tissular structures causes hemorrhages and edemas (swelling caused by trapped fluids) which progressively increases spinal pressure and can lead to further damage. Vascular rupture impedes proper oxygen and nutrients supply resulting in local ischemia which derives in the formation of reactive oxygen and nitrogen species [6]. Moreover, permeability of blood-spinal barrier is comprised which results in cerebrospinal fluid leakage and allowing the massive entrance of immune cells [7]. On the top of that, the patient may present systemic life-threatening conditions such as hypotension and cardiovascular, respiratory and thermoregulation disfunctions.

At a cellular level many cells collapse due to the primary lesion, their content being discharged to the extracellular space. Surviving cells have to cope with a highly aggressive environment that can result in the loss of their plasmatic membrane integrity, in ionic imbalance (specially characterized by a massive calcium influx), mitochondrial dysfunction, free radical generation and lipid and protein peroxidation and ultimately may lead to necrotic or apoptotic cell death [8]. The extracellular neurotransmitter accumulation around the injury site become neurotoxic for surrounding cells, including glial cells (oligodendrocytes, astrocytes and microglia) and neurons, due to the excessive activation of their receptors; an event that is known as excitotoxicity [9].

In functional terms at the acute phase patients may experience a spinal shock, a temporary condition characterized by the absence of reflexes, loss of motor control, sensory disfunction and flaccid paralysis [10].

The subacute phase comprises the following weeks after injury. This stage involves a cascade of coordinated events resulting in progressive damage to the surrounding tissue [1].

Approximately 2 days after injury resting astrocytes, the specialized supporting cells of the central nervous system (CNS), become reactive and proliferate and arranged around the perilesional area forming a glial GFAP + (glial fibrillary acidic protein) border surrounding the unsalvageable tissue to contain the core of inflammation. The benefits and detriments of astroglial contribution has been largely debated by SCI scientist, with some authors claiming that the astrocytes actively contribute to the formation of what has been traditionally denominated as “the glial scar”, representing a major impediment for later axonal growth across the injury [11]. Others claim that the ‘astrocytic border’

plays a neuroprotective role preventing the spreading of inflammation to adjacent uninjured tissue and so rejecting the term “glial scar” [12-14]. Apart from the resident glia (astrocytes and microglia), other immune cells massively invade the spinal cord shortly after the injury (including neutrophils, macrophages, fibroblast and monocytes, among others) where they can reside for several months. Due to environmental signals (proinflammatory cytokines) their phenotype is switched mainly into an activated proinflammatory state (M1) to clear cell and myelin debris and further propagate the immune reaction by inflammatory factors secretion [12, 15]. A minor percentage of microglia and macrophages can be also activated towards an anti-inflammatory proregenerative state (M2) [16]. The immune response after SCI remains controversial, having both beneficial and deleterious outcomes for the recovery, so many therapeutical strategies are focused on neuromodulators to unbalance in favor to positive effects.

Moreover, during the subacute phase denervated axons suffer from demyelination (in part due to the loss of oligodendrocytes) what leaves the axons directly exposed and triggers a self-destructive process of axonal fragmentation known as Wallerian degeneration resulting in further functional loss [17].

Functionally, during the subacute stage (first few months following a SCI) patients will experience discrete spontaneous motor and sensory improvements due to the progressive recovery from the initial spinal shock.

Lastly, **the chronic phase** extends over the lifespan of patients and is characterized by the establishment of cyst cavities and the maturation of the astrocytic border. More importantly the chronic phase entails the stabilization of the functional deficits, typically occurring 9 months after injury, when the initial recovery reaches a life-lasting plateau [18].

Clinical Management of SCI patients

Unfortunately, nowadays there are no available curative options for SCI in the clinic therefore, the functional prognosis for patients is currently bearish (though exciting advances are being made in the last few years). The acute clinical management of SCI patients nowadays consists in the evaluation of severity by neuroimaging and preventing further damage of the spinal cord by spinal immobilization and surgical decompression. Surgical decompression aims to alleviate the pressure caused by the increasing edema shortly after the injury. In support to that, rodent models of SCI have robustly shown that the histological and functional impairments are mitigated when the duration of the compression is reduced [19, 20], fact that led some authors to claim that “time is spine” [21]. Sadly, early surgical decompression (<24h) might not be feasible for all patients

depending on their manifestation of other life-threatening complications or limitations on surgical care availability (as is the case for developing countries). Pharmacological treatment at the acute stage may include methylprednisolone (a synthetic glucocorticoid, with anti-inflammatory and anti-peroxidative properties) with beneficial outcomes for the locomotion but contraindications such as risk of pneumonia, wound infections and gastrointestinal hemorrhage [22]. At later stages, treatment for SCI patients include the administration of pregabalin and gabapentin for the alleviation of neuropathic pain and rehabilitation which aims to maintain muscle strength, bone density and to provide psychological support [23, 24].

Spinal cord injury Research

The intricated nature of spinal cord injury made it a challenging and inspiring puzzle for researchers in the search for regeneration. Though SCI research has been an ongoing endeavor for over a century, in the past decade our understanding in the underlying molecular, cellular and systemic mechanisms occurring after SCI has remarkably increased, with every single finding contributing to a whole. We are living an exciting era, since SCI repair seems to be getting closer and closer with every passing year, as shown by outstanding advances in human patients [25].

This exponential knowledge acquisition has been possible thanks to the use of molecular tools and advanced techniques such as refined neuronal tracers, in vivo imaging, chemogenetics/optogenetics and tissue clearing techniques, among others. Moreover, SCI research requires the use of animal models to unveil the spontaneous mechanism of remodeling (known as neural plasticity) or to test developing therapeutical approaches. For its extensive use in the purpose of this thesis, it is worth mentioning the value of rodent SCI models which allow the generation of clinically relevant injury types (such as contusion, compression, hemisection, among others) depending on the experimental requirements. Rodent is the best suited and most used (92%; 72.4% of which are rats) model for basic SCI research due to the ease of their manipulation allowing for testing on higher sample size, their low cost, well-established SCI guidelines, and fewer ethical considerations compared to non-human primates [26]. However, it is important to also consider that rats exhibit specific anatomical and functional variations compared to humans, as discussed in following section. Therefore, direct extrapolation of conclusions drawn from rat models of SCI is not possible and additional testing of hypothesis in non-human primates and, ultimately, in pilot clinical research are required prior to human translation.

Despite the last advances, much still needs to be done both in the pre-clinical and clinical stages, and the intention of this work is to further contribute to the still unsolved questions.

CNS anatomy and function

The process of walking

Our motor system is involved in multiple roles; it allows the maintenance of posture and balance and controls autonomic functions such as breathing and gut movements. The execution of voluntary movements is one of the most relevant outputs of our nervous system activity, essential for performing daily tasks [27].

The elementary units of motor system for the transmission of information are: upper neurons and lower neurons. The somas of upper motor neurons are located in the brain, projecting their axons down to the spinal cord. Lower neurons reside within the spinal cord and their axons can either descend to innervate lower segments of the spinal cord (propriospinal neurons) or exit through the nerve roots to innervate muscles (motor neurons) [28].

Even seemingly trivial movements such as leg flexion requires a complex circuit coordination of multiple neurons of the motor system. For the generation of purposeful movement, first, executive commands from the brain travel through descending tracts into the spinal cord to synapse with motoneurons or spinal interneurons. Then, this motoneuron synapse into neuromuscular junctions governing the contraction and relaxation of the engaged muscle. The coordinated engagement of hundreds of neuromuscular junctions will produce the appropriate movement [27].

While one might regard the spinal cord as a rudimentary communication pathway to the muscles under the brain authority, the spinal cord actually represents a highly sophisticated organizational circuitry. It houses a large number of transcriptionally and functionally distinct neurons that work together to coordinate various aspects of locomotion [29].

Principles on spinal cord anatomy

The human spinal cord is organized segmentally along the rostral-caudal axis of the body into 8 cervicals, 12 thoracics, 5 lumbar, 5 sacral and 1 coccygeal spinal segments (Figure 1, left) which are protected by three connective tissue layers (termed meninges) and the spinal column, composed of 33 vertebrae: 7 cervicals, 12 thoracic, 5 lumbar, 5

fused sacral and 3-5 coccygeal [30] [31]. This organization is evolutionary conserved, with slight variations in rodents [32].

Structurally the spinal cord is composed by the white and the grey matter, distinguishable for its cross-sectional appearance: the grey matter forming a butterfly-like shape surrounded by the white matter[30] (Figure 1, right). The grey matter is composed by cell bodies of motor and sensory neurons, interneurons and unmyelinated axons, being the central canal in its middle part. The dorsal and ventral aspects of the grey matter are referred as “horns” (in charge of the sensory and motor function, respectively). Furthermore, the grey matter is stratified in 10 different laminae according to Rexed’s organization [33] (I-IX from dorsal to ventral, being lamina X around the central canal) based on the density, topography and function of the resident neurons. The white matter is composed by ascending and descending myelinated axons owing its color to this whitish component, being referred their dorsal, ventral and lateral aspects as “funiculus” (Figure 1, right).

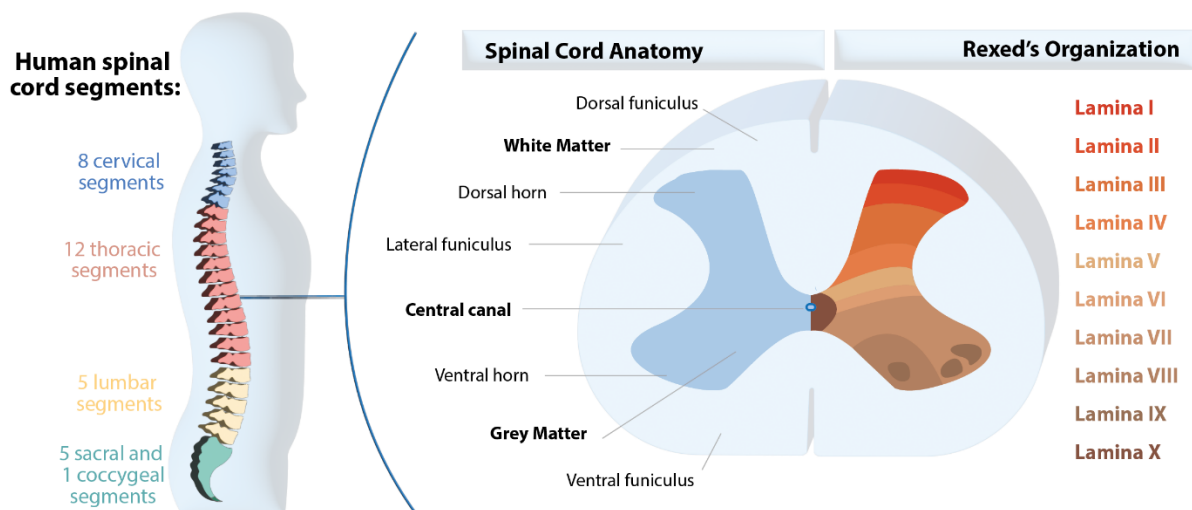


Figure 1: Principles of the anatomy of the spinal cord. Segmental organization of the human cord (left). Coronal section of the thoracic spinal cord showing its grey and white matter organization and the distribution of grey matter laminae according to Rexed’s description (right).

Spinal pathways: Ascending and Descending

In the white matter the spinal cord contains ascending and descending tracts that transmit information to and from the brain [34]. The directionality of the transmission determines whether a tract is ascending (sensory or afferent) or descending (motor or efferent). Each tract occupies a specific location in the white matter. With the development of anterograde and retrograde tracing techniques, the distribution of the major ascending and descending tracts in white matter as well as their termination

patterns in the grey matter has been mapped in a wide variety of vertebrates [35]. The anatomic course of the tracts is a noteworthy aspect in the context of spinal cord injury, as some tracts are more putative to remain preserved after injury depending on their trajectory in the spinal cord [36].

Ascending pathways

The ascending tracts are those in charge of processing the peripheral sensory information from the peripheral nerves up to the brain. The ascending pathways are comprised by first-order neurons with their soma in the dorsal root ganglion (DRG), second-order neurons located in the dorsal horn of the grey matter and third-order neurons located in the subcortical structures (i.e., thalamus or brainstem) [37]. These tracts can process conscious (i.e., pain, temperature, tactile sensation, vibration) or unconscious information (i.e., proprioception) [38]. The different types of sensory tracts are reviewed elsewhere [37] and won't be further discuss in this section given or main focus on motor function.

Descending pathways.

Descending tracts, also known as supraspinal or motor pathways, arise from several regions of the brain (motor centers) and travel down the spinal cord to reach their targets (Figure 2). The pattern of origin of the descending tracts is well conserved across mammals; while their trajectory within the spinal cord white matter may vary across species [39].

Extensive retrograde tracing studies has so far identified the motor centers in the brain projecting descending tracts into the spinal cord [35]. Of those the major ones are the corticospinal (CST), reticulospinal (RtST), raphespinal (RpST) and rubrospinal (RST) tracts (Figure 2), which will be studied in the Chapter 2 [34]. Signature characteristics of each tract (such as their origin, trajectory, termination pattern, targets and neurotransmitter phenotype) will be discuss in this section with a special emphasis in the rat and human anatomy given their relevance in this work.

- **The corticospinal tract:**

The corticospinal tract originates mainly from the pyramidal neurons of the layer V of the primary motor (M1) and sensory (S1) cortex, with other regions of the cortex (i.e. somatosensory and prefrontal) making smaller contributions [40]. From there, dense bundles of corticospinal fibers travel down the brain through the internal capsule and cerebral peduncle into the pons to reach the ventral side of the medulla oblongata, the “pyramids”, reason why the CST has also been called as “pyramidal tract”, in contrast to

the other descending tracts (“extrapyramidal”). At the level of the caudal hindbrain most of CST fibers decussate (80%-95% in rodents and 75–90% in humans, with interindividual variability), crossing the midline to the opposite side, before entering the spinal cord [41-43].

The decussation confers the CST its contralateral feature, meaning that each hemisphere of the motor cortex controls the movements of the opposite side of the body. The main CST navigates through the dorsal column of the rat spinal cord (Figure 2, magenta), while in primates and humans the CST mainly occupies the lateral column (Figure 3). The small proportion of tracts that do not cross in the pyramidal decussation forms a small bundle of axons in the ventral funiculus of the human spinal cord or in the ventral and dorsolateral funiculus in the rat spinal cord [43]. While the main CST travels all the rostro-caudal extension of the spinal cord, the minor CST gradually diminish in size terminating in the lower thoracic segments.

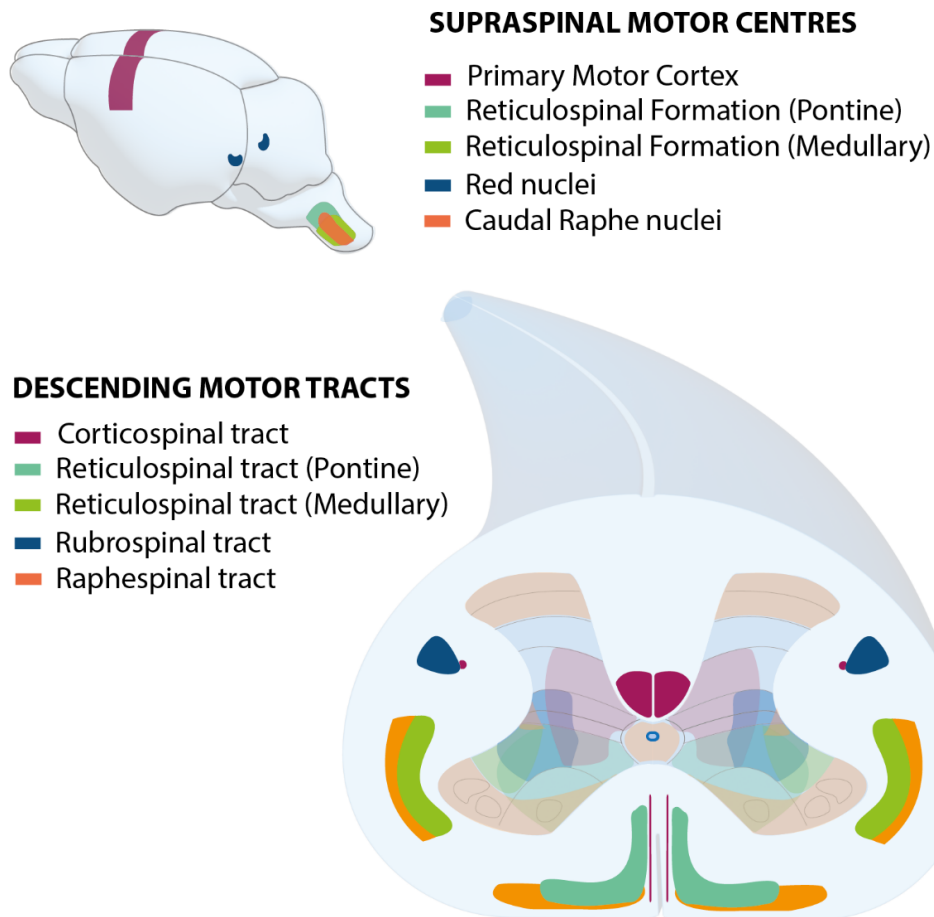


Figure 2: Descending motor pathways from the brain to the spinal cord. Illustration showing the approximate anatomical location on the brain of supraspinal centers projecting descending motor tracts into the spinal cord. The spinal trajectory of the motor tracts (dark color) as well as

their approximate termination patterns (light color) in the grey matter are shown as described by Sengul et al (2015) [39] and Liang et al (2015) [44].

As the CST descend, their axons leave the white matter at the appropriate spinal segment to enter into the grey matter to reach their intended targets. Neurochemically corticospinal neurons are glutamatergic (that is, excitatory) and establish vesicular glutamate transporters 1 positive (VGlut1) synapsis with their targets (please note that VGlut1 also labels synaptic inputs from the afferents). In rodents CST innervates neurons located mainly in the dorsomedial horns (laminae I-VII), while in human and primates the CST terminates mainly in the intermediate and ventral horns (laminae V-IX) (Figure 3). In agreement to that observation direct corticospinal innervation of motor neurons (located in the laminae IX) are characteristics of primates, while non-primates relay on segmental interneuron and propriospinal neurons to ultimately transmit cortical command to motoneurons [40]. This evolutionary feature may derive from the quadrupedal to bipedal transition and the need of acquisition of finger dexterity.

Regarding its function the CST has been recognized as the major pathway controlling voluntary movements. In human and non-human primates, the CST plays an essential role in controlling purposeful fine motor movements of the extremities [45]. However, in rats, the CST has a less relevant contribution in forepaw movement [46].

Besides its direct projection to the spinal cord, pyramidal neurons also project as the **corticobulbar pathway** terminating in the brainstem [47]. Corticobulbar fibers terminate and multisynaptically contact lower motor neurons of the cranial nerves. Unlike the CST, only half of the corticobulbar fibers decussate, meaning that cranial nerve nuclei receive bilateral innervation coming from both hemispheres [48]. The corticobulbar pathway has the function of controlling the movement of the heart, lungs, and digestive tract, facial musculature, ocular movements, chewing, swallowing, etc. [49].

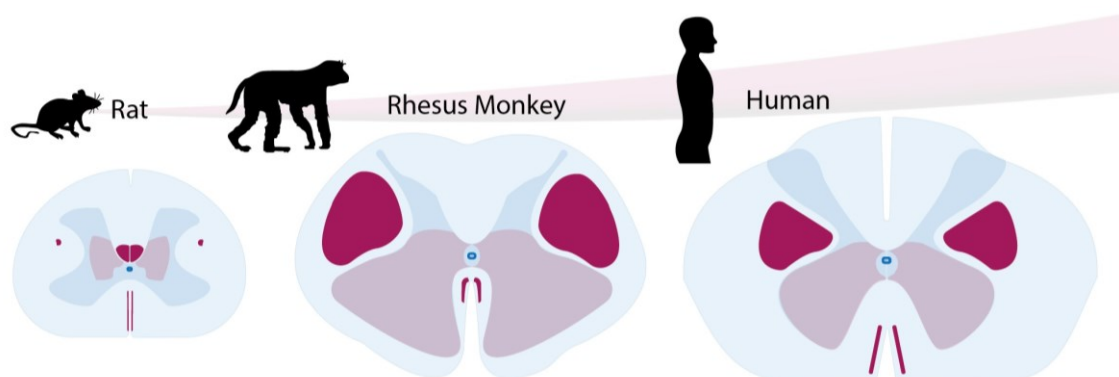


Figure 3: Evolution of the CST in mammals. CST projections (dark color) and terminations (light color) have gradually change through evolution. Adapted from Roze et al. 2016. The

evolutionary changes are thought to derive from the transition from quadrupedal to bipedal and the need to acquire manual dexterity.

- **The reticulospinal tract**

The RtST originates at the medial pontine (more rostrally) and gigantocellular nuclei (Gi, more caudally) of the reticular formation of the brainstem [39] (Figure 2, light and dark green). The medial pontine includes the subnuclei reticularis pontine oralis (PnO) and caudalis (PnC). The gigantocellular nuclei contains large cells and is composed by the ventral (VGI or GiA) and the lateral paragigantocellular nuclei (LPGi) [50]. Many authors have use the term “reticulospinal” in a broad sense, including both the raphespinal and reticulospinal pathways due to their close anatomical origin and diffuse boundaries (the caudal raphe nuclei and the reticular nuclei in the ventromedial aspect of the brainstem) [39, 51, 52]. The inconsistent nomenclature in the literature represents a summed difficulty for deciphering the individual features of raphe and reticulospinal pathways.

The reticulospinal neurons project to the ventromedial (pontine origin) and the ventrolateral (gigantocellular origin) horns of the spinal cord (Figure 2, light and dark green). Although they are referred as a tract, actually they do not form a distinct bundle of axons, instead their fibers are intermingled with other ascending or descending pathways [53]. Importantly the mainly ventral distribution of the RtST confers it an advantageous position for remaining partially intact after incomplete spinal cord injuries, compare to others such as the CST [36]. The majority of the reticulospinal neuron are glutamatergic and express the vesicular glutamate transporter 2 (VGLUT2), though a small proportion of (Gamma-aminobutyric acid, GABA) GABAergic and glycinergic have been also described [52].

- **The raphespinal tract**

The raphespinal tract has its origin in the caudal raphe nuclei within the medulla oblongata that includes the raphe magnus, obscurus y pallidus [44]. The raphespinal tract is composed mainly by serotonin (also known as 5-hydroxytryptamine, 5-HT) expressing neurons (receiving the name of serotonergic tract) and a subset (1/3) of non-serotonergic neurons, both showing similar termination patterns [44]. Non-serotonergic neurons can be GABAergic and peptidergic [54, 55]. The raphe magnus neurons project to the dorsolateral funiculus terminating in the dorsal horn (laminae I and II), while neurons of the raphe pallidus and obscurus project into the ventrolateral funiculus and innervate intermediate and ventral horns motoneurons (laminae VIII, IX and X)) specially at the thoracic, lumbar and sacral segments (Figure 2, orange). Given their serotonergic

nature the serotonergic terminations in the spinal cord can be easily visualized by 5-HT immunolabelling, which confers technical advantage compare to other tracts that require specific tracing [44].

- **Rubrospinal tract**

The RST has its origin in the red nucleus of the midbrain and decussates in the tegmental decussation of the caudal midbrain. Their projections forms a tract in the dorsolateral funiculus terminating in the ventral horn lamina V, VI, and VII where it synapses motor neurons [39] (Figure 2, blue). The functional relevance of this tract consists controlling the muscle tone and rudimentary motor skills over flexor muscles [56].

In bipedal species the rubrospinal pathway is underrepresented, probably compensated by the overrepresentation of the CST during evolutionary adaptations. Thus, the RST may have much more implication in functional recovery in rats than in humans [57].

- **Cortico-reticulospinal, cortico-raphespinal and cortico-rubrospinal**

Projections from cortical regions and synaptic contacts with the reticular formation, the red nuclei and the caudal raphe nuclei have been reported establishing indirect routes between the cortex and the spinal cord through the reticulospinal, raphespinal and rubrospinal axons [47, 58-60].

Among these, the most extensively documented is the cortico-reticular tract, which is considered to have significant motor relevance in humans, second only to the corticospinal tract. Clinical cases of local brain hemorrhages or stroke specifically damaging the cortico-reticular tract, presented motor weakness in their proximal joint muscles (shoulder abductor and hip flexor), unveiling the motor role of this pathway even when the CST remains intact. Based on these studies the cortico-reticulospinal tract is thought to account for 30-40% of the motor function of proximal joint muscles. Moreover, the cortico-reticular tract has been involved in gait function recovery (in human stroke patients) and postural stability[61, 62]. In addition the relevance of the cortico-reticulospinal pathway has been recently proven after SCI in rodent models [25] and indirectly observed in human patients [62]

CNS reorganization upon injury

Traditionally the adult CNS was thought to be stagnant and neural remodeling restricted to earlier developmental stages. This dogma was first established in 1928 by Ramon y Cajal, the so-called father of neuroscience with his famous statement: "In adult centers

the nerve paths are something fixed, ended, immutable. Everything may die, nothing may be regenerated” [63]. However, a century later, it is currently widely accepted that the adult CNS can undergo substantial reorganization (namely as “plasticity”) in response to spinal cord injury or other pathologies (i.e., brain stroke or limb amputation). Spinal cord injury cause mayor impact in the vicinity of the epicenter, however substantial circuit remodeling can occur far from the injury site including cortical, subcortical and spinal levels [64]. The majority of the injuries even when functionally complete, are anatomically incomplete, meaning that some tracts are spare across the injury. The spared tracts often serve as a substrate for circuit reorganization and functional improvements after SCI.

Brain plasticity

The motor repertoire is topographically mapped onto the cortex, meaning that specific body parts are controlled by distinct motor cortex subregions. Cortical plasticity is defined as a shift in the boundaries that delineate the representation of a particular motor skill within the cortical region and has proven to be well conserved trait among mammals [65, 66].

Cortical motor map plasticity is observed both under physiological (i.e. learning a new motor skill) and pathological conditions (i.e. limb amputations, CNS damage). For instance, in humans learning how to play the piano involves an increase in the representation of finger movements in the cortical area; while the repetition of other tasks that do not involve learning do not trigger cortical remodeling [67].

After spinal cord injury numerous studies have revealed substantial motor map reorganization as a compensatory mechanism for the impaired limbs [68]. Complete thoracic spinal cord transections in rat, leads to a chronic abolishment of the hindlimb representation in the motor cortex and an expansion in the cortical boundaries controlling muscles of the trunk and forepaws. On the other hand, in incomplete SCI such as unilateral hemisection, cortical remodeling enables the functional recovery of the affected paw. In those cases, the hindlimb motor cortex undergo spontaneous bilateral reorganization characterized by the unaffected motor hemisphere taking up the control of the affected limb, and the elimination of limb motor representation in the deafferented hemisphere [69]. Of note, studies using transcranial magnetic stimulation in tetraplegic patients revealed enlargement of cortical areas that represent the muscles above the level of the injury, indicating that cortical reorganization also occurs in human patients [65].

The molecular mechanisms underlying cortical remodeling include alterations in protein synthesis, dendritic changes, synapse remodeling and potentiation and depotentiation of cortical horizontal connections [70-73].

Plastic mechanisms can also occur at subcortical levels as shown by the injured-induced growth of corticofugal projections into neurons of the red nucleus [74] or the reticular formation [60]. Electrophysiological and cell-specific silencing experiments have revealed that this type of plastic remodeling represent a functionally relevant mechanism, relaying cortical commands to subregional spinal segments [60].

Spinal cord plasticity

The spinal cord is a key site for injury-induced neuroplasticity, being corticospinal the most studied pathway. Two different kinds of reorganization may occur: the functional modification of pre-existing circuits by synaptic modulation (synaptic/functional plasticity) or the generation of new circuits by structural reorganization of the tracts through sprouting (anatomical/structural plasticity)

Synaptic plasticity refers to the ability of neurons to modify the intensity of their connections by changes in the conduction velocity, synaptic strength and transmission efficiency (namely long-term potentiation or depression, LTP and LTD respectively) [75]. Synaptic plasticity may lead to silencing of neuronal pathways that are no-longer functional after axotomy or unsilencing of dormant circuits which overall can result in profound functional circuit remodeling [76]. The mechanism underlying synaptic modulation involves the insertion/removal of AMPA receptor in the postsynaptic membrane enabling/impeding (respectively) electrical firing upon neurotransmitter release. Moreover, synaptic remodeling is thought to regulate anatomical plasticity since LTP induces sprouting and synaptogenesis while LTD induces synaptic pruning [76].

Regarding **structural plasticity** spinal cord injuries affecting the CST, have shown to promote spontaneous axonal branching (known as sprouting) from this tract in many species [77-79]. When SCI left intact CST fibers, for example unilateral hemisection, the injured tracts can sprout caudal to the injury into the grey matter of the ipsilesional side to reinnervate the interneurons or motor neurons of the affected hemisphere. Moreover, if all CST tracts are interrupted by SCI, CST sprouting rostral to the lesion can allow the establishment of newly functional synapsis with propriospinal neurons with spare axons projecting caudal to the injury [80]. In that manner CST remodeling enable supraspinal input to be rerouted and reach spinal areas below the injury[81].

Apart from the CST, other descending tracts (RST, RpST and RtST) are known to exert significant growth after incomplete SCI. Importantly, this growth tends to reinnervate their natural patterns suggesting and attempt to recapitulate their original connectivity [82, 83].

Maladaptive plasticity

Although plastic reorganization plays a crucial role in the recovery of motor dysfunction, it can also have maladaptive consequences. This undirected plasticity comes at a cost, as it may lead to the formation of aberrant neuronal circuits. For instance, spinal circuit rearrangement can lead to co-activation of antagonistic muscle resulting in muscular exhaustion [82].

Studies using rat models of chronic SCI have demonstrated that changes in fiber and synapse density caudal to the injury correlates with neurological dysfunction, such as long latency reflex responses in hindlimb muscles [82]. This neurological dysfunction is also frequently observed in chronic human patients presenting a clinical profile that include reflex responses, bladder overactivity, dysreflexia or spontaneous spasms [64].

Of note, patients may also experience pain hypersensitivity as a result of plastic changes in neural circuits that control nociceptive information, a condition termed as nociplastic pain [84]. The underlying mechanism for this type of pain involves an amplified processing or decreased inhibitory response to peripheral nociceptive input as a result of either peripheral or CNS plasticity. For example, unsilencing of synapses in dorsal horn neurons after injury has also been suggested to participate in central sensitization and chronic pain [76]. Chronic pain is considered of the mayor clinical problems in SCI patients being associated with the development of opioid dependence, problems in mental health and overall decreased quality of life [76].

We can learn from the basis of naturally-occurring mechanisms of neural plasticity for the development of new therapeutical strategies. Though spontaneous plasticity results in extensive functional improvements (to barely unnoticeable impairment) in several species, in humans, spontaneous locomotor recovery is very limited. This consideration has led the scientific SCI community to the belief that therapeutical intervention must aim to further exploit the potential of our intrinsic neuroplastic capacity to achieve significant locomotor outcomes [85]. Many mechanisms of plasticity are known to be activity-dependent, so treatments focused on maintaining or inducing the activity of circuits above or below the injury are an emerging therapeutical scope [76].

Treatments for spinal cord injury: from basic to clinical research

Overview of the main therapeutical approaches

It is currently pretty well-established that therapeutical strategies for SCI injury must aim to combat the following barriers to regeneration: i) intrinsic factors such as the lack of sufficient endogenous axonal regeneration, the inefficient plastic reorganization and the massive neuronal loss [86] and ii) extrinsic factors such as the unpermissive environment within the injury epicenter due to the presence of inhibitory factors (i.e. Nogo A, myelin and chondroitin sulfate proteoglycans, CSPG) [87]

At the preclinical stage there is a plethora of strategies to overcome the devastating impact of SCI. Some of the most promising approaches include the use of biomaterials, neurotrophic factor support, extracellular matrix degraders, neuromodulation, cell transplantation or combination of them to achieve synergistic effects [88-92].

Biomaterial-based strategies are based on the use of scaffold (temporary biodegradable supporting structures) with the aim to provide physical support to the injured spinal cord, to prevent scarring and to serve as a permissive support for axonal regeneration [22]. For example, the application of injectable hydrogels (i.e., chitosan) is a minimally invasive technique to fill cyst cavities due to their three-dimensional porous structures, providing a matrix for the ingrowth of supportive tissue. Also, the use of aligned nanofibers and scaffolds (consisting mainly in synthetic polymers) has gained popularity for allowing directionally assisted growth thanks to the organized configuration of nanofibers imitating the size scale of natural extracellular components [89]. Importantly, biomaterial efficacy can be further improved by combination with stem cell therapies (facilitating their integration and survival within the spinal cord) or biofunctionalization with trophic factors or active biopeptides [88]. In this regard, in the last year it is worth to highlight the great advances made by Stupp et al. who developed highly dynamic peptide amphiphile supramolecular polymers containing a peptide to activate the transmembrane receptor β 1-integrin (colloquially referred to as “dancing molecules”) which demonstrated outstanding potential to promote vascular and axonal growth, myelination, neuronal survival, attenuation of gliosis and functional recovery in mouse model of SCI [93].

Other recurrent therapeutical scope has focused on the inability of axons to regrowth over the inhibitory environment of the lesion. Some strategies such as the treatment with enzyme chondroitinase ABC (ChABC) aim to minimize the unpermissiveness of the environment by the degradation of CSPG at the injury core what has proven remarkable pro-regenerative effects over injured tracts resulting in significant functional recovery in

animal models [90]. Moreover, the potentiation of intrinsic regenerative capacity of neurons has been also extensively targeted for example by deletion of PTEN or pharmacological inhibition of Rho/Rock signaling, among others [94].

Undoubtedly one of the most extensively explored interventions over the last 50 years has been the stem cell transplantation. Various cell types including mesenchymal stem cells (MSCs), induced-pluripotent stem cells (IPSCs), oligodendrocyte progenitor cells (OPCs) and olfactory ensheathing cells (OECs) or even stem-cell derived exosomes have proven to be viable options for SCI treatment [95, 96]. Among those, the transplantation of neural progenitor cells (NPCs) stand out for its multipotency (ability to differentiate into any neural lineage) and its biosafety [97].

NPCs transplantation

NPCs are multipotent self-renewing progenitor cells with the ability to derive into neurons, oligodendrocytes and astrocytes. NPCs are found in the developing CNS and persist in the adulthood in the subventricular zone (SVZ) of the forebrain, the subgranular zone (SGZ) of the dentate gyrus and the central canal (CC) of the spinal cord. NPCs can be isolated from all these anatomical niches and from different developmental stages, however for its applicability as SCI therapy the most widespread option are NPCs extracted from fetal spinal cord [97].

NPCs' transplantation attractiveness relies in its pleiotropic spectrum of effects [98]. First, NPCs serve as a tri-potent cell source for the replacement of the massive cellular loss occurring after the primary insult [99]. Second, NPCs grafts can help to restore the integrity of the spinal cord and to provide a more permissive environment by the release of trophic factors such as BDNF or GDNF [100]. Moreover, NPCs graft can support the growth of regenerating axons and can form synaptic connections with them serving as a relay of the information across the injury [98]. Specifically, *Tuszynski et al.* have extensively contributed to establish the guidelines for efficient engraftment and to increase our current understanding of NPC mechanisms. Over the years their findings have demonstrated that NPCs grafts are able to: i) survive for at least 3 months after transplantation, ii) differentiate into astrocytes and neurons (which extend axons into the endogenous tissue and express synaptic markers), iii) support the growth of serotonergic and corticospinal axons, and ultimately iv) to promote significant locomotor recovery in several animal models of SCI (including rodents and non-human primates) [101, 102].

An important consideration for NPCs therapy is the appropriate timing of the transplantation. While during the acute and subacute phases the spinal cord environment

is especially aggressive what can dramatically impact on the graft survival, during the chronic stage the functional impairments are already established and scarcely reversible. Therefore, finding the most adequate therapeutic time window is an essential aspect for transplantation success [103].

Despite its potential NPCs therapy still accounts for several limitation for its clinical translation into human patients. Some of these include: i) ethical complications derived from NPCs source (human fetal tissue) ii) the technical difficulties of expansion and storage of sufficient number of cells in a standardized manner; iii) the need for immunosuppression of the receptor due to the allogeneic origin of the graft and iv) invasiveness delivery of the transplantation (particularly by intraspinal injections) [98]. So far clinical trials in SCI patients have shown that NPCs transplantation is safe for human application, however it showed limited outcomes over sensory and motor function recovery in SCI patients [98, 104].

cAMP as a master regulator of CNS repair

cAMP therapies in SCI

One of the molecules that have been shown to play a major role in CNS regeneration is the cyclic adenosine monophosphate (cAMP), with extensive literature support [105-107]. Specifically, three naturally-occurring phenomena perfectly illustrate the relevance of cAMP in neural regeneration. First, retinal ganglion and spinal neurons at an early-developmental stages exhibit high cAMP and substantial regenerative capacity as shown by their ability to display neurite outgrowth even under the exposure to inhibitory molecules (i.e., MAG or myelin). cAMP concentrations dramatically decay after birth which parallel a marked developmental loss of their intrinsic regenerative capacity [108]. Thus, cAMP is considered to be responsible for the switch from regenerative to non-regenerative states in the transition from embryonic to adult neurons [105]. Second, cAMP signaling activation has proved to be the underlying mechanism to the growth-promoting effects elicited by neurotrophic factors. Specifically, one set of experiments showed that only when cerebellar neurons were previously exposed to BDNF or GDNF their neurite growth inhibition was totally blocked when subsequently cultured over MAG or myelin substrates. Among a wide panel of agents tested, only cAMP analogs were able to simulate the preconditioning effect of the neurotrophins, which was further confirmed by measurements of cAMP by immunoassay revealing a two-fold increase in cAMP concentrations upon neurotrophic treatment [109]. Third, after a peripheral injury, cAMP levels increase threefold in the DRG neurons enabling the regeneration of its central axon if subsequently injured (what has been call “the conditioning lesion effect”);

and effect that is perfectly mimicked by injections of cAMP analogs in the DRGs [110, 111]. Further insights about this issue are provided in chapter 2.

The cAMP signaling starts with the generation of intracellular cAMP by adenylate cyclases (ACs), a family of enzyme comprised by 10 different subtypes [107]. ACs activity is modulated by calcium or by G-protein coupled receptors that recruit a G- α . Stimulatory (Gs) subunit upon binding with extracellular factors (i.e., BDNF). Once activated ACs catalyze the conversion of ATP into cAMP and pyrophosphate. Subsequently, elevating intracellular levels of cAMP stimulate its effector proteins: protein kinase A (PKA) and exchange protein activated by cAMP (EPAC) [107]. These two effectors are highly-coordinated and can modulate numerous downstream targets. PKA is composed by two different subunits which are ubiquitously expressed in almost all cell types. EPAC possess two different isoforms (Epac1 and Epac2) which differentially expressed, being EPAC2 specifically expressed in adult CNS and adrenal gland [112]. PKA and EPAC may act independently, antagonistically or synergistically to exert wide-range of cellular functions [113]. One of their most relevant downstream effects is the nuclear phosphorylation and subsequent activation of cAMP response element binding protein (CREB). P-CREB forms a complex with co-activator CREB binding protein, recruiting the RNA polymerase II and resulting the activation of the transcription of hundreds of regenerative-associated genes (i.e., BDNF, Arginase I). Ultimately, cAMP levels are returned to basal concentrations via cAMP degradation by phosphodiesterase (PDEs) a family of cAMP hydrolyzing enzymes.

cAMP signaling activation has been linked with numerous neural beneficial effects including increased neuronal survival, stem cell neuronal differentiation, axonal regeneration, remyelination and synaptic plasticity among others [114-117]. All the aforesaid facts clearly convey the significance of cAMP signaling in promoting CNS regeneration and unveil its huge potential as a therapeutic intervention after CNS damage. Several authors have arisen to the same conclusions based on their experience but still, cAMP-targeted therapies for SCI are not as popularized as they should, considering their greatest potential.

There are several ways of achieving cAMP manipulations in vivo: i) administration of Adenylate cyclase activators (i.e., forskolin), ii) phospho-diesterase (PDE) inhibitors (i.e., rolipram, roflumilast) or iii) direct administration of synthetic cAMP analogs (i.e., dibutyryl-cyclic AMP [db-cAMP] and 8-Br-cAMP) (Figure 4, left). Several of them have been applied as SCI treatments over the last decade alone or in combination with other therapeutical interventions. For instance, studies performed by Costa et al in 2013

showed that the subcutaneous administration of rolipram (a PDE4 inhibitor) for 2 weeks by and osmotic pump in rats suffering a contusion injury resulted in improved BBB (Basso, Beattie and Bresnahan locomotor test) and beam walking scores starting at 7 and 3 dpi respectively and maintained for at least 56 dpi. Moreover, the intrathecal administration of 8-Br-cAMP after a C2 hemisection allowed the restoration of phrenic nerve output and improved the of respiratory motor recovery in Sprague Dawleys (SD) rats [118]. Other examples of successful cAMP-targeted therapies are compiled in Table 1.

Reference	Treatment Regime	Functional Outcomes	Proposed mechanism
Goshgarian et al. (2008) [118]	Intrathecal administration of 8-Br-cAMP on left C2 hemisectioned rats	Enhanced phrenic nerve output and restored respiratory deficits	Not specified
Schaal et al.(2012) [119]	Daily intravenous administration of rolipram for 2 weeks after a T8 contusion	Increased BBB scores 6 weeks post-injury	<ul style="list-style-type: none"> · Increased neuronal and oligodendrocyte survival in the lesion · Reduced number of phagocytes 2 weeks post-injury
Xingang Li et al.(2017)[120]	Microfibrils impregnated with (db-cAMP) and chondroitinase ABC in hemisection injury	Improved scores in BBB and narrow beam tests	<ul style="list-style-type: none"> ·Promoted axonal sprouting ·Reduced glial scar formation
Jeoung Soo Lee et al. (2018)[121]	Rolipram-Loaded into polymeric micelle nanoparticle intraspinally injected in rat model of compression injury.	Not specified	<ul style="list-style-type: none"> · Reduced apoptosis · Reduced infiltrated macrophages and inflammatory response
Moradi et al, (2020) [122]	Intraperitoneal administration of roflumilast 30 min before T9 contusive injury in male rats	Increased BBB scores 28 dpi Increased mechanical allodynia and decreased thermal sensibility 28 dpi	<ul style="list-style-type: none"> · Decreased cavity size · Increased anti-inflammatory responses 28 dpi
A.Silva et al.(2023)[123]	Roflumilast in a thoracic contusion rat model.	Improved BBB scores, and decreased foot errors in Gridwalk test.	<ul style="list-style-type: none"> · Decrease in cavity size · Less reactive microglia · Higher axonal regeneration

Table 1: Compilation of in vivo studies investigating the effects of pharmacological cAMP modulators as SCI treatment in rodents. Expanded from Mussen et al. (2023) [124]

Reported underlying mechanisms of cAMP-targeted therapies include white matter preservation, increased neuronal and oligodendrocyte survival, decreased infiltration of phagocytes, decreased inflammatory markers and free radical formation [122, 123, 125, 126]. However, others studies arouse some controversy due to the inconsistency in the

results what might be explained by variations in the route of administration, drug dosage and time of application[127].

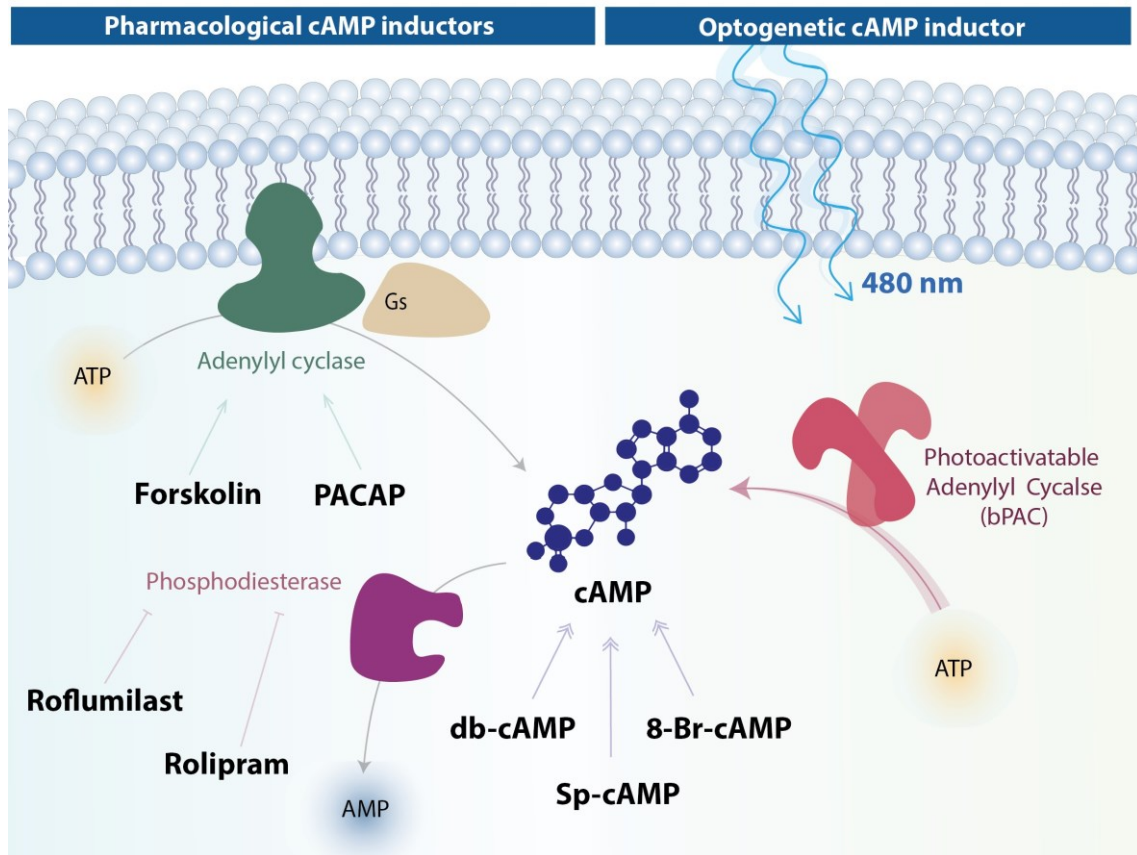


Figure 4: Outstanding methods for cAMP manipulation. Illustration showing critical points for pharmacological targeting in drug-based cAMP modulation. As shown pharmacological cAMP signaling induction can be achieved by either adenylyl cyclase activation (via Forskolin or PACAP), phosphodiesterase inhibition (via Rolipram or Roflumilast) or by direct administration of cAMP analogs (i.e., db-cAMP, sp-cAMP or 8-Br-cAMP). On the other hand, novel tools of cAMP elevation include the use activatable adenylyl cyclase that promote highly efficient cAMP generation upon blue light exposure (right side of the panel).

Novel tools for cAMP manipulations

Is important to note that the administration of cAMP modulators is contraindicated for its clinical use due to their side effects [128]. Since cAMP serves as a ubiquitous second messenger, the systemic administration of cAMP modulators does not represent a safe strategy for clinical translation, making imperative the need of developing strategies with cellular specificity. Beside to the safety concern, pharmacological cAMP modulation does not allow the generation of controllable cAMP peaks that mimic natural dynamism of cellular mechanisms.

For these reasons in the recent years novel tools have emerged to enable non-invasive on-demand manipulation of intracellular cAMP with spatio-temporal precision. Alongside the discovery of DREADDs and Channelrhodopsins to modulate calcium influx and neuronal depolarization [129], analogous genetically-encoded tools have been developed to modulate cAMP: Gs-DREADDs chemoreceptors (rM3Ds) and photo-activatable adenylyl cyclase (PAC) or. rM3D is based on the coupling of a Gs protein with a DREADD receptor that becomes activated and activates adenylyl cyclase upon binding of CNO[130]. However, Gs-DREADD application is less popularized compared to PACs.

The discovery of photo-activatable adenylyl cyclases (PACs) opened a new path for the light-inducible modulation of intracellular cAMP levels [131] (Figure 4, right). PACs were characterized and isolated from photo-sensitive microorganisms, being the first one discovered in 2002 in *Euglena*, a unicellular flagellated algae (euPAC) [132]. The protein structure is based on two subunits, each with two blue light receptor domains (BLUF) coupled to two ACs, that upon blue light exposure elicit a ~ 80-fold increase in their enzymatic activity. More recently, in 2010, a novel PAC was discovered in the bacteria *Beggiatoa* (bPAC). Compare to euPAC, bPAC possess smaller protein structure (only 350 amino acids compare to 1019) which makes it more feasible for transgenic delivery [133]. Additionally, bPAC displays greater sensitivity to blue light exposure, an important aspect for its applicability due to limited penetration of blue light in tissues, as well as lower dark activity [133]. Different studies have reported a 300-to-1600-fold increase in cAMP levels upon bPAC light activation depending on measurements from purified proteins or soluble protein extracts [134, 135]. Albeit low dark-to-light ratio, bPAC has shown to increase basal cAMP levels even in the dark ($1.48 \pm 0.1 \mu\text{M}$ of cAMP in non-bPAC expressing xenopus oocytes versus $24.7 \pm 4.7 \mu\text{M}$ cAMP in bPAC-oocytes in the absence of light and $267 \pm 65 \mu\text{M}$ in the presence of light) [135]. Genetic modifications by punctual mutations have been recently implemented to minimize bPAC dark activity if required [135]. Moreover, the genetic sequence of bPAC has been modified to be fused with fluorescent reporters, tagged for its translocation to presynaptic vesicles (synaptoPAC) or transmembrane domains (PACmn) or expressed under the control of specific promoter according to experimental requirements [135, 136]. The addition of fluorescent proteins to the N-terminus or C-terminus (i.e., bPAC-eYFP) have also shown to also decrease dark activity (i.e., $9.7 \pm 1.9 \mu\text{M}$ cAMP in bPAC-eYFP xenopus-oocytes) without affecting its light activity [135].

So far bPAC has been implemented in vivo in several neuroscience fields. For instance, transgenic mice expressing bPAC in the astrocytes showed that cAMP inductions in

hippocampal astrocytes increased synaptic plasticity and modulated memory by an astrocyte-neuron lactate shuttle [137]. In the context of CNS damage bPAC has so far only be described in vivo in a Zebrafish model in 2015. Outstandingly, the light-stimulation of bPAC in afferent neurons of Zebrafish dramatically increased the regeneration of their axotomized central axons, which re-targeted their correct area of the brain forming new functional synapsis [138]. This fact, established a justified basis for our willingness to unprecedentedly implement of bPAC in a mammal animal model of SCI.

HYPOTHESIS AND OBJETIVES

Given the current lack of a significantly effective clinical strategy for spinal cord injury (SCI) patients, we firmly believe in the need to further delve into basic understanding of spinal cord injury pathology for the development of new therapeutic strategies. To give a response to this urgent and yet unmet clinical need, in the present thesis, our main objective is: **to contribute with new insights into how the central nervous system (CNS) responds to injury and upon treatments, which could yield meaningful findings for consideration in the development of future therapeutical approaches.** This objective has been explored in well-established and clinically-relevant models of SCI such as thoracic contusion and dorsal hemisection in rats.

In order to experimentally approach this thesis and its main objective, we have pursued various sub-objectives organized across the two main chapters:

Chapter 1 entitled “*NPC transplantation rescues sci-driven cAMP/EPAC2 alterations, leading to neuroprotection and microglial modulation*”. In this chapter we hypothesize that a comprehensive transcriptional characterization of the temporal evolution following a spinal cord injury (SCI) and an exploration of the transcriptional changes induced by neural progenitor cells (NPCs) transplantation could help to unveil relevant molecular processes for SCI pathophysiology and its potential treatment. For that we have developed the following objectives (O):

O1.1: To describe transcriptional profiles during the temporal progression after severe contusive injury. The study of temporal transcriptional patterns after SCI may help to unveil interactions between relevant molecular processes and can serve to establish the more convenient time for therapeutical intervention considering their targeted molecular pathways.

O1.2: To transcriptionally characterize the molecular processes underlying NPC transplantation. Deeper understanding of the influence of NPC transplantation into the injured spinal cord transcriptional profile and NPCs mechanism of action description can serve to unveil new target pathways for the conceptualization of potential synergistic future strategies.

O1.3: To investigate the potential involvement of EPAC2 in NPC transplantation therapeutical mechanism after SCI via lost-of-function experiments. Having demonstrated the dichotomy of EPAC2 regulation by SCI and NPC transplantation in O1.1 and O1.2, next we aimed to mechanistically understand the role of exchange

protein activated by cAMP (EPAC2) in the context of immunomodulation and neuro-preservation

Chapter 2 entitled “*Stimulation of corticospinal neurons by optogenetic cAMP inductions promotes motor recovery via raphespinal tract modulation*”. cAMP signaling has been demonstrated a crucial function for adult nervous system regeneration. Our finding in chapter 1 also revealed the dramatic alterations of cAMP signaling after SCI as well as the upregulating effects mediated by NPC transplantation over this pathway, emphasizing the imperative need to further intervene over cAMP modulation after injury. Thus, in chapter 2 we postulate that daily optogenetic cAMP stimulation in corticospinal neurons immediately after SCI may help to overcome regeneration failure after injury. We hypothesize that cAMP-mediated stimulation of corticospinal projecting neurons would trigger a pro-regenerative response, facilitating neuroplastic changes of the corticospinal tract (CST) and ultimately leading to improvements in locomotor function. This main was approached by the following sub-objectives:

O2.1: To set up an optogenetic inducible system for neuronal cAMP signaling activation; including i) an in vitro neuronal model, to allow the validation of the optogenetic and ii) an in vivo model of dorsal hemisection consisting on bPAC-expressing animals in CST neurons with implanted wireless devices for cortical light stimulation.

O2.2: To study the functional effects of daily cortical bPAC stimulation on the motor and sensory outcomes in rat models of dorsal hemisection.

O2.3: To investigate the anatomical basis of bPAC-mediated functional recovery. For that aim intend to explore the changes in the corticospinal system via direct visualization by anterograde and retrograde tracing techniques in bPAC and control animals. Additionally, retrograde tracing bellow the injury allows to explore the involvement of other important supraspinal centers on functional regeneration.

O2.4: To explore putative corticospinal relay formation with serotonergic neurons at the brainstem level. Based on the premise that CST may form new relay circuits with anatomically intact pathways at the brainstem, here we aim to i) explore the synaptic targets of corticospinal system with brainstem motor centers by using a trans-synaptic tracer Wheat Germ Agglutinin (WGA) and ii) to characterize the electrophysiological behavior of serotonergic neurons in subcortical regions in bPAC and control rats.

O2.5: To study the serotonergic tract implication in bPAC-mediated functional recovery by functional evaluation in loss-of-function experiments by 5,7-Dihydroxytryptamine (DHT) abolishment of serotonergic system.



RESULTS: CHAPTER 1

RESULTS

CHAPTER 1: NPC transplantation rescues sci-driven cAMP/EPAC2 alterations, leading to neuroprotection and microglial modulation

The content of this chapter was published on the 29th of July of 2022, in Cellular and Molecular Life Sciences Journal with the following complete reference:

[*NPC transplantation rescues sci-driven cAMP/EPAC2 alterations, leading to neuroprotection and microglial modulation.*](#)

Martínez-Rojas B, Giraldo E, Grillo-Risco R, Hidalgo MR, López-Mocholi E, Alastrue-Agudo A, García-García F, Moreno-Manzano V.

Cell Mol Life Sci. 2022 Jul 29;79(8):455.

doi: 10.1007/s00018-022-04494-w.

PMID: 35904607

My contribution to the present research article encompassed theoretical conceptualization, interpretation of the output datasets provided by the bioinformatic unit, management of experiments and data acquisition and analysis (always counting with technical assistance and support from my thesis supervisors and co-authors). I also contributed with the original manuscript writing and subsequent edition, as well as with figures and supplementary material generation.

NPC TRANSPLANTATION RESCUES SCI-DRIVEN cAMP/EPAC2 ALTERATIONS, LEADING TO NEUROPROTECTION AND MICROGLIAL MODULATION

Beatriz Martínez-Rojas¹, Esther Giraldo^{1,2,3}, Rubén Grillo-Risco⁴, Marta R. Hidalgo⁴, Eric López-Mocholi¹, Ana Alastrue-Agudo¹, Francisco García-García⁴, Victoria Moreno-Manzano^{1*}

¹Neuronal and Tissue Regeneration Laboratory, Centro de Investigación Príncipe Felipe, E-46012 Valencia, Spain

²Department of Biotechnology, Universitat Politècnica de València, Valencia, Spain

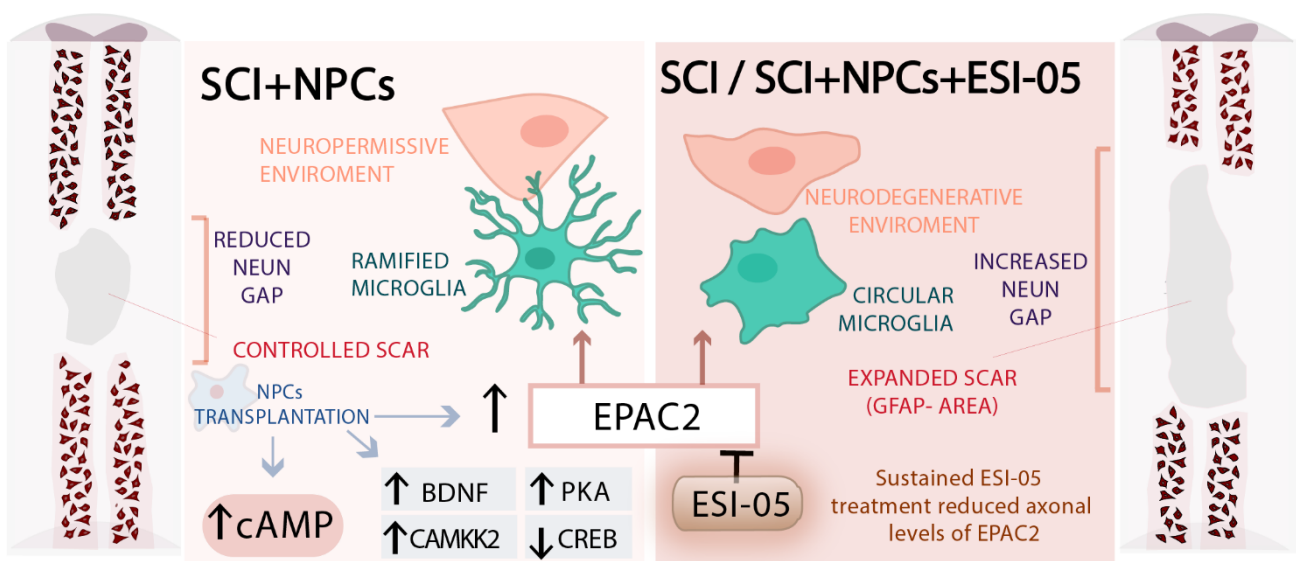
³UPV-CIPF Joint Research Unit Disease Mechanisms and Nanomedicine, Centro de Investigación Príncipe Felipe, 46012 Valencia, Spain

⁴Bioinformatics Unit, Centro de Investigación Príncipe Felipe, E-46012 Valencia, Spain

*Corresponding author. Email: vmorenom@cipf.es; ORCID: [0000-0002-6035-9491](https://orcid.org/0000-0002-6035-9491)

Keywords: NPC transplantation, transcriptomic analysis, spinal cord injury, cAMP, EPAC2.

GRAPHICAL ABSTRACT



ABSTRACT

Neural progenitor cell (NPC) transplantation represents a promising treatment strategy for spinal cord injury (SCI); however, the underlying therapeutic mechanisms remain incompletely understood. We demonstrate that severe spinal contusion in adult rats causes transcriptional dysregulation, which persists from early subacute to chronic stages of SCI and affects nearly 20,000 genes in total tissue extracts. Functional analysis of this dysregulated transcriptome reveals the significant downregulation of cAMP signalling components immediately after SCI, involving genes such as EPAC2, PKA, BDNF, and CAMKK2. The ectopic transplantation of spinal cord-derived NPCs at acute or subacute stages of SCI induces a significant transcriptional impact in spinal tissue, as evidenced by the normalized expression of a large proportion of SCI-affected genes. The transcriptional modulation pattern driven by NPC transplantation includes the rescued expression of cAMP signalling genes, including EPAC2 (exchange protein directly activated by cAMP). We also explore how the sustained *in vivo* inhibition of EPAC2 downstream signalling via the intrathecal administration of ESI-05 for one week impacts therapeutic mechanisms involved in the NPC-mediated treatment of SCI. NPC transplantation in SCI rats in the presence and absence of ESI-05 administration prompts increased rostral cAMP levels; however, NPC and ESI-05 treated animals exhibit a significant reduction in EPAC2 mRNA levels compared to animals receiving only NPCs. Compared with transplanted animals, NPCs+ESI-05 treatment increases the scar area (as shown by GFAP staining), polarizes microglia into an inflammatory phenotype, and increases the magnitude of the gap between NeuN+ cells across the lesion. Overall, our results indicate that the NPC-associated therapeutic mechanisms in the context of SCI involve the cAMP pathway, which reduces inflammation and provides a more neuropermissive environment through an EPAC2-dependent mechanism.

INTRODUCTION

Spinal cord injury (SCI) occurs when a traumatic insult disrupts the communication of impulses through the central nervous system (CNS), resulting in the loss of motor and sensory function below the injured area. Even given recent advances, we still lack effective strategies that restore spinal cord functionality after injury [1]. The search for SCI treatments remains challenging, given the highly complex physiopathological events induced by the initial injury and the involvement of multiple cell types and thousands of transcriptional events [2]. Our incomplete understanding of the molecular mechanisms underlying the dynamic pathophysiology of SCI represents a significant impediment to the development of efficient therapeutic strategies and makes the selection of

rationalized therapies for acute, sub-acute, and chronic disease states a challenging task.

Cell-based therapies [3] are an attractive alternative to conventional neuronal preservation and regeneration approaches for acute or chronic SCI [4]. Neural progenitor cell (NPC) transplantation represents a promising therapeutic approach, as these multipotent cells can re-establish and replace damaged neuronal circuits (reviewed by Lane, Lepore, and Fischer [5]). The transplantation of adult-derived NPCs obtained from naïve [6] or injured [7] spinal cord tissue has been extensively explored in SCI models; however, the limited availability of NPCs in human adult tissues has hampered clinical translation and prompted the widespread application of NPCs prepared from earlier developmental stages (i.e., from neonatal or foetal tissues) [8].

NPCs differentiate into three different lineages (including neurons and glia) after transplantation into the injured spinal cord. Differentiated neurons can synaptically integrate into the disrupted circuitry and create novel neuronal relays across the injury [9], while glia [10] (astrocytes and oligodendrocytes) provide support to both host and NPC-derived neurons, attenuate glial scar formation [11], and enhance the remyelination of injured axons [12]. NPC transplantation simultaneously provides multiple therapeutic activities and, as such, represents an intrinsically multifactorial therapy. NPCs can i) serve as a source of new cells to restore the structural integrity of the injured spinal cord [13], ii) provide neurotrophic support through the secretion of specific factors (such as nerve growth factor, brain-derived neurotrophic factor [BDNF], and glial cell-derived neurotrophic factor) into the injured microenvironment [14, 15], iii) modulate inflammatory responses [16], and iv) protect against glutamate-mediated excitotoxicity [17, 18]. Of note, the precise molecular mechanisms driving the NPC-induced pleiotropic spectrum of effects remain minimally defined.

Elevating cyclic adenosine monophosphate (cAMP) levels also represents a promising means of promoting neural regeneration after SCI, as studies have revealed that high levels of cAMP promote axonal growth in a range of species [19, 20]. Throughout development, endogenous levels of cAMP decrease in dorsal root ganglia neurons in parallel with the loss of axon-growing capacity; thus, the decay in basal cAMP levels associates with a switch from the regenerative state of embryonic neurons to the non-regenerative state of the adult CNS [21].

Unfortunately, cAMP levels decay by around four-fold after SCI, thus generating a non-conducive environment for CNS regeneration [22]. Pearse et al. reported that cAMP levels decayed by 64.3% in the spinal cord rostral to the injury, 68.1% in the brainstem,

and 69.7% in the sensorimotor cortex for at least two weeks after SCI [20]; however, the mechanism driving cAMP decay and whether decay occurs in all spinal cord cell types or a specific subpopulation remains unclear. Overall, findings from a range of related studies have provided insight into the importance of cAMP signalling during CNS regeneration; therefore, a more profound study of this pathway may provide therapeutic targets for CNS pathologies in general and, more specifically, SCI.

Reports have suggested that the cAMP signalling cascade signals solely through protein kinase A (PKA) activation; however, recent research has demonstrated that cAMP binding activates a guanine nucleotide exchange factor - Rap guanine nucleotide exchange factor (GEF) 4 (RAPGEF4), also known as exchange protein directly activated by cAMP 2 (EPAC2) [23]. Guijarro-Belmar *et al.* demonstrated that an EPAC2 activator (S-220) delivered to *ex vivo* spinal cord slices modulated the lesion environment, prompted axonal outgrowth by reducing astrocyte/microglial activation, and resulted in significantly better locomotor performance for up to four weeks after treatment when applied *in vivo* [24].

To date, cAMP-targeted SCI treatments have focused on the application of general modulators of the pathway, such as adenylate cyclase (AC) stimulators, phosphodiesterase (PDE) inhibitors [25, 26], or cAMP analogs [27] alone or in combination with cell therapies [20, 28-30]. While many of these studies reported functional recovery, applying more specific drugs may provide a deeper understanding of the individual implications of EPAC2/PKA in driving regeneration in the context of SCI and NPC transplantation.

The present study aimed to define alterations to transcriptional profiles during SCI evolution and the molecular processes underlying NPC-based therapies, focusing primarily on cAMP signalling. Furthermore, we investigated the potential involvement of EPAC2 in NPC transplantation-mediated regeneration after SCI through the *in vivo* administration of the specific EPAC2 inhibitor ESI-05.

RESULTS

SCI Induces Robust and Persistent Transcriptional Dysregulation

We evaluated transcriptional profiles at early and chronic stages after SCI to understand the evolving mechanisms occurring after severe traumatic SCI, induced by applying a 250 kdyn contusion at the thoracic vertebrae 8 level in adult Sprague Dawley female rats (**Figure 1A**, upper panel displays a schematic diagram of the experimental design). We

collected 1.5 cm long samples of the spinal cord tissue (including the injury epicentre) at time points representing early subacute (one week; T1) [31], late subacute (two weeks; T2) [32], early chronic (four weeks; T4), and late chronic (eight weeks; T8) [33] stages to generate transcriptional profiles using the Rat Gene Expression microarray platform (Agilent-014879 Whole Rat Genome Microarray 4x44K G4131F, Agilent). **Figure 1A** (lower panel) depicts the bioinformatics workflow employed for data processing.

Principal component analysis (PCA) of the samples comprising this data set provided evidence of the clear segregation of the uninjured and injured animals and amongst all time points after SCI (**Figure 1B**). While we detected small intra-group dispersion between the animals of the same experimental condition, we observed higher dispersion during earlier stages when compared to later stages (**Figure 1B**).

Transcriptional analysis at each time point after SCI provided evidence for robust transcriptional dysregulation compared to the uninjured group (T0), which affected 19,675 differentially expressed genes (DEGs) during SCI progression (representing 55.48% of the rat transcriptome - **Online Resource Figure 1**). We observed evident transcriptional alterations from the first week after injury (up to 15,655 genes) that persisted over time, as evidenced by the similar numbers of DEGs observed at two-, four-, and eight-weeks post-injury compared to uninjured spinal cords (14,178, 13,641, and 14,097 DEGs, respectively) (**Figure 1C**, upper panel). All comparisons provided more downregulated genes than upregulated genes (**Figure 1C**); **Online Resource Table 1** lists all DEGs for each comparison.

We next performed a differential expression analysis of each stage versus subsequent time points to explore the evolution of SCI, which revealed the most significant transcriptional differences at the earliest stages - between the first and second weeks after injury (522 DEGs) - and a lower number of DEGs between the second to fourth (27 DEGs) and fourth to eighth weeks after injury (32 DEGs) (**Figure 1C**, lower panel). These findings suggest that an initial burst of transcriptional activity stabilizes two weeks after injury. Furthermore, we discovered that most DEGs (9993 genes) appeared for every time point after SCI when compared to the uninjured spinal cord, as represented by the high number of transcripts at the central intersections of the Venn diagram shown in **Figure 1D**. **Online Resource Table 2** lists the genes comprising each Venn diagram intersection.

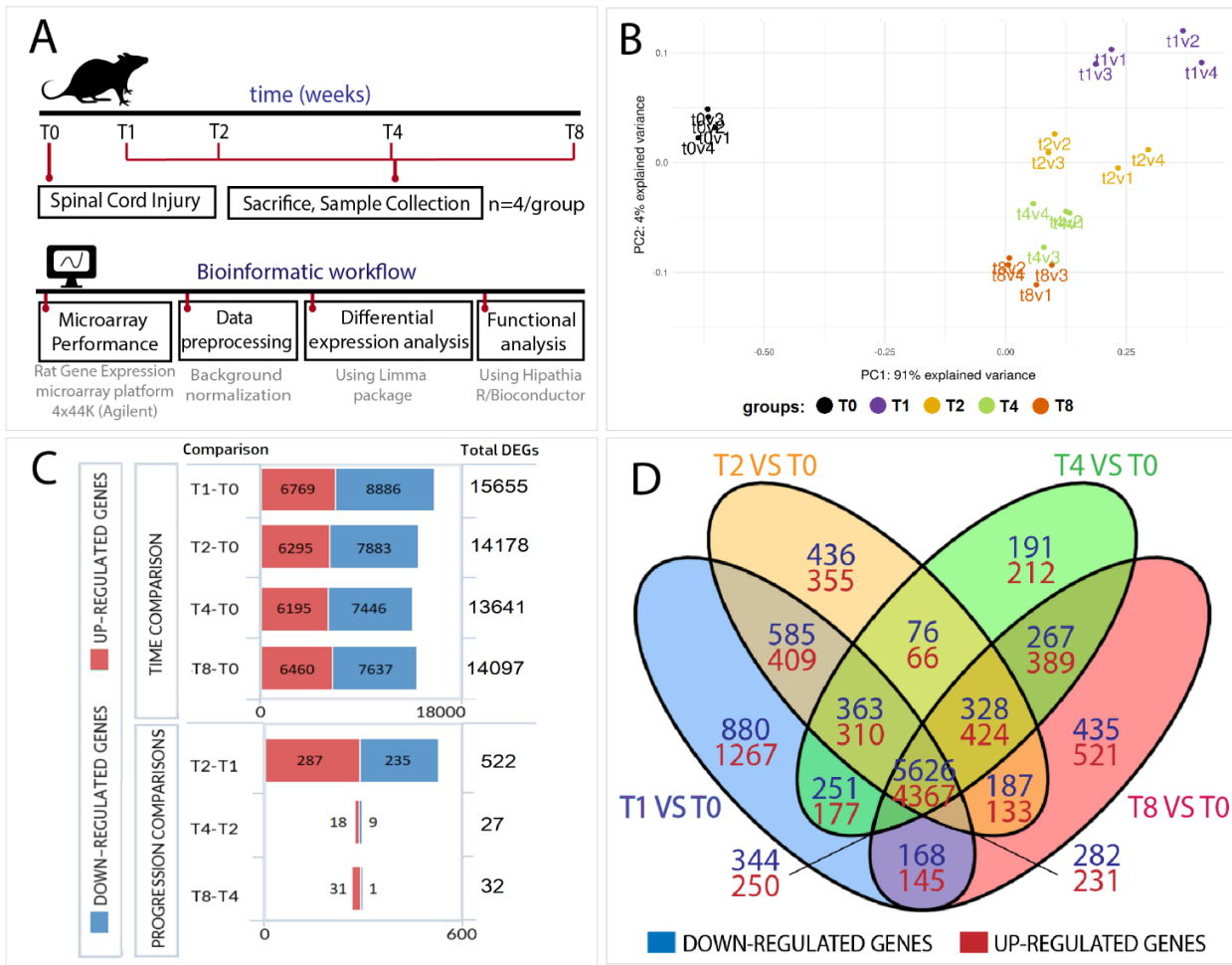


Figure 1: Differential expression analysis during SCI evolution. (A) Schema describing the experimental design, including the in vivo SCI model and the bioinformatic workflow followed in the transcriptional analysis. **(B)** Principal component analysis (PCA) of our data set, showing clear segregation between the different experimental groups used to analyse the evolution of transcriptional alterations after SCI. Please note that v1, v2, v3, v4 denotes the different biological replicates. **(C)** Graphical representation of DEGs from the indicated comparisons during SCI evolution (genes considered differentially expressed with corrected p-values of <0.05). **(D)** Venn diagram depicts DEGs for each time point versus the uninjured spinal cord (T0) and overlapping DEGs between comparisons.

Functional Pathway Analysis Clusters Altered Biological Functions According to their Temporal Regulation Pattern

We functionally analysed the temporal evolution of SCI-induced transcriptomic alterations using the Hipathia algorithm for pathway activity analysis and computed the activation level of each altered function [34]. The functional analysis represented in the heatmap (**Figure 2A, Online Resource Table 3**, and interactive heat map in **Online Resource File 1**) demonstrated the aggregation of altered biological functions into eight different clusters according to their temporal regulation pattern. Functions included in

clusters 1-4 become upregulated after SCI, while functions included in clusters 5-8 become downregulated after SCI (**Figure 2B**). **Figure 2B** depicts individual representations of selected functions in clusters 3 and 7 (which display opposite profiles), while **Online Resource Figure 2** depicts selected functions for clusters 1, 2, 4, 5,6, and 8. **Online Resource Table 3** describes additional information on cluster composition.

Cluster 3 (**Figure 2A-B**) comprises a group of strongly upregulated functions at early stages after SCI (one to four weeks post-injury) that resolve at later chronic stages (eight weeks after SCI). These functions include the "Adenosine Receptor signalling pathway" (GO:0060167) and "G-protein coupled glutamate receptor signalling" (GO:0007216). The alteration of these functions may result from the deleteriously high concentrations of ATP [35] and glutamate [36] associated with SCI, which ultimately derive from cell disruption. The upregulation of these functions suggests that these molecules can trigger secondary signalling pathways within the post-injury tissue to induce excitotoxicity by binding to their respective receptors [37].

In contrast to Cluster 3, Cluster 7 (**Figure 2A-B**) comprises functions that become downregulated at early stages (from one to four weeks) after injury but return to pre-injury levels during chronic stages (eight weeks) and includes terms such as "Cellular response to cAMP" (GO:0071320). The close temporal coincidence with the upregulated functions in Cluster 3 may indicate that these functions induce the downregulation of Cluster 7 functions. Interestingly, we detected a recurrent representation of cAMP signalling during the exploration of altered functions. We also encountered cAMP-related GO terms among the differentially activated functions (listed in **Figure 2C** - indicating the corresponding adjusted p-value and logFC at each temporal comparison). The common overrepresentation of cAMP functions discovered during transcriptional comparisons suggests that SCI profoundly impacts cAMP-related processes.

Cluster 1 comprises a set of functions that became highly upregulated one week after injury and then exhibited a slow but progressive downregulation while remaining significantly elevated compared to the uninjured spinal cord. Among these sets of functions, we encountered "Actin cytoskeleton reorganization" (GO:0031532) and "positive regulation of JAK/STAT cascade" (GO:0046427), with the latter triggering the proliferation and differentiation of multipotent and self-renewing adult stem cells [7] (Sox2/Sox3+ ependymal cells) in response to SCI [38], promoting glial scar formation (preventing secondary damage) [39], and enabling successful axonal regeneration [40]. Previous studies reported that SCI regeneration requires the precise temporal control of JAK/STAT activity, with an early and transient upregulation observed in regenerative

species but a slightly delayed and sustained upregulation (at least 30 days) in non-regenerative species [41]. Thus, this temporal profile of JAK/STAT functions may relate to a non-regenerative response.

Cluster 2 includes persistently upregulated functions at all time points after SCI and displays an enrichment in functions related to immunological processes, including "Positive regulation of interleukin-8 production" (GO:0032637), "Neutrophil chemotaxis" (GO:0030593), "Positive regulation of leukocyte migration" (GO:0002687), and "NK T cell proliferation" (GO:0001866). The presence of these functions suggests that immunological processes induced by primary injury remain unresolved with time, leading to a chronic inflammatory state (as previously described by Schwab et al. [42]).

Cluster 4 comprises functions that display progressive upregulation over time after SCI and includes terms such as "Cholesterol metabolic process" (GO: 0008203), which has been previously linked to SCI and other CNS disorders [43]. Similarly, we encountered additional cholesterol-related processes such as "Cholesterol transport" (GO:0030301), which displayed an upward tendency over time (as found in Cluster 6), and "Cholesterol biosynthetic process" (GO:0006695), which displayed a downward tendency over time (as found in Cluster 8) [44] among the significantly altered biological functions. Importantly, studies have shown that glutamate excitotoxicity mediates cholesterol-related alterations in CNS injury and disease [45].

SCI Severely Alters cAMP Signalling

We next undertook a deeper evaluation of SCI-induced alterations to cAMP signalling components at the transcriptional level. **Figure 3A** depicts a schema describing the most relevant components of cAMP signalling and their roles. cAMP signalling pathway initiation occurs after the activation of adenylate cyclases (ADCY), a family of enzymes devoted to cAMP production. cAMP molecules bind and activate the PKA and EPAC effector proteins, which then activate the mitogen-activated protein kinase (MAPK) cascade via Ras-related protein 1 (RAP1) by PKA-mediated protein phosphorylation or the EPAC2-mediated conversion of guanosine diphosphate/guanosine triphosphate [46]

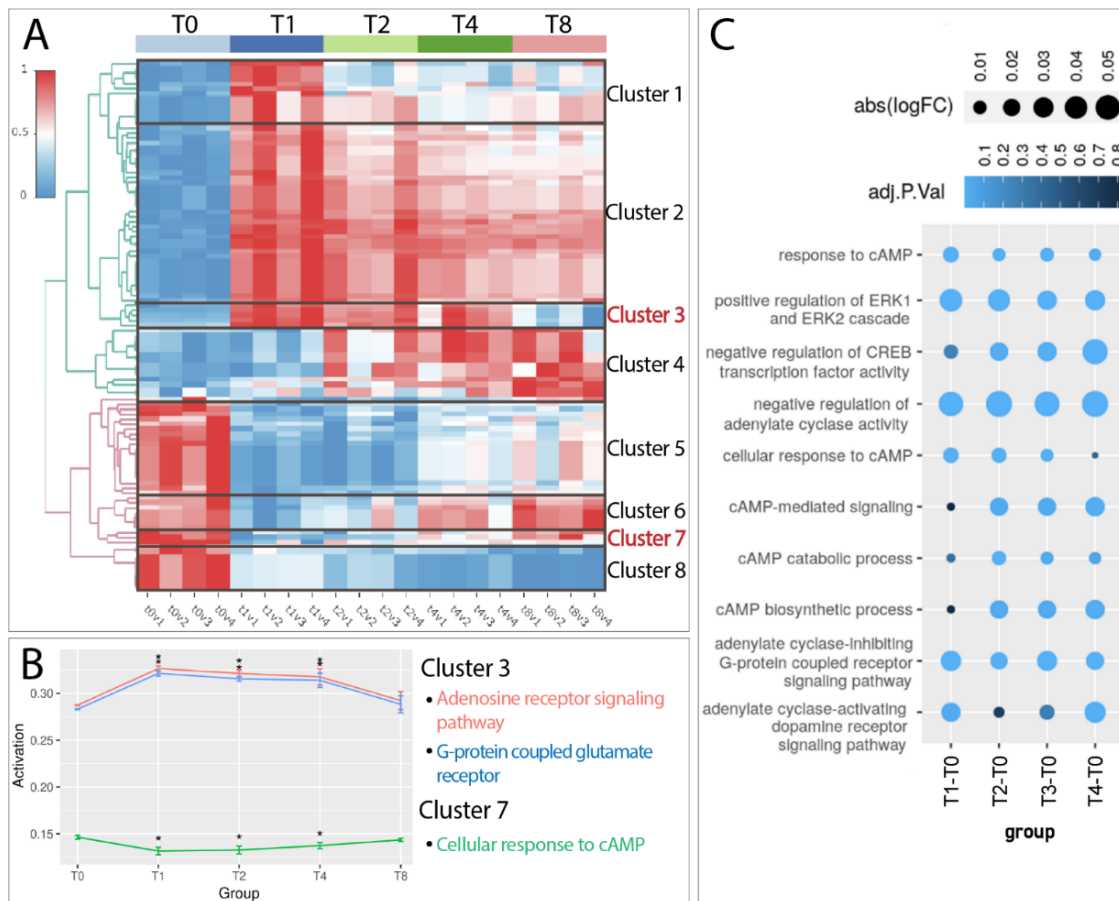


Figure 2: Functional analysis during SCI evolution. (A) Heatmap representing the activation level computed by Hipathia algorithm of differentially activated GO functions for the comparisons on weeks one, two, four, and eight after SCI relative to the uninjured spinal cord (T0). Red, upregulation; blue, downregulation; v1-v4 indicates replicates for each condition. **(B)** Graphical representation of the mean activation levels and associated standard deviation for selected functions encountered in clusters 3 and 7 (*, adjusted p-value < 0.05). **(C)** Dot plot depicting significantly altered cAMP-related GO terms after SCI. Colour intensity represents the corresponding adjusted p-value, while dot size indicates the logFC.

The MAPK cascade culminates with cAMP response element-binding protein (CREB) phosphorylation, which acts as a transcriptional factor to induce the expression of regenerative-associated genes [47]. Such genes include BDNF, an essential axon regeneration modulator that promotes neural plasticity and neurogenesis, exerts nociceptive perception in the uninjured spinal cord, and elicits neuroprotective effects after injury to promote functional recovery [48]. BDNF mediates its effects by binding to tyrosine receptor kinase B (TRKB), which activates the Ras/MAPK cascade through a feedback mechanism [49]. PKA also phosphorylates dopamine- and cAMP-regulated neuronal phosphoprotein (DARPP-32 - a complex integrator of dopaminergic signalling) at Thr34 to inhibit the activity of protein phosphatase 1 (PP1) on CREB; however, DARPP32 also acts as a PKA inhibitor when phosphorylated at Thr75 [50]. In myocytes,

EPAC2 evokes intracellular Ca²⁺ spikes via calmodulin kinase II (CAMKII) activation and ryanodine receptor (RyR) modulation, thereby linking the cAMP pathway to Ca²⁺ signalling [51].

For all evaluated time points after SCI, we confirmed the significant dysregulation of multiple critical genes involved in the cAMP signalling pathway (as represented in **Figure 3A** and shown in an associated heatmap in **Figure 3B** [interactive version in **Online Resource File 1**]) compared to the uninjured spinal cord (T0) when using a false discovery rate (FDR) of < 0.05. We discovered the significant downregulation of ADCY2, 3, 5, and 8 and upregulation of ADCY1, 4, and 6, which agrees with previous observations made in dorsal root ganglia neurons after SCI [52]. We also observed the downregulated expression of the direct cAMP targets PKA and EPAC2 after SCI; however, EPAC2 levels suffered a more robust downregulation than PKA at all evaluated time points, with fold changes ranging from -2.04 to -2.89 for EPAC2 and -0.66 to -0.88 for PKA in comparison with the uninjured spinal cord (T0). Similarly, we encountered the repression of TRKB2, CAMKK2, and BDNF in all groups after SCI (**Figure 3B**, lower section), the upregulation of RAP1B, PPP1CA, and CREB, and the maintained expression of MEK, ERK, and other cAMP-related genes (**Figure 3B**). A closer analysis of DARPP32 expression revealed a biphasic behaviour, with downregulated expression occurring at early stages after injury followed by subsequent upregulated expression at chronic stages (**Figure 3B**).

We further validated EPAC2, BDNF, PKA, CAMKK2, and CREB transcriptional changes by qPCR analysis of independent samples in rostral (thoracic vertebrae 5 to 7), injury-affected (thoracic vertebrae 8 to 9), and caudal (thoracic vertebrae 10 to 11) segments (1.5 cm long each) (**Figure 3C**). The segmental analysis of EPAC2 expression demonstrated significant downregulation at the epicentre of the injury at one (T1), two (T2), and eight (T8) weeks after injury. At week one, we also encountered significantly downregulated EPAC2 expression within rostral segments (**Figure 3C**). BDNF mRNA expression levels significantly diminished caudal to the injury at every time point after SCI compared to the uninjured spinal cord (T0) (**Figure 3C**), which agrees with the independent microarray dataset. At chronic stages (T8), BDNF expression became significantly reduced within the injury zone, suggesting an extended lack of neurotrophic factors within more rostral zones. The slight downregulation detected in PKA by the microarray could not be reproduced by qPCR; this discrepancy may arise from the difference in the relative sensitivities of the associated techniques. We found a significant downregulation of CAMKK2 expression at the injury site one and four weeks after SCI, which partially replicates previous results from the microarray data set. In agreement

with microarray data, qPCR analysis replicated the bi-phasic behaviour of DARPP32 expression with an early downregulation at one week (rostral and caudally to the lesion site) that became upregulated eight weeks after SCI (within rostral and injury segments). Meanwhile, we observed upregulated CREB expression one week after SCI in the injury site and the rostral region two weeks after SCI. Hence, qPCR analysis faithfully replicated the majority of the transcriptional changes observed in the whole rat spinal cord transcriptional analysis in separate sets of samples. The results provide more evidence for the significant alteration of genes related to cAMP signalling after SCI.

NPC Transplantation Rescues SCI-induced Alterations to the cAMP Signalling Pathway

The functional evaluation of rats receiving NPC transplantation after contusive injury demonstrated significant improvements starting from the third week after therapy (Figure 4A). Thus, we aimed to transcriptionally evaluate the early impact of NPC therapy on SCI to reveal those mechanisms that could be eliciting the later functional recovery. Therefore, we compared the transcriptional profile of animals one week after receiving NPC transplants at acute (right after injury) or subacute (one week after injury) stages after SCI with time-matching non-transplanted animals (Figure 4B).

PCA analysis showed clear segregation of the different experimental groups, demonstrating consistency between the experimental replicates (Figure 4C). The differential expression analysis of transplanted versus non-transplanted injured animals revealed that acute NPC transplantation (T1NPC) transcriptionally modulated a total of 4227 genes (1933 upregulated and 2294 downregulated), impacting 1032 SCI-related genes (846 early subacute-SCI DEGs and 186 subacute-SCI DEGs) (Online Resource Figure 3). The subacute transplantation of NPCs (T2NPC) modulated a lower number of genes than acute transplantation (3364 genes; 1639 up- and 1725 down-regulated) but had a more significant impact (1281 genes) on SCI-related genes (1019 early subacute-SCI DEGs and 262 late subacute-SCI DEGs). These findings suggest that NPC transplantation at acute and subacute stage SCI significantly impacts transcription in spinal cord tissue; however, subacute NPC transplantation provided a more specific effect regarding the modulation of SCI-induced alterations.

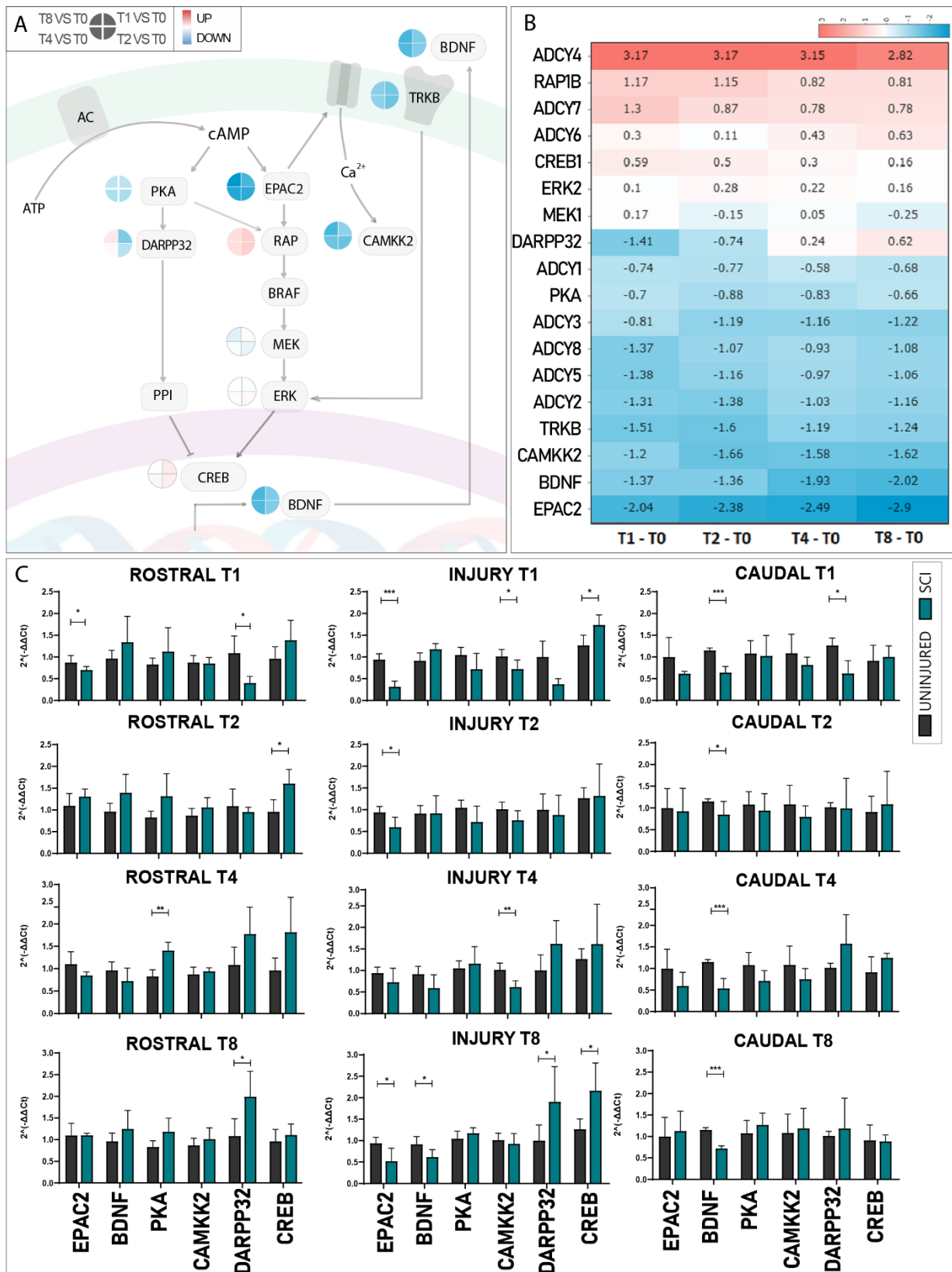


Figure 3: qPCR-mediated Confirmation of transcriptional alterations to the cAMP signalling pathway after SCI. (A) Schematic representation of the cAMP pathway depicting relevant components. The clock icon next to each component represents the evolution of gene expression alterations (from one week [T1] to eight weeks [T8]) as indicated in the legend. **(B)** Heatmap of

cAMP signalling pathway genes showing logFC for each gene over time. Red, upregulation; Blue, downregulation. (C) Microarray expression data validation by qPCR-mediated assessment of gene expression of cAMP-related genes for evolution (from top to bottom) and tissue localization (from left to right) in uninjured spinal cord/control (Black) versus SCI (Green). Data shown as mean \pm SEM. Each gene independently assessed for normality using the Shapiro-Wilk test and then analysed using a one-tailed unpaired t-student; * $p < 0.05$, ** $p < 0.01$, *** $p < 0.001$.

We next functionally analysed the mechanism underlying NPC therapy by applying the Hipathia algorithm to calculate the activation levels of GO biological functions. **Online Resource Figure 4** and **Online Resource Table 4** depict some functions that reported differential activation levels in injured non-transplanted versus injured NPC transplanted animals. Among the differentially modulated functions, we encountered GO terms related to immunomodulation, such as "Interferon-gamma mediated signalling" (GO:0060333), "Positive regulation of interleukin-1 beta secretion" (GO:0032731), and "Positive regulation of T-cell proliferation" (GO:0042102). We also observed the modulation of neural functions such as "Regulation of short-term neuronal synaptic plasticity" (GO:0048172), "Neuron projection morphogenesis" (GO:0048812), or "Regulation of cell communication by electrical coupling" (GO:0010649) after NPC transplantation (Figure 3D, blue panel). NPC-modulated GO terms also included "Removal of superoxide radicals" (GO:0019430), "Ion transmembrane transport" (GO:0034220), and "Regulation of generation of L-type calcium current" (GO:1902514), suggesting the scavenger function and ionic modulatory capacity of NPCs. Furthermore, NPCs modulated functions related to cell survival ("Negative regulation of mitochondrial membrane permeability involved in apoptotic process," GO:1902109) and cell proliferation and differentiation ("Astrocyte differentiation," GO:0048708; "Endothelial cell morphogenesis," GO:0001886). NPC transplantation also regulated molecular pathways such as "Notch signalling" (GO:0007219), "Neurotrophin TRK receptor signalling" (GO:0048011), "Cellular response to cAMP" (GO:0071320) and "Inositol-phosphate mediated signalling" (GO:0048016) (**Online Resource Figure 4**).

While focusing on cAMP functions, we discovered that NPC transplantation during acute stages after SCI significantly reversed the downregulation of cAMP cellular responses compared to time-matched injured non-transplanted animals (**Figure 4E**). We detected the same tendency for subacute transplantation, although this failed to reach significance. We assessed gene expression of cAMP-related targets by qPCR (**Figure 4F**) to further characterize the impact of NPC therapy on cAMP signalling. We reproduced the experiment using neonatal NPCs, as a more clinically relevant model, to

validate previous high content gene transcriptional results (which employed adult NPC transplantation). We found that acute neonatal NPC transplantation rescued SCI-induced reductions in EPAC2 expression in rostral and caudal segments, while subacute NPC transplantation prompted increased EPAC2 expression compared to the non-transplanted group rostral to the injury. Additionally, NPC transplantation increased BDNF expression in the caudal region when applied at acute or subacute stages compared to injured non-transplanted animals. Furthermore, we found a significant increase in BDNF levels in the injured site for the subacute transplantation group. After sub-acute transplantation, we observed a significant induction in PKA and CAMKK2 mRNA levels throughout the spinal cord in rostral, injury, and caudal regions. While we observed a similar trend for acute transplantation, these results failed to reach significance. Finally, NPC transplantation reduced the upregulated levels of CREB encountered after SCI to control levels. Overall, our results suggest that both adult and neonatal NPC transplantation can correct most SCI-driven alterations to the expression of cAMP signalling components.

NPC Transplantation after SCI Increases cAMP and rostral Axonal Levels of EPAC2

To evaluate the influence of EPAC2 on therapeutic outcomes after NPC transplantation at the sub-acute stage after SCI, we administered a specific EPAC2 inhibitor (ESI-05) alongside NPC transplantation (schema shown in **Figure 5A**). The quantification of cAMP concentrations in rostral and caudal spinal cord homogenates (0.5 cm distal from the injury epicentre; **Figure 5B**) by ELISA immunoassay revealed that animals with SCI exhibited significantly lower cAMP levels in rostral segments compared to the corresponding caudal segment, which indicates an area-dependent depletion of cAMP induced by SCI (**Figure 5B**). Interestingly, NPC transplantation (in the absence and presence of ESI-05) prompted a significant increase in rostral cAMP levels compared to control, indicating that NPC transplantation inhibits the SCI-induced rostral depletion of cAMP levels. In agreement, anti-cAMP staining in the injured segment revealed a higher percentage of total immunolabeled area in injured animals receiving NPC transplantation (SCI+NPCs) and injured animals receiving NPC transplantation and ESI-05 (SCI+NPCs+ESI-05) compared to untreated injured animals (SCI) (**Figure 5C**).

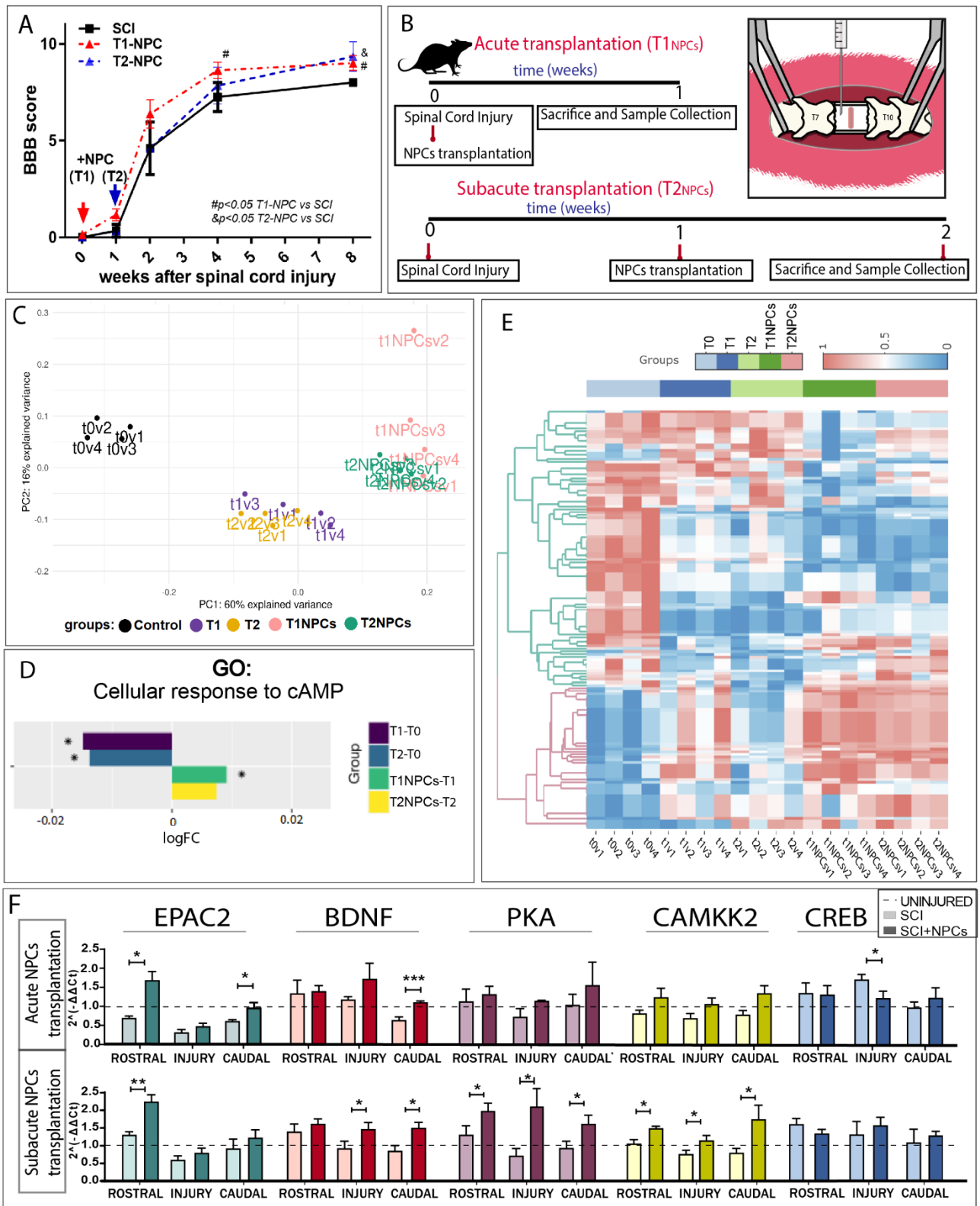


Figure 4. Transcriptional profile analysis after acute/subacute NPC transplantation and analysis of transcriptional changes in cAMP-related genes. (A) Functional locomotor evaluation by open-field BBB scale over eight weeks post-SCI and after acute or sub-acute NPC transplantation (parallel animals to those used for the microarray analysis). Data expressed as mean \pm S.E.M., determined by two-way mixed model ANOVA with Tukey's multiple comparison

test (# $p < 0.05$ T1-NPC versus SCI; & $p < 0.05$ T2-NPC versus SCI) ($n = 6$ animals). **(B)** Schema describing the in vivo experimental design. **(C)** Principal component analysis (PCA) of our data set, showing clear segregation between the different experimental groups used to analyse the impact of NPC transplantation on SCI-induced transcriptional alterations; v1-v4 indicates replicates for each condition **(D)** Bar-graph representing logFC regarding cellular responses to cAMP for indicated comparisons, showing that NPC transplantation reverses the SCI-induced downregulation in this biological function. **(E)** Heatmap representing differentially-activated GO functions computed by the Hipathia algorithm, which provided significant results between uninjured (light blue), injured at week one (T1 - dark blue) or week 2 (T2 - light green), acute (dark green), and subacute (pink) NPC transplantation; v1-v4 indicates replicates for each condition (interactive version at Online Resource File 1) **(F)** qPCR analysis of cAMP-related genes after acute (upper row) and subacute (bottom row) NPC transplantation. Data shown as mean \pm SEM, evaluated with the Shapiro-Wilk test to assess normality and one-tailed unpaired t-student or Mann-Whitney test to compare groups: * $p < 0.05$, ** $p < 0.01$, *** $p < 0.001$.

Next, we evaluated the expression of the direct cAMP target EPAC2 in our experimental groups (SCI, SCI+NPCs, and SCI+NPCs+ESI-05). qPCR analysis revealed a significant increase in rostral EPAC2 mRNA levels following NPC transplantation (SCI+NPCs) compared to injured non-transplanted rats (SCI) (**Figure 5D**), which agrees with our previous findings (**Figure 4F**); however, the addition of ESI-05 (SCI+NPCs+ESI-05) inhibited the NPC-mediated increase in EPAC2 mRNA levels, suggesting that EPAC2 may participate in a positive feedback loop regulating its expression.

Protein immunoreactivity analysis in spinal cord tissues revealed EPAC2 staining within the cytoplasm or plasma membrane of B-III-Tubulin+ neuronal bodies in the grey matter and B-III-Tubulin+ axonal tracts of the white matter (**Online Resource Figure 5** and **Figure 5E, respectively**). We failed to encounter significant differences in the proportion of cytoplasmic or plasma membrane-resident EPAC2+ cells after normalizing data to the total number of EPAC2+ neuronal bodies; however, we observed a significant accumulation of EPAC2 protein in the axonal tracts 0.5 cm rostral to the injury in NPC-transplanted animals (SCI+NPCs) compared to injured non-transplanted animals (SCI) (in agreement with our qPCR data), as supported by a previous study showing elevated levels of EPAC2 only in neurites and growth cones [53]. In contrast, NPC transplantation combined with ESI-05 treatment (SCI+NPCs+ESI-05) reduced the amount of EPAC2 encountered in rostral axonal tracts (**Figure 5E**). This result agrees with previous observations showing that EPAC2 inhibition leads to a reduction in the number of vesicles expressing EPAC2 after prolonged synaptic activity, given that EPAC2 activity remains essential for the maintenance of the readily-releasable vesicle pool [54]. Although we failed to detect EPAC2 staining in non-neuronal cells, previous data support

the expression of EPAC2 in many other cell types, including astrocytes, ependymal cells, and NPCs [55, 56].

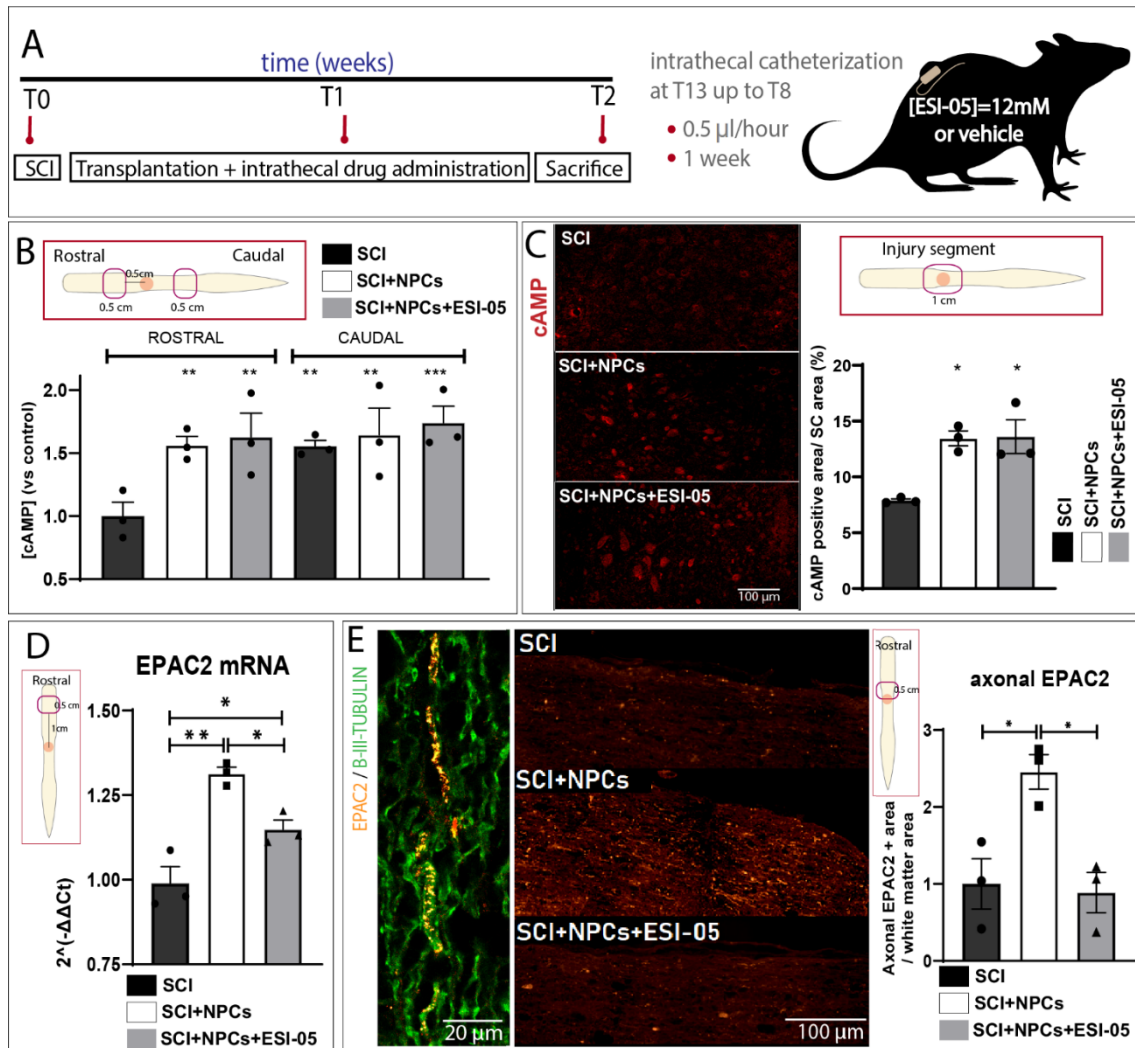


Figure 5. In vivo transplantation of NPCs with the EPAC2 inhibitor ESI-05. (A) Experimental design for the in vivo administration of ESI-05 or vehicle (in SCI and SCI+NPCs groups). Experimental groups: SCI, SCI+NPCs, and SCI+NPCs+ESI-05 (n=3/group). (B) Determination of cAMP concentrations by ELISA immunoassay of the regions rostral and caudal to the injury epicentre relative to injured non-transplanted (SCI) animals. (C) cAMP immunostaining (left panel) and quantification (right panel) in the injured region (D) qPCR analysis of EPAC2 expression in the rostral spinal segment (one-way ANOVA: *, p<0.05; **, p<0.01). (E) Histological visualization of EPAC2 immunostaining (orange) overlapping with B-III-Tubulin+ tracts (green) (left panel). Representative images (middle panel) of EPAC2 staining in rostral white matter areas for each experimental condition and its quantification (right panel) (one-way ANOVA: *, p<0.05).

EPAC2 inhibition reverses NPC-mediated effects resulting in enlarged injury-affected areas

We next assessed the influence of NPC transplantation in the presence/absence of ESI-05 during the early stages of scar resolution (two weeks after injury) by measuring the

extent of the area delimited by the astrocytic barrier (the GFAP- area). Analysis of the GFAP- area throughout the central slices of the injured spinal cord revealed that NPC-treated animals (SCI+NPCs) displayed a significantly reduced scar area compared to injured non-transplanted animals (SCI); however, co-treatment with ESI-05 (SCI+NPCs+ESI-05) abolished the effect of NPCs on scar resolution, resulting in the development of a scar area similar to injured non-transplanted animals (**Figure 6A-B**). Overall, our results describe a critical role for EPAC2 during the early stages of glial scarring in vivo.

ESI-05 Treatment Evokes a Phenotypical Microglial Shift towards Amoeboid-like Cells Reversing the Ramified Phenotype Induced by NPC Transplantation

We next evaluated microglial morphology in Iba-1 staining in terms of circularity [57]. Microglia are morphologically dynamic cells that change from a multi-branched "ramified" state under homeostatic conditions to an amoeboid-like shape under pathological conditions [58]. Circular microglia generally display a proinflammatory M1 profile, while ramified microglia have been associated with an anti-inflammatory and neuroprotective M2 state [59]. To focus on the microglial cell population with greater relevance to neuroprotection, we specifically studied the morphology of microglia in white matter regions rich in NeuN+ neurons. Furthermore, the study of Iba-1 staining in those specific regions allows the exclusion of macrophages from our analysis since they localize to peri-injury areas. We discovered that NPC transplantation (SCI+NPCs) increased the percentage of ramified microglia (**Figure 6C**) up to $54.0 \pm 2.6\%$ in comparison to untreated injured animals (SCI) in these areas, thereby creating a larger anti-inflammatory microglial population (**Figure 6D**).

Overall, these findings suggest that NPC transplantation prompts a shift in microglial morphology in the NeuN+ cell microenvironment within the injured spinal cord. Strikingly, dual treatment with NPCs and ESI-05 (SCI+NPCs+ESI-05) partially reversed the effect of NPCs on microglial status (resulting in a population of $41.9 \pm 5.4\%$ ramified-like cells), which suggests that EPAC2 mediates the NPC-induced alterations in the microglial population (**Figure 6C-D**). Accordingly, animals receiving NPC transplantation (SCI+NPCs) displayed a reduction in the area positive for P2X4 receptor expression (**Figure 6E**), which becomes upregulated in pathological conditions in activated microglia/macrophages [60], when compared to injured untreated animals (SCI) or animals receiving NPC transplantation and ESI-05 treatment (NPCs+ESI-05).

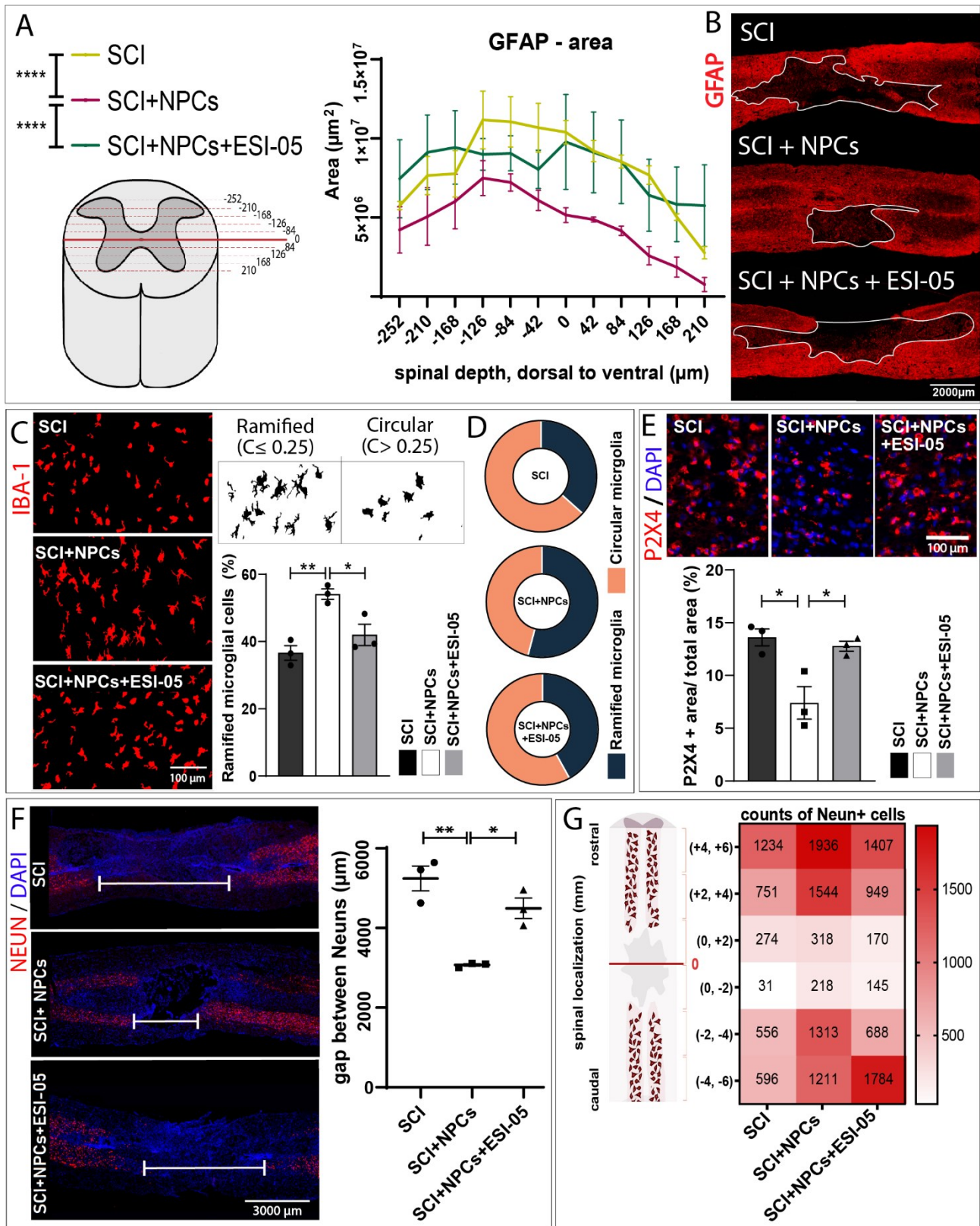


Figure 6 Effects of dual NPC and ESI-05 treatment on scar area, microglial phenotype, and Neun+ cell gap. **(A)** Quantification of the scar area (GFAP-) throughout longitudinal slices in the mid-region of the injured spinal cord. Two-way ANOVA: ****, $p < 0.0001$. **(B)** Representative images of GFAP immunostaining and traced GFAP+ area (white line). **(C)** Morphological

visualization of microglial cells by Iba-1 staining and determination of the percentage of ramified microglial cells. (D) Pie charts representing the microglial population segregated in ramified or circular cells for each experimental group. (E) Representative images of P2X4 immunostaining and its quantification. One-way ANOVA: *, $p < 0.05$. (F) Representative images (left panel) of the sparsity of NeuN+ cells through the injury and quantification of the gap distance (right panel). (G) Heat map showing the mean number of NeuN+ cells per experimental group in each spinal segment of 2 mm.

EPAC2 Mediates NPC Transplantation-related Neuroprotection after SCI

Finally, we measured the gap between rostral and caudal NeuN+ cells across the injury to evaluate the effects of various treatments on neuronal sparsity caused by SCI. Interestingly, NPC transplantation (SCI+NPCs) significantly reduced the gap between NeuN+ cells (**Figure 6F**) and increased the density of NeuN+ cells encountered in the areas surrounding the injury epicentre (**Figure 6G**) compared to injured untreated animals (SCI). Of note, animals receiving NPC transplantation and ESI-05 treatment (NPCs+ESI-05) exhibited a similar gap distance and NeuN density to injured non-transplanted animals (SCI), thereby demonstrating the involvement of EPAC2 in NPC-mediated neuroprotection (**Figure 6F-G**).

DISCUSSION

The primary injury to spinal cord tissues initiates an interconnected and evolving molecular cascade of secondary events [32], with transcriptional analysis providing a comprehensive view of the molecular mechanism underlying SCI pathophysiology [61, 62]. Advanced technologies for transcriptional studies applied to the SCI field, which include RNA-sequencing [62, 63], single-cell analysis [64], and/or axoplasmic fractioning [65], have provided novel insight into the cellular and molecular behaviour of the spinal cord under physiological or injured conditions. Here, we present a transcriptional analysis of spinal cord homogenates, which provides tissular (though not cell-type specific) information regarding critical time points after SCI (from early subacute to late chronic stages). Our approach provides wide temporal coverage to allow the study of the temporal dynamics of SCI evolution. Furthermore, we evaluated the impact of intramedullary acute or subacute transplantation of NPCs on transcriptional profiles within the SCI to define the functional outcomes of NPC therapy.

Whole spinal cord differential transcriptomic analysis revealed two critical issues – i) the substantial number of DEGs found after SCI demonstrates the strong transcriptional impact of SCI (affecting up to 55.48% of the total transcripts), and ii) most DEGs (up to

9993) display commonality at all time points under study (from one to eight weeks after SCI) indicating a lack of efficient transcriptional resolution. Nevertheless, comparisons made during injury progression established that the most significant number of DEGs occurred between the first and the second weeks after SCI; therefore, early therapeutic interventions may prevent later transcriptional dysregulation. Transcriptional characterization indicated that NPC transplantation transcriptionally modulates those SCI-related and non-SCI-related genes necessary for injury resolution. Interestingly, NPC-related DEGs comprise functional blocks relevant to CNS regeneration, such as neural function, immune response, or ionic homeostasis.

Temporal clustering provided evidence that functions such as "G-protein coupled glutamate receptor signalling" and "Adenosine Receptor signalling pathway" (GO:0007216; listed in cluster 3) became upregulated during the first four weeks after SCI before returning to preinjury levels by week eight. The transcriptional upregulation of genes implicated in glutamate receptor transduction may be a consequence of the high availability of this neurotransmitter during SCI. Similarly, the elevated levels of extracellular ATP observed after SCI (which undergoes metabolism to form adenosine [66]) may cause the overactivation of adenosine receptors and thus lead to the upregulation of related signalling components. Interestingly, in close temporal convergence, we discovered the downregulation of the "Cellular response to cAMP" within the first four weeks after SCI before recovering at chronic stages. Given the temporal overlap between the upregulation of glutamate and adenosine receptor cascade with the downregulation of the cAMP response, we suggest the implication of glutamate and ATP leakage in cAMP decay after SCI through G_i protein activation linked to metabotropic glutamate receptors or adenosine receptors [67, 68]; however, we note the need for further experimental validation to fully explore and validate this hypothesis.

We also note the recurrent appearance of cAMP-associated GO terms among altered functions after SCI. Reports have described the regenerative efficacy of cAMP-directed therapies in SCI and provided evidence for the involvement of distinct mechanisms. For instance, cAMP treatment helped axons to overcome growth inhibition by the myelin-associated glycoprotein (MAG) [69, 70] and promoted axon regeneration in the spinal cord, as shown by the capacity of intraganglionic dibutyryl cAMP (db-cAMP) microinjections to induce the growth of injured sensory branches [71]. Similarly, in vivo imaging of fluorescently labelled reticulospinal axons of injured lampreys demonstrated that treatment with a cAMP analog inhibited axon retraction and enhanced axon growth [72]. Furthermore, db-cAMP treatment induced axons to grow in straighter paths and increased the number of surviving axotomized neurons [19, 73]. Importantly, these in

vivo studies apply general methods that prompt cAMP accumulation, which impedes the exploration of the specific involvement of EPAC2 or PKA on cAMP-related effects in spinal cord regeneration; however, Lin et al. reported that the cortical infusion of a selective PKA antagonist enhanced functional improvements after rehabilitative training in injured rats after SCI (contrary to their initial hypothesis) [74]. This finding suggested EPAC2 as a mediator of cAMP-derived-neuronal regeneration and neuroplasticity in the context of SCI for the first time.

cAMP signalling begins by cAMP binding to PKA or EPAC2 and the subsequent activation of distinct signalling pathways, which gives rise to the duality of EPAC2 and PKA functions. The differential activation of PKA and EPAC2 may derive from the regulatory activities of intracellular cAMP levels and the prolongation of cAMP stimulation [75]. Since both PKA and EPAC2 play relevant neuroregenerative functions, we believe that PKA/EPAC2 interplay may have significant implications for SCI; therefore, a deeper understanding of this process remains of great interest.

Although PKA and EPAC2 trigger CREB phosphorylation through MAPK signalling, they possess differential mechanisms of action; for instance, PKA activation in cultured dentate granule cells promotes axonal branching, while EPAC2 activation promotes axonal elongation [53]. EPAC2 participates in a wide range of neural functions, including axonal growth and guidance [21], synapse remodelling through Rap-dependent AMPA GluR2/3 removal [69], and attenuation of microglial and astrocytic activation [22]; however, EPAC2-specific functions remained relatively unexplored in the context of SCI. We employed a combination treatment comprising a specific EPAC2 inhibitor (ESI-05) and NPC transplantation to investigate any possible EPAC2-dependent neuroprotective and neuroregenerative capacities. Although ESI-05 targets EPAC2 protein activity, qPCR and immunohistological analysis indicated that the sustained inhibition of EPAC2 resulted in the downregulation at the protein and mRNA levels.

Previous reports indicated that cAMP induction modulated astrocytic reactivity and reduced scar tissue in vivo [25] and that the specific activation of EPAC2 within the lesion in an ex vivo model of SCI resulted in the generation of astrocytes with elongated processes that were permissive to axon regrowth [24]. We evaluated whether NPC transplantation and EPAC2 inhibition by ESI-05 impacted the extension of GFAP delimited scars. NPC transplantation reduced the extension of GFAP- areas two weeks after SCI; however, cotreatment of NPCs with ESI-05 increased the scar area to a level similar to that observed in injured non-transplanted animals. NPCs may serve as an extra supply of astrocytes [13] or induce astrocyte mobilization in the initial stage of glial

scaring, which is essential for optimal injury preservation of the remaining healthy tissue (reviewed by Falnikar, Li, and Lepore [76]). Overall, our results indicate that EPAC2 inhibition during NPC transplantation may impede gliogenic potential and avoid appropriate astroglial scaring, prompting lesion enlargement. In agreement, cortical NPCs obtained from EPAC2-knockout mice cannot undergo astrocytogenesis induced by pituitary adenylate cyclase-activating peptide (PACAP) [55]. Although our results suggest a role for EPAC2 in the initial formation of the astrocytic border, we hope that further investigations during chronic scenarios will provide further insight.

We morphologically evaluated Iba-1+ cell morphology as an indicator of microglial phenotype in our in vivo model of SCI; specifically, we analysed NeuN+ rich areas, considering the high relevance of the microglia-neuron interaction. Morphological analysis indicated that NPC transplantation increased the percentage of ramified microglia compared to injured non-transplanted animals, suggesting that NPC transplantation could polarize microglia into an anti-inflammatory state (thereby providing a more permissive environment) in neuron-rich areas through an EPAC2-associated mechanism. Previous observations supporting these results described how co-culturing NPCs with brain slices induced neuron survival through microglial polarization into an anti-inflammatory phenotype, which included a reduction in tumour necrosis factor-alpha (TNF α) secretion and an increase in insulin like-growth factor 1 (IGF-1), chemokine (C-X3-C motif) receptor 1 (CX3CR1), and triggering receptor expressed on myeloid cells 2 (TREM2) secretion [77]. Interestingly, ESI-05 administration reversed the effect of NPC transplantation on microglial polarization, thereby suggesting the involvement of EPAC2. Similarly, previous data noted that EPAC2 activation with S-220 in lipopolysaccharides (LPS)-stimulated microglia significantly reduced their inflammatory-like activation status by reducing inducible nitric oxide synthase (iNOS) expression and NO release in vitro, which led to a decreased cell body perimeter that resembled the non-injured morphology in an ex vivo model of SCI [24].

We also employed immunostaining to demonstrate that NPC transplantation decreased P2X4 levels, which agrees with results from a previous study [78], and that cotreatment with an EPAC2 inhibitor avoided this effect. A previous study reported that P2X4 receptor levels increase after SCI upon microglia/macrophage activation [60], while others have shown that P2X4 receptor expression promotes local inflammatory responses and neuropathic pain [60, 79]. Thus, the decrease in P2X4 receptor expression mediated by NPC transplantation suggests that NPC therapy results in an anti-inflammatory outcome. The reversion of P2X4 receptor expression status after ESI-05 treatment suggests a

dependency on EPAC2 for the anti-inflammatory activities exerted by administered NPCs.

In addition to the attenuation of the proinflammatory environment, we also aimed to explore whether NPC transplantation altered neuropreservation in injured tissue by measuring the distance between NeuN+ cells across lesions. Interestingly, we discovered that NPC transplantation favoured neuropreservation, with a two-fold lower gap distance between NeuN+ cells and higher NeuN+ density proximal to the injury epicentre observed. A reduction in the distance between neurons across the injury may indicate a more neuropermissive microenvironment and/or represent a crucial stage in facilitating neuronal plasticity and the formation of new relays, as rostral regenerating axons will cross shorter distances to reach caudal targets. Of particular interest, ESI-05 treatment reversed NPC-mediated neuroprotection, supporting a similar NeuN+ cell gap observed in injured non-transplanted animals. A review of the literature provided evidence of some debate regarding the role of EPAC2 in mediating neuronal apoptosis/survival. While some studies indicate the involvement of EPAC2 in p38-mediated neuronal apoptosis in traumatic brain injury [80], others report improved locomotor recovery after S-220 treatment for SCI, thereby suggesting a neuroprotective role of EPAC2. The regulation of apoptosis or survival via EPAC2 may depend on different scenarios of neural injury pathogenesis [81]. In the context of SCI, we believe that EPAC2 mediates neuronal survival by globally impacting the tissue environment to reduce scar expansion and local proinflammatory processes mediated by M1-polarized microglia. Thus, the detrimental contribution of ESI-05 on the neuroprotective effect of NPCs may derive from an aggressive micro environmental context due to lesion expansion and exacerbated microglial proinflammatory responses caused by an absence of EPAC2.

Considering the short-time window of NPC intervention (one week after transplantation), the ability of NPCs to provide trophic factors into the injured environment (as previously described [15]) should have relevant contribution in their therapeutic effects. Grafted NPCs constitutively secrete neuronal growth factor (NGF), brain and glial-derived neurotrophic factors (BDNF, GDNF) in vivo to inhibit neuronal loss after secondary excitotoxic damage, reduce the activation of both microglia and astrocytes, and impact the growth of sensory and motor axons, which are sensitive to those cues [15].

Overall, our data suggest that NPC transplantation promotes a more neuropermissive microenvironment during SCI by reducing scar extension, attenuating microglial activation, and promoting neuropreservation through EPAC2-dependent mechanisms.

Conclusions

Overall, we provide a comprehensive, wide-ranging temporal profile of the physiopathological evolution of SCI combined with a transcriptional characterization of the impact of NPC transplantation. We have deposited the transcriptional data sets generated in the GEO under accession code GSE183591. We also propose a new hypothesis for cAMP decay after SCI, which may provide the impetus for additional research. We describe the tissue-specific and temporal expression of cAMP signalling components after SCI and experimentally demonstrate that NPC transplantation counteracts a significant proportion of SCI-induced cAMP signalling dysregulation. Finally, we demonstrated the influence of EPAC2 on the immunomodulatory and neuroprotective outcomes associated with NPC transplantation.

METHODS AND MATERIALS

Spinal Cord Injury Model

Sprague Dawley rats (~200 g) were bred at the Animal Experimentation Unit of the Research Institute Príncipe Felipe (Valencia, Spain). Only female rats were used due to the ease of manual bladder emptying required after SCI, the reduced frequency of urinary infections after SCI [82], and more stable body weight during the experimental timeframe [83] compared to male rats. The maintenance and use of all animals were in accordance with guidelines established by the European Communities Council Directive (86/609/ECC) and the Spanish Royal Decree 53/2013. All experimental procedures were approved by the Animal Care and Use Committee of the Research Institute Prince Felipe (2021/VSC/PEA/0032). Rats were housed under standard temperature conditions with controlled 12 h light/dark cycles with *ad libitum* access to food and water. All animals were maintained by professionally trained staff.

For the surgical interventions, female rats were subcutaneously pre-medicated with morphine (2.5 mg/kg) and anesthetized with 2% isoflurane in a continuous oxygen flow of 1 L/min. Laminectomy was performed of the thoracic vertebrae 8-9 to expose the spinal cord and induce severe SCI at thoracic vertebrae 8 level by contusion applying 250 kdyn force using Infinite Horizon Impactor, as previously described [7, 84]. All animals were subjected to post-surgery care consisting of manual drainage of bladders twice a day until vesical reflex was recovered and subcutaneous administration of 5 mg/kg of Enrofloxacin (Alsir) for seven days, 0.1 mg /kg of Buprenorphine twice a day for four days after each intervention, and 1 mg/kg of Tacrolimus starting from one day

before NPC transplantation until the experimental endpoint. The experimental protocol included humane endpoint criteria when severe signs of distress were observed.

NPC Culture and Transplantation

NPC isolation and culture were performed as previously described [85]. Briefly, spinal cords were harvested from adult (for the microarray performance) or neonatal (for the qPCR validation and combinatory transplantation with ESI-05 or vehicle) spinal cords (P3-P5) in cold Hank's balanced saline solution (HBSS) with 10 µL penicillin/streptomycin (P/S; Sigma). Dissected tissue was gently pipetted to induce mechanical disaggregation, and cells were then cultured on ultra-low attachment plates as neurosphere-like cultures. Proliferation culture media comprised NeuroCult™ Proliferation Medium (StemCell Technologies, Grenoble, France) supplemented with NeuroCult™ Proliferation Supplement (Stem Cell Technologies) and 0.7 U/mL heparin (Sigma), 10 µL P/S (Sigma), 20 ng/mL epidermal growth factor (EGF; Thermo Fisher, Horsham, UK), and 20 ng/mL basic fibroblast growth factor (bFGF; Invitrogen). NPC transplantation was carried out directly after (acute model) or one week after (subacute model) contusion. 1×10^6 NPCs at passages 3-4 were intramedullary administered at two injection points (2 mm caudal and rostral to the lesion epicentre) using a 26 G Hamilton pipette coupled to a siliconized glass pipette containing the cell suspension. NPCs were infused at a rate of 2 µL/min in a total volume of 5 µL/injection, waiting 2 min before removing the syringe to allow cell deposition into the tissue (as previously described [84]). Control injured animals were injected with the same volume of the cell-free medium. All animals were sacrificed one week after transplantation.

For the transcriptional study, animals were distributed into the following groups: animals sacrificed at one (T1), two (T2), four (T4), or eight (T8) weeks after SCI; and SCI animals with NPC transplantation at acute (T1_{NPCs}) or sub-acute stages (T2_{NPCs}) (n=8 animals/group; n= 4 for microarray performance and n=4 for qPCR validations). The in vivo combinatory treatment of NPC and the EPAC2 inhibitor (ESI-05) employed the following groups: SCI, SCI+NPCs, and SCI+NPCs+ESI-05 (n=3 animals/group).

Drug Administration

Drug administration was performed by intrathecal catheterization starting one week after injury. Partial laminectomy and dura mater perforation were performed at T13 to introduce the catheter (Alzet Corp., Cupertino, CA, USA; previously filled with 0.9% saline solution) to the injured segment (Thoracic vertebrae 8 level). Catheters were coupled to osmotic pumps (Model 1007D, Alzet Corp. Germany) previously filled with 100 µL of drug solutions (either DMSO 60% [vehicle] for SCI and SCI+NPCs animals or

ESI-05 12 mM in DMSO 100% for SCI+NPCs+ESI-05 animals) and incubated overnight at 37°C in a saline solution following the manufacturer's instructions. Pumps delivered 0.5 µl/hour for one week to achieve a sustained concentration of 15 µM of ESI-05 (assuming a cerebrospinal fluid volume of 400 µl after injury).

Sacrifice and Sample Processing

Animals were overdosed with sodium pentobarbital (100 mg/kg) and transcardially perfused with 0.9% saline solution. For further processing, spinal cord tissue was carefully removed and dissected into rostral, injured, and caudal sections (as described in each experimental design, see **Figures 1A, 4A, and 5A**). Samples destined for histological analysis were fixed by immersion in 4% paraformaldehyde in phosphate buffer saline (PBS) for 24 h and then maintained in 0.1M phosphate buffer (PB). Samples destined for RNA and protein isolation, obtained from 0.5 cm of the tissue adjacent (caudal and rostral) to the injury epicentre, were frozen in liquid nitrogen and stored at -80°C until use.

Microarray Analysis

Total RNA was extracted using the RNeasy Mini Kit (QIAGEN) for transcriptional analysis according to the manufacturer's instructions. Labelled cRNA (3 µg) was hybridized with the Whole Rat Genome Oligo Microarray Kit (Agilent p/n G2519F-014879). The protocol and the raw and normalized data were deposited in the Gene Expression Omnibus (GEO) as open access at www.ncbi.nlm.nih.gov/geo/query/acc.cgi?acc=GSE183591.

Data Processing and Bioinformatic Workflow

Agilent raw data were pre-processed by normalization and background correction using Agilent methodology. The intensity signal was standardized across arrays via quantile normalization [86].

The normalized expression matrix was used as input for two different analyses.

1. Differential expression analysis: Pair-wise analyses between conditions were designed to study: i) the temporal evolution of the injury (every time point condition (T1-T8) versus uninjured (T0): T1-T0; T2-T0; T4-T0; T8-T0, ii) the progression evaluation (each time point condition versus its previous time point), and iii) treatment intervention (acute and subacute transplantation versus untreated and early subacute or late subacute SCI animals). Then, differential gene expression assessment for all comparisons was carried out using limma moderated t-statistics [87]. Multiple testing p-value corrections used the Benjamini-Hochberg procedure to derive adjusted p-

values. Genes were called differentially expressed if their corrected p-value was smaller than 0.05.

2. Functional analysis: pathway analysis using the Hipathia R/Bioconductor package was first performed to estimate the level of activation of each subpathway in every sample from gene expression data. The effector proteins of a subpathway can be linked to GO terms (Biological Processes); Hipathia computes the level of activation of each function, summarizing the activity of all subpathways annotated in a GO term. Finally, a function activity analysis for all comparisons was performed using the limma package. The p-values were adjusted using the Benjamini-Hochberg method [34]. Those functions with an adjusted p-value lower than 0.05 were considered significant.

All bioinformatic steps were performed with the programming language R. Principal Component analysis was performed using the `pca` function from the `mixOmics` package. Unsupervised hierarchical clustering heatmaps (using the euclidean distance) were generated with the `heatmaply` package.

RNA extraction and RT-qPCR

Tissue samples were mechanically disrupted in 1 ml of TriZol Reagent (Invitrogen, Massachusetts, USA) using an ultraturrax. RNA extraction was performed according to Trizol standard method and afterward submitted to an additional step of clean-up by RNeasy MinElute Cleanup (Qiagen, Germany) to ensure the quality of the sample ($A_{260/280} \approx 2$ and $A_{260/230} \geq 1.8$)

1 μ g of total RNA was reverse-transcribed using the high-capacity RNA-to-cDNA™ kit (Applied Biosystems, Massachusetts, USA) in a 30 min reaction at 42°C. Specific primers were designed for each gene of interest- (**Online Resource Table 5**) using primer-BLAST (NCBI, Maryland, USA) and evaluated by efficiency curve performance. qPCR was performed in triplicate using AceQ SYBR qPCR Master Mix (ThermoFisher) in the Light-Cycler 480 detection System (Roche, Basel, Switzerland). Ct data were obtained with the LightCycler 480 relative quantification software (Roche, Basel, Switzerland). GAPDH mRNA level was used as an internal control for normalization. Changes in expression relative to control samples were calculated as $2^{-\Delta\Delta Ct}$.

cAMP Determination

~20 mg of each frozen tissue sample from rostral and caudal regions was weighed and homogenized in 10X volume of 0.1M HCl. Determination of cAMP was performed using cAMP Direct Immunoassay Kit (ab65355, Abcam) following the manufacturer's

instructions. The absorbance of each sample (in duplicate) at OD_{450nm} was measured by a VICTOR2 D fluorometer (PerkinElmer). The calculation of cAMP concentration was assessed by extrapolation to a standard curve.

For the cAMP analysis in the injury site, three longitudinal slices per animal in mid-depth of the spinal cord (taking the central canal as reference) were immunostained. The area positive for cAMP signal was normalized to the slice's total area.

Histological Assessment

After carefully removing the meninges, tissues were placed into paraffin blocks using a Modular tissue embedding center (Myr, SL). Spinal segments were cut into longitudinal sections of 7 μ m thickness using an HM340E Electronic rotary microtome (VWR International, Barcelona, Spain).

Paraffin tissue slices were first baked and washed. Prior to immunofluorescence, slices were incubated at 97°C for 25 min in Tris-EDTA Buffer (10 mM Tris Base, 1 mM EDTA Solution, 0.05% Tween 20, pH 9) to unmask the epitopes and then blocked and permeabilized with 0.1% Triton X-100, 5% horse serum, and 10% foetal bovine serum in PBS. Immunofluorescence double staining was performed by overnight incubation at 4 °C with primary antibodies and 1 h with secondary antibodies at room temperature.

Primary antibodies used were - anti-B-III-Tubulin (α -ms,1:400, MO15013, Neuromics, Edina, MN, USA), anti-NeuN (α -CK,1:600, ABN91, Merck Millipore, Massachusetts, USA), anti-GFAP (α -CK, 1:1000 PA1-10004, Thermo Fisher, Massachusetts, USA), anti-cAMP (α -Rb,1:100, 07-1497, Merck Millipore, Massachusetts, USA), anti-Epac2 (α -Rb,1:400, 43239, Cell Signalling Technology, Massachusetts, USA), Iba-1 (α -Rb,1:400, 019-19741, WAKO, Osaka, Japan), P2X4 (α -Rb, 1:400, purchased from Alomone Labs, Jerusalem, Israel). Secondary antibodies used were either AlexaFluor-488, -555, or -647 (1:400, Invitrogen, Massachusetts, USA) conjugated antibodies against the respective IgG of the primary antibody. DAPI (1:1000, Sigma, Missouri, USA) was used to stain cell nuclei.

Fluorescence images of each spinal cord slice were acquired using an Aperio Versa scanner (Leica Biosystems, Wetzlar, Germany). Images were visualized and quantified with the Image Scope software or ImageJ/Fiji software.

Analysis of GFAP- Areas

The glial scar is delimited by border-forming astrocytes expressing GFAP [88]. The analysis of the extension of the scar was carried out by quantifying the area delimited by

GFAP staining (GFAP negative area) in at least twelve longitudinal slices per animal in a central range of -252 to + 210 microns from dorsal to ventral, including the central canal (0), as represented in the illustration in **Figure 6A**.

Analysis of Microglial Circularity and P2X4 Expression

Iba-1 immunostaining was employed to study the microglial morphology associated with their inflammatory profile [59]. As Iba-1 can also label engrafted macrophages, microglial populations within NeuN+ dense areas of the white matter (which differ from the tissular location where the macrophages are found [into and surrounding injury zone]) were selectively studied.

ImageJ was used to compute the circularity of each Iba+ cell in two different slices obtaining populations of more than 3800 cells per animal. Microglial cells were categorized by their activation level into subpopulations according to their circularity: i) ≤ 0.25 (circular microglia) and ii) > 0.25 (ramified microglia). P2X4 quantification employed the analysis of spinal cord slices, including the injury epicenter, by calculating the percentage of P2X4+ staining/total spinal area for each animal, as represented in **Figure 6E**.

Analysis of NeuN+ Cell Gap

The distance between NeuN+ cells across the injury site was measured to evaluate the sparsity of neurons caused by SCI. Additionally, the number of NeuN+ cells in tissue ranges of 2 mm from the injury epicenter towards rostral or caudal was counted, and the total number of NeuN+ cells detected in each range per animal was calculated. The heat map representation in **Figure 6G** shows the mean value per group. Twelve spinal cord slices per animal in a central range of -252 to + 210 microns from dorsal to ventral, including the central canal (0).

Statistical Analyses

Bar plots are represented as mean \pm standard error mean (SEM), and data were statistically analysed by Graph Pad Prism Software. First, the normality test Shapiro-Wilk was performed to test for the Gaussian distribution of each data set. If normality was met, homoscedasticity was evaluated using Bartlett's test. Heat maps, clustering graphics, and dot plots were generated with R. Comparisons between two groups used a one-tailed t-test with a confidence level of 95%. Comparisons between more than two groups were performed using a one-way ANOVA and Bonferroni's post-test for normal and homoscedastic data sets. If normality was not met, Kruskal-Wallis One-way ANOVA with Dunn's method or Tukey test post hoc correction was used. In the case of repeated

measurements per variable, a nested ANOVA was performed. In the case of repeated measurement throughout the spinal depth, we used a two-way ANOVA and Tukey post-test.

Acknowledgments

The authors would like to thank Dr Vicente Felipo for his scientific discussion and suggestions, Maravillas Mellado for her technical support in molecular analysis, and Stuart P. Atkinson for English editing. This research was funded by FEDER/Ministerio de Ciencia e Innovación – Agencia Estatal de Investigación [RTI2018-095872-B-C21/ERDF]. Part of the equipment employed in this work was funded by Generalitat Valenciana and cofinanced with ERDF funds (OP ERDF of Comunitat Valenciana 2014–2020) and the UE; Fondo Europeo de Desarrollo Regional (FEDER) incluido en el Programa Operativo FEDER de la Comunidad Valenciana 2014-2020. B. Martinez-Rojas was supported by a grant from the Conselleria de Educació, Investigació, Cultura y Deporte de la Generalitat Valenciana and the European Social Fundation ACIF/2019/120.

Competing Interests

The authors have no relevant financial or non-financial interests to disclose.

Author Contributions:

B. Martinez-Rojas: CHA

E. Giraldo: Data curation; Writing - review & editing; Supervision

R. Grillo-Risco, F. García-García, M.R. Hidalgo, E. Lopez Mocholi, A. Alastrue: Methodology; Data curation; Formal analysis

V. Moreno-Manzano: Conceptualization; Data curation; Formal analysis; Writing - original draft; Writing - review & editing; Funding acquisition; Supervision; Project administration

Data Availability

The data that support the findings of this study are available on request from the corresponding author. The protocol and the raw and normalized data were deposited in the GEO for open access at

<https://www.ncbi.nlm.nih.gov/geo/query/acc.cgi?acc=GSE183591>, with the accession number GSE183591.

Ethics approval

The maintenance and use of all animals were in accordance with guidelines established by the European Communities Council Directive (86/609/ECC) and the Spanish Royal Decree 53/2013. All experimental procedures were approved by the Animal Care and Use Committee of the Research Institute Prince Felipe (2021/VSC/PEA/0032).

Consent to participate

Informed consent was obtained from all individual participants included in the study.

Supplementary material and online resources:

The following are available online at <https://link.springer.com/article/10.1007/s00018-022-04494-w#Sec27> : Online Resource File 1: Interactive heatmaps corresponding to Figures 2A, 3B, and 4D; Online Resource Table 1: DEG file; Online Resource Table 2: Sets of DEGs from Venn diagram intersections; Online Resource Table 3: Temporal clustering of altered biological functions; Online Resource Table 4: GO terms altered by NPC transplantation; Online Resource Table 5: Primer sequences; Online Resource Figure 1: Cumulative number of DEGs during SCI progression; Online Resource Figure 2: Temporal clusters of altered biological functions after SCI; Online Resource Figure 3: Venn diagram depicting DEGs impacted by acute and subacute NPC transplantation; Online Resource Figure 4: Highlighted GO terms altered by NPC transplantation; Online Resource Figure 5: EPAC2 staining in B-III-Tubulin positive somas

References

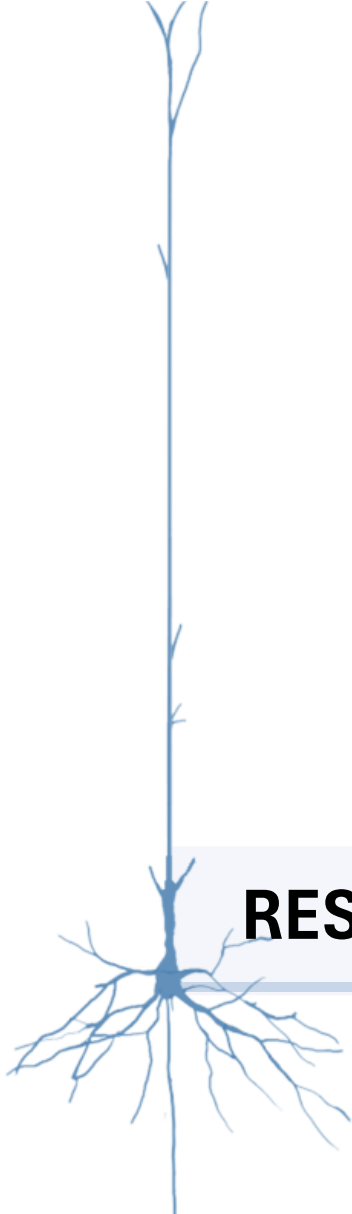
1. Ahuja, C.S., et al., *Traumatic Spinal Cord Injury-Repair and Regeneration*. Neurosurgery, 2017. **80**(3S): p. S9-S22.
2. Sofroniew, M.V., *Dissecting spinal cord regeneration*. Nature, 2018. **557**(7705): p. 343-350.
3. Assinck, P., et al., *Cell transplantation therapy for spinal cord injury*. Nat Neurosci, 2017. **20**(5): p. 637-647.
4. Jin, Y., et al., *Transplantation of neural progenitor cells in chronic spinal cord injury*. Neuroscience, 2016. **320**: p. 69-82.
5. Lane, M.A., A.C. Lepore, and I. Fischer, *Improving the therapeutic efficacy of neural progenitor cell transplantation following spinal cord injury*. Expert Rev Neurother, 2017. **17**(5): p. 433-440.
6. Pfeifer, K., et al., *Adult neural progenitor cells provide a permissive guiding substrate for corticospinal axon growth following spinal cord injury*. Eur J Neurosci, 2004. **20**(7): p. 1695-704.
7. Moreno-Manzano, V., et al., *Activated spinal cord ependymal stem cells rescue neurological function*. Stem Cells, 2009. **27**(3): p. 733-43.
8. Ogawa, Y., et al., *Transplantation of in vitro-expanded fetal neural progenitor cells results in neurogenesis and functional recovery after spinal cord contusion injury in adult rats*. J Neurosci Res, 2002. **69**(6): p. 925-33.

9. Bonner, J.F. and O. Steward, *Repair of spinal cord injury with neuronal relays: From fetal grafts to neural stem cells*. Brain Res, 2015. **1619**: p. 115-23.
10. Sankavaram, S.R., et al., *Adult Neural Progenitor Cells Transplanted into Spinal Cord Injury Differentiate into Oligodendrocytes, Enhance Myelination, and Contribute to Recovery*. Stem Cell Reports, 2019. **12**(5): p. 950-966.
11. Mao, Y., K. Mathews, and C.A. Gorrie, *Temporal Response of Endogenous Neural Progenitor Cells Following Injury to the Adult Rat Spinal Cord*. Front Cell Neurosci, 2016. **10**: p. 58.
12. Nagoshi, N., et al., *Human Spinal Oligodendrogenic Neural Progenitor Cells Promote Functional Recovery After Spinal Cord Injury by Axonal Remyelination and Tissue Sparing*. Stem Cells Transl Med, 2018. **7**(11): p. 806-818.
13. Lepore, A.C. and I. Fischer, *Lineage-restricted neural precursors survive, migrate, and differentiate following transplantation into the injured adult spinal cord*. Exp Neurol, 2005. **194**(1): p. 230-42.
14. Lu, P., et al., *Neural stem cells constitutively secrete neurotrophic factors and promote extensive host axonal growth after spinal cord injury*. Exp Neurol, 2003. **181**(2): p. 115-29.
15. Schizas, N., et al., *Neural crest stem cells protect spinal cord neurons from excitotoxic damage and inhibit glial activation by secretion of brain-derived neurotrophic factor*. Cell Tissue Res, 2018. **372**(3): p. 493-505.
16. Karova, K., et al., *Transplantation of neural precursors generated from spinal progenitor cells reduces inflammation in spinal cord injury via NF-kappaB pathway inhibition*. J Neuroinflammation, 2019. **16**(1): p. 12.
17. Butti, E., et al., *Subventricular zone neural progenitors protect striatal neurons from glutamatergic excitotoxicity*. Brain, 2012. **135**(Pt 11): p. 3320-35.
18. Geranmayeh, M.H., et al., *Paracrine Neuroprotective Effects of Neural Stem Cells on Glutamate-Induced Cortical Neuronal Cell Excitotoxicity*. Adv Pharm Bull, 2015. **5**(4): p. 515-21.
19. Lau, B.Y., et al., *Cyclic AMP promotes axon regeneration, lesion repair and neuronal survival in lampreys after spinal cord injury*. Exp Neurol, 2013. **250**: p. 31-42.
20. Pearse, D.D., et al., *cAMP and Schwann cells promote axonal growth and functional recovery after spinal cord injury*. Nat Med, 2004. **10**(6): p. 610-6.
21. Cai, D., et al., *Neuronal cyclic AMP controls the developmental loss in ability of axons to regenerate*. J Neurosci, 2001. **21**(13): p. 4731-9.
22. Macks, C., et al., *Rolipram-Loaded Polymeric Micelle Nanoparticle Reduces Secondary Injury after Rat Compression Spinal Cord Injury*. J Neurotrauma, 2018. **35**(3): p. 582-592.
23. Peace, A.G. and D.A. Shewan, *New perspectives in cyclic AMP-mediated axon growth and guidance: The emerging epoch of Epac*. Brain Res Bull, 2011. **84**(4-5): p. 280-8.
24. Guijarro-Belmar, A., et al., *Epac2 Elevation Reverses Inhibition by Chondroitin Sulfate Proteoglycans In Vitro and Transforms Postlesion Inhibitory Environment to Promote Axonal Outgrowth in an Ex Vivo Model of Spinal Cord Injury*. J Neurosci, 2019. **39**(42): p. 8330-8346.
25. Nikulina, E., et al., *The phosphodiesterase inhibitor rolipram delivered after a spinal cord lesion promotes axonal regeneration and functional recovery*. Proc Natl Acad Sci U S A, 2004. **101**(23): p. 8786-90.
26. Kajana, S. and H.G. Goshgarian, *Systemic administration of rolipram increases medullary and spinal cAMP and activates a latent respiratory motor pathway after high cervical spinal cord injury*. J Spinal Cord Med, 2009. **32**(2): p. 175-82.
27. Xia, T., et al., *The combination of db-cAMP and ChABC with poly(propylene carbonate) microfibers promote axonal regenerative sprouting and functional recovery after spinal cord hemisection injury*. Biomed Pharmacother, 2017. **86**: p. 354-362.

28. Nout, Y.S., et al., *Glial restricted precursor cell transplant with cyclic adenosine monophosphate improved some autonomic functions but resulted in a reduced graft size after spinal cord contusion injury in rats*. *Exp Neurol*, 2011. **227**(1): p. 159-71.
29. Bretzner, F., et al., *Combination of olfactory ensheathing cells with local versus systemic cAMP treatment after a cervical rubrospinal tract injury*. *J Neurosci Res*, 2010. **88**(13): p. 2833-46.
30. Lu, P., et al., *Combinatorial therapy with neurotrophins and cAMP promotes axonal regeneration beyond sites of spinal cord injury*. *J Neurosci*, 2004. **24**(28): p. 6402-9.
31. Gong, L., et al., *Changes in transcriptome profiling during the acute/subacute phases of contusional spinal cord injury in rats*. *Ann Transl Med*, 2020. **8**(24): p. 1682.
32. Anjum, A., et al., *Spinal Cord Injury: Pathophysiology, Multimolecular Interactions, and Underlying Recovery Mechanisms*. *Int J Mol Sci*, 2020. **21**(20).
33. Li, X., et al., *Comparison of subacute and chronic scar tissues after complete spinal cord transection*. *Exp Neurol*, 2018. **306**: p. 132-137.
34. Hidalgo, M.R., et al., *High throughput estimation of functional cell activities reveals disease mechanisms and predicts relevant clinical outcomes*. *Oncotarget*, 2017. **8**(3): p. 5160-5178.
35. Sangsiri, S., et al., *Spinal cord injury alters purinergic neurotransmission to mesenteric arteries in rats*. *Am J Physiol Heart Circ Physiol*, 2020. **318**(2): p. H223-H237.
36. Nolan, J.K., et al., *Ex vivo electrochemical measurement of glutamate release during spinal cord injury*. *MethodsX*, 2019. **6**: p. 1894-1900.
37. Li, S. and P.K. Stys, *Mechanisms of ionotropic glutamate receptor-mediated excitotoxicity in isolated spinal cord white matter*. *J Neurosci*, 2000. **20**(3): p. 1190-8.
38. Tapia, V.S., M. Herrera-Rojas, and J. Larrain, *JAK-STAT pathway activation in response to spinal cord injury in regenerative and non-regenerative stages of *Xenopus laevis**. *Regeneration (Oxf)*, 2017. **4**(1): p. 21-35.
39. Herrmann, J.E., et al., *STAT3 is a critical regulator of astrogliosis and scar formation after spinal cord injury*. *J Neurosci*, 2008. **28**(28): p. 7231-43.
40. Bareyre, F.M., et al., *In vivo imaging reveals a phase-specific role of STAT3 during central and peripheral nervous system axon regeneration*. *Proc Natl Acad Sci U S A*, 2011. **108**(15): p. 6282-7.
41. Wang, T., et al., *The role of the JAK-STAT pathway in neural stem cells, neural progenitor cells and reactive astrocytes after spinal cord injury*. *Biomed Rep*, 2015. **3**(2): p. 141-146.
42. Bachmann, L.C., et al., *Sprouting of brainstem-spinal tracts in response to unilateral motor cortex stroke in mice*. *J Neurosci*, 2014. **34**(9): p. 3378-89.
43. Adibhatla, R.M. and J.F. Hatcher, *Altered lipid metabolism in brain injury and disorders*. *Subcell Biochem*, 2008. **49**: p. 241-68.
44. Kim, J.H., et al., *Changes in cholesterol biosynthetic and transport pathways after excitotoxicity*. *J Neurochem*, 2010. **112**(1): p. 34-41.
45. Ong, W.Y., et al., *Changes in brain cholesterol metabolome after excitotoxicity*. *Mol Neurobiol*, 2010. **41**(2-3): p. 299-313.
46. Lewis, A.E., R. Aesoy, and M. Bakke, *Role of EPAC in cAMP-Mediated Actions in Adrenocortical Cells*. *Front Endocrinol (Lausanne)*, 2016. **7**: p. 63.
47. Ma, T.C., et al., *cAMP-responsive element-binding protein (CREB) and cAMP co-regulate activator protein 1 (AP1)-dependent regeneration-associated gene expression and neurite growth*. *J Biol Chem*, 2014. **289**(47): p. 32914-25.
48. Garraway, S.M. and J.R. Huie, *Spinal Plasticity and Behavior: BDNF-Induced Neuromodulation in Uninjured and Injured Spinal Cord*. *Neural Plast*, 2016. **2016**: p. 9857201.
49. Chen, T., et al., *Brain-Derived Neurotrophic Factor Increases Synaptic Protein Levels via the MAPK/Erk Signaling Pathway and Nrf2/Trx Axis Following the Transplantation of*

- Neural Stem Cells in a Rat Model of Traumatic Brain Injury*. *Neurochem Res*, 2017. **42**(11): p. 3073-3083.
50. Fernandez, E., et al., *DARPP-32 is a robust integrator of dopamine and glutamate signals*. *PLoS Comput Biol*, 2006. **2**(12): p. e176.
 51. Pereira, L., et al., *The cAMP binding protein Epac modulates Ca²⁺ sparks by a Ca²⁺/calmodulin kinase signalling pathway in rat cardiac myocytes*. *J Physiol*, 2007. **583**(Pt 2): p. 685-94.
 52. Bavencoffe, A., et al., *Persistent Electrical Activity in Primary Nociceptors after Spinal Cord Injury Is Maintained by Scaffolded Adenylyl Cyclase and Protein Kinase A and Is Associated with Altered Adenylyl Cyclase Regulation*. *J Neurosci*, 2016. **36**(5): p. 1660-8.
 53. Zhou, Z., et al., *Photoactivated adenylyl cyclase (PAC) reveals novel mechanisms underlying cAMP-dependent axonal morphogenesis*. *Sci Rep*, 2016. **5**: p. 19679.
 54. Fernandes, H.B., et al., *Epac2 Mediates cAMP-Dependent Potentiation of Neurotransmission in the Hippocampus*. *J Neurosci*, 2015. **35**(16): p. 6544-53.
 55. Seo, H. and K. Lee, *Epac2 contributes to PACAP-induced astrocytic differentiation through calcium ion influx in neural precursor cells*. *BMB Rep*, 2016. **49**(2): p. 128-33.
 56. Seo, H. and K. Lee, *Cell-specific expression of Epac2 in the subventricular and subgranular zones*. *Mol Brain*, 2019. **12**(1): p. 113.
 57. Fang, M., et al., *Connexin 30 Deficiency Attenuates Chronic but Not Acute Phases of Experimental Autoimmune Encephalomyelitis Through Induction of Neuroprotective Microglia*. *Front Immunol*, 2018. **9**: p. 2588.
 58. Kuo, T.T., et al., *Post-stroke Delivery of Valproic Acid Promotes Functional Recovery and Differentially Modifies Responses of Peri-Infarct Microglia*. *Front Mol Neurosci*, 2021. **14**: p. 639145.
 59. Franco, R. and D. Fernandez-Suarez, *Alternatively activated microglia and macrophages in the central nervous system*. *Prog Neurobiol*, 2015. **131**: p. 65-86.
 60. Ulmann, L., et al., *Up-regulation of P2X4 receptors in spinal microglia after peripheral nerve injury mediates BDNF release and neuropathic pain*. *J Neurosci*, 2008. **28**(44): p. 11263-8.
 61. Zhao, S.J., et al., *Bioinformatics analysis of the molecular mechanisms underlying traumatic spinal cord injury*. *Mol Med Rep*, 2018. **17**(6): p. 8484-8492.
 62. Poplawski, G.H.D., et al., *Injured adult neurons regress to an embryonic transcriptional growth state*. *Nature*, 2020. **581**(7806): p. 77-82.
 63. Kong, G., et al., *AMPK controls the axonal regenerative ability of dorsal root ganglia sensory neurons after spinal cord injury*. *Nat Metab*, 2020. **2**(9): p. 918-933.
 64. Sathyamurthy, A., et al., *Massively Parallel Single Nucleus Transcriptional Profiling Defines Spinal Cord Neurons and Their Activity during Behavior*. *Cell Rep*, 2018. **22**(8): p. 2216-2225.
 65. Phay, M., H.H. Kim, and S. Yoo, *Dynamic Change and Target Prediction of Axon-Specific MicroRNAs in Regenerating Sciatic Nerve*. *PLoS One*, 2015. **10**(9): p. e0137461.
 66. Matsuoka, I. and S. Ohkubo, *ATP- and adenosine-mediated signaling in the central nervous system: adenosine receptor activation by ATP through rapid and localized generation of adenosine by ecto-nucleotidases*. *J Pharmacol Sci*, 2004. **94**(2): p. 95-9.
 67. Prezeau, L., et al., *Characterization of a metabotropic glutamate receptor: direct negative coupling to adenylyl cyclase and involvement of a pertussis toxin-sensitive G protein*. *Proc Natl Acad Sci U S A*, 1992. **89**(17): p. 8040-4.
 68. Oka, M., et al., *Involvement of metabotropic glutamate receptors in Gi- and Gs-dependent modulation of adenylyl cyclase activity induced by a novel cognition enhancer NS-105 in rat brain*. *Brain Res*, 1997. **754**(1-2): p. 121-30.
 69. Qiu, J., et al., *Spinal axon regeneration induced by elevation of cyclic AMP*. *Neuron*, 2002. **34**(6): p. 895-903.

70. Hannila, S.S. and M.T. Filbin, *The role of cyclic AMP signaling in promoting axonal regeneration after spinal cord injury*. *Exp Neurol*, 2008. **209**(2): p. 321-32.
71. Neumann, S., et al., *Regeneration of sensory axons within the injured spinal cord induced by intraganglionic cAMP elevation*. *Neuron*, 2002. **34**(6): p. 885-93.
72. Jin, L.Q., et al., *Axon regeneration in the absence of growth cones: acceleration by cyclic AMP*. *J Comp Neurol*, 2009. **515**(3): p. 295-312.
73. Pale, T., E.B. Frisch, and A.D. McClellan, *Cyclic AMP stimulates neurite outgrowth of lamprey reticulospinal neurons without substantially altering their biophysical properties*. *Neuroscience*, 2013. **245**: p. 74-89.
74. Lin, C.C., et al., *The Therapeutic Effectiveness of Delayed Fetal Spinal Cord Tissue Transplantation on Respiratory Function Following Mid-Cervical Spinal Cord Injury*. *Neurotherapeutics*, 2017. **14**(3): p. 792-809.
75. de Rooij, J., et al., *Mechanism of regulation of the Epac family of cAMP-dependent RapGEFs*. *J Biol Chem*, 2000. **275**(27): p. 20829-36.
76. Falnikar, A., K. Li, and A.C. Lepore, *Therapeutically targeting astrocytes with stem and progenitor cell transplantation following traumatic spinal cord injury*. *Brain Res*, 2015. **1619**: p. 91-103.
77. Wu, H.M., et al., *Microglial activation mediates host neuronal survival induced by neural stem cells*. *J Cell Mol Med*, 2014. **18**(7): p. 1300-12.
78. Gomez-Villafuertes, R., et al., *Purinergic Receptors in Spinal Cord-Derived Ependymal Stem/Progenitor Cells and Their Potential Role in Cell-Based Therapy for Spinal Cord Injury*. *Cell Transplant*, 2015. **24**(8): p. 1493-509.
79. Tsuda, M., et al., *P2X4 receptors and neuropathic pain*. *Front Cell Neurosci*, 2013. **7**: p. 191.
80. Zhang, L., et al., *Inhibition of Epac2 Attenuates Neural Cell Apoptosis and Improves Neurological Deficits in a Rat Model of Traumatic Brain Injury*. *Front Neurosci*, 2018. **12**: p. 263.
81. Guijarro-Belmar, A., et al., *The therapeutic potential of targeting exchange protein directly activated by cyclic adenosine 3',5'-monophosphate (Epac) for central nervous system trauma*. *Neural Regen Res*, 2021. **16**(3): p. 460-469.
82. Onifer, S.M., A.G. Rabchevsky, and S.W. Scheff, *Rat models of traumatic spinal cord injury to assess motor recovery*. *ILAR J*, 2007. **48**(4): p. 385-95.
83. Walker, C.L., et al., *Functional and Histological Gender Comparison of Age-Matched Rats after Moderate Thoracic Contusive Spinal Cord Injury*. *J Neurotrauma*, 2019. **36**(12): p. 1974-1984.
84. Alastrue-Agudo, A., et al., *FM19G11 and Ependymal Progenitor/Stem Cell Combinatory Treatment Enhances Neuronal Preservation and Oligodendrogenesis after Severe Spinal Cord Injury*. *Int J Mol Sci*, 2018. **19**(1).
85. Giraldo, E., et al., *A rationally designed self-immolative linker enhances the synergism between a polymer-rock inhibitor conjugate and neural progenitor cells in the treatment of spinal cord injury*. *Biomaterials*, 2021. **276**: p. 121052.
86. Bolstad, B.M., et al., *A comparison of normalization methods for high density oligonucleotide array data based on variance and bias*. *Bioinformatics*, 2003. **19**(2): p. 185-93.
87. Ritchie, M.E., et al., *limma powers differential expression analyses for RNA-sequencing and microarray studies*. *Nucleic Acids Res*, 2015. **43**(7): p. e47.
88. Requejo-Aguilar, R., et al., *Combined polymer-curcumin conjugate and ependymal progenitor/stem cell treatment enhances spinal cord injury functional recovery*. *Biomaterials*, 2017. **113**: p. 18-30.



RESULTS: CHAPTER 2

CHAPTER 2: Stimulation of corticospinal neurons by optogenetic cAMP inductions promotes motor recovery via raphespinal tract modulation.

The content of this chapter is under final preparation to be soon submitted for evaluation and publication under the following reference:

Stimulation of corticospinal neurons by optogenetic cAMP inductions promotes motor recovery after spinal cord injury via raphespinal tract modulation.

Martinez-Rojas B, Giraldo E, López-Mocholi E, Alastrue-Agudo A, Paniagua G, Pedraza M, Sonia Hingorani Jai Prakash, Rost BR, Javier Monreal Trigo, Alcaniz Filloi M, Andrade-Talavera Y, Rodríguez-Moreno A and Moreno-Manzano V.

In this research article, I have contributed in the conceptualization of the working hypothesis, the design of the theoretical framework, the development of the experimental work as well as the collection, analysis and interpretation of the data (always with the help of the technical staff, my thesis supervisors and collaborators). Also, I have generated the original draft of the manuscript, figures and supplementary material.

STIMULATION OF CORTICOSPINAL NEURONS BY OPTOGENETIC cAMP INDUCTIONS PROMOTES MOTOR RECOVERY VIA RAPHESPINAL TRACT MODULATION.

Martínez Rojas B^{1,2}, Giraldo E^{1,2}, Lopez-Mocholi E¹, Alastrue A¹, Paniagua G¹, Pedraza M¹, Hingorani Jai Prakash S^{1,2}, Monreal Trigo J³, Alcaniz Filloi M³, Ros BR⁴, Andrade-Talavera Y⁵, Rodríguez-Moreno A⁵ and Victoria Moreno-Manzano^{1,2}

¹Neuronal and Tissue Regeneration Laboratory, Centro de Investigación Príncipe Felipe, E-46012 Valencia, Spain

²Department of Biotechnology, Universitat Politècnica de València, Valencia, Spain

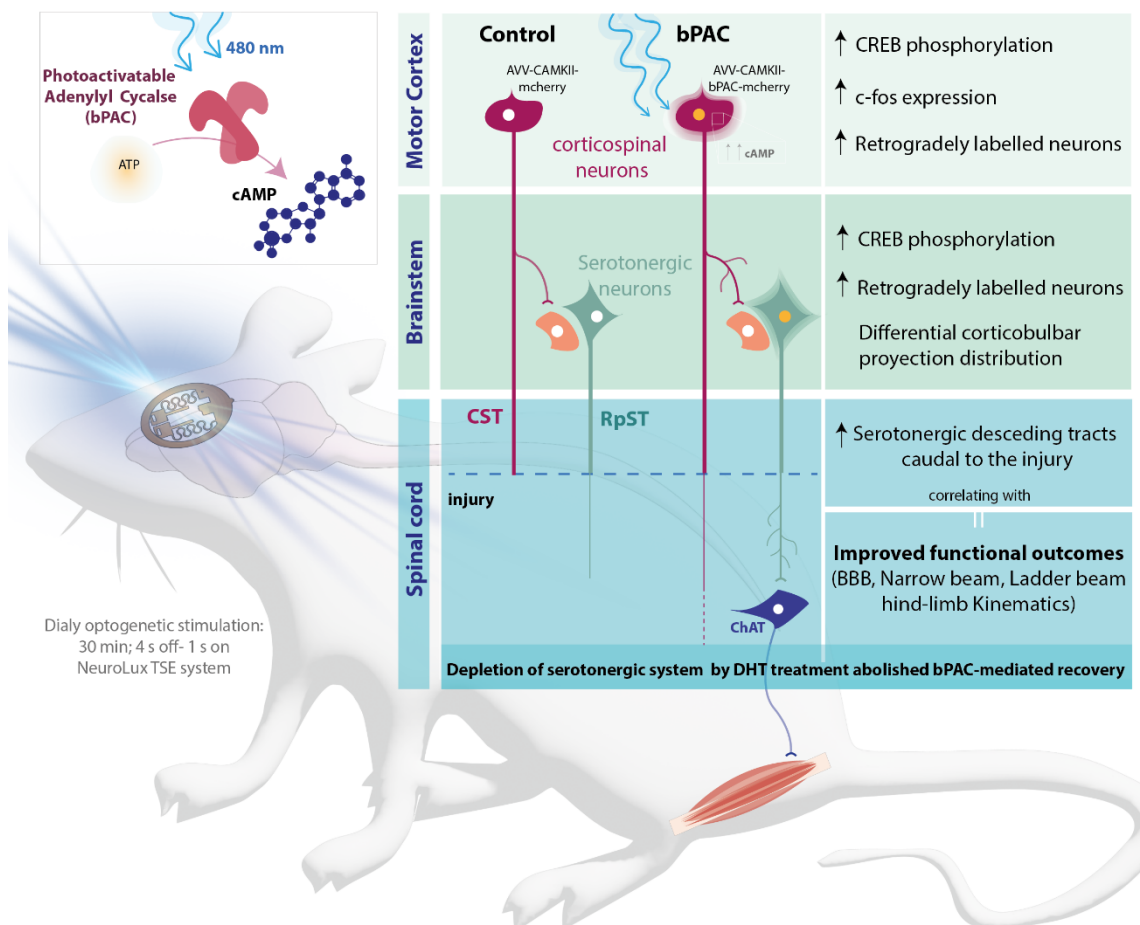
³UPV-CIPF Joint Research Unit Disease Mechanisms and Nanomedicine, Centro de Investigación Príncipe Felipe, 46012 Valencia, Spain

⁴German Center for Neurodegenerative Diseases (DZNE), Berlin, Germany

⁵Laboratory of Cellular Neuroscience and Plasticity, Department of Physiology, Anatomy and Cell Biology, University Pablo de Olavide, 41013 Seville, Spain.

*Corresponding author. Email: vmorenom@cipf.es; ORCID: **0000-0002-6035-9491**

Keywords: cAMP, bPAC, spinal cord injury, optogenetics, corticospinal tract, serotonergic tract.



ABSTRACT:

Cyclic adenosine monophosphate (cAMP) has emerged as a pivotal inductor of CNS regeneration. Inconveniently, cAMP levels exhibit a dramatic decline within the spinal cord, brain stem, and motor cortex following spinal cord injury (SCI). Here we propose daily optogenetic cAMP inductions in corticospinal neurons after SCI to address the regeneration failure after injury. We developed a novel strategy involving the adenoviral delivery of photoinducible adenylyl cyclase (bPAC) into corticospinal neurons followed by wireless daily blue light stimulation of motor cortex in living rats. Daily optogenetic cAMP stimulation in rats subjected to thoracic dorsal hemisection results in early and sustained locomotor recovery when compared to non-treated controls. bPAC stimulated rats display increased number of retrogradely traced neurons from the lumbar segment both in the motor cortex and the raphe-reticular formation, but not in the red nuclei. Intriguingly, the immunolabeling of the raphespinal tract with 5-hydroxytryptamine (5-HT) reveals that bPAC stimulation increased the ratio of descending serotonergic axons caudal to the injury site, a change that significantly correlates with enhanced functional outcomes. Insights gleaned from our studies into corticobulbar projection, WGA trans-synaptic tracing, and P-CREB analysis suggest that bPAC influence over the serotonergic pathway might take place at the brainstem level. Notably, depleting the serotonergic system through the administration of 5,7-Dihydroxytryptamine abrogates bPAC-mediated recovery, reinforcing the pivotal role of the serotonergic tract in bPAC-mediated functional improvement. Overall, our findings underscored the efficacy of cAMP elevation in corticospinal neurons in mediating functional recovery and allowed to unveil a cortical rerouting pathway via the serotonergic descending tract.

INTRODUCTION

During the process of walking the brain send executive commands through descending tracts into the spinal cord where they synapse with interneurons or motor neurons that engage the target muscle [1]. Spinal cord injury disrupts this sophisticated array of connections depriving lower spinal neurons of supraspinal inputs that, ultimately, render them non-functional [2] and results in dramatic locomotor deficits [3].

The corticospinal tract (CST) represents the most relevant supraspinal descending pathway for the motor control due to its functional relevance in controlling skilled voluntary movements in humans, especially finger dexterity[4]. The CST originates from pyramidal neurons in layer V of the sensory-motor cortex, raising bundles of corticospinal axons that travel down the brain. While most axons (95%) decussate before entering the dorsal funiculus in the rat spinal cord [5], a small percentage (5%) do not and run along

the ventral and lateral funiculus [6]. Apart from the motor cortex, other phylogenetically older motor centers of the brain also directly connect to the spinal cord as well [7]. Within the brainstem, neurons located in the gigantocellular nucleus (Gi), the lateral paragigantocellular nuclei (LPGi) and the ventral gigantocellular nuclei (VGi or GiA) of the reticular formation originate the reticulospinal tract (RtST) descending through the ventral and lateral funiculus of the spinal cord [8-10]. In close anatomic proximity, the serotonergic tract (the major component of the raphespinal tract, RpST) arises from the serotonergic cells distributed in the caudal raphe nuclei, including the raphe magnus, pallidus and obscurus but also scattered through the reticular formation [11]. Given that the term 'reticular formation' refers to a complex network of hundreds of nuclei, and their diffuse anatomical boundaries, there exists certain inconsistency in nomenclature of RtST and RpST, with some authors including the raphespinal system within the broader category of reticulospinal pathways [9, 12, 13]. Of note, neurons of the layer V of the motor cortex also send cortico-bulbar projections to the brainstem, delineating an alternative indirect pathway to the spinal cord [14, 15].

After SCI, the CST is especially reluctant to axonal regeneration and shortly after the injury corticospinal axons form retracting bulbs and dieback from the lesion site [16, 17]. Promising therapies using bioactive biomaterials [18], modulators of the non-permissive matrix [19], trophic support [20], cell transplantation [21] or a combination hereof [22], have achieved varying degrees of CST axonal outgrowth into the injury site; however long-distance CST elongation remains inconceivable and there is scarcely any future optimism in this regard.

Luckily, new evidences have suggested that CST sparing below the injury level is not strictly required to recover cortical control over leg motor neurons [23]. CST regeneration across the injury represents only one means for cortical commands to reach sublesional areas after SCI [24]. In fact, alternative naturally occurring plastic mechanisms are putative to accomplish this purpose; for example, supraspinal CST sprouting to contact propriospinal neurons [25] with spared connections caudal to the injury or cortico-brainstem rewiring [26] represent validated mechanisms to reroute the cortical networks bypassing the injury. Thus, the field has recently faced a new paradigm shift towards therapies focused on exploiting the potential of spare tracts by promoting their plasticity via neuromodulation, leaving behind the conventional focus on injury containment, cell replacement or damaged fiber regeneration. In that context, neuromodulatory therapies mediated by either electrical [27], optogenetical [28], chemogenetical [29] or magnetical [30] means and applied at cortical, deep-brain or spinal levels have proven to be effective in promoting functional recovery after SCI in animal models, shedding light into the

circuits critical for functional recovery in humans. Excitingly, neuromodulatory therapies have already been successfully translated into human patients [31, 32].

In the present study we ought to explore the therapeutic potential of neuromodulation of corticospinal neurons by dialy cyclic adenosine monophosphate (cAMP) inductions after SCI. Our therapeutical approach takes inspiration from the conditioning lesion effect: cAMP levels triple in dorsal root ganglion (DRG) neurons one day after a conditioning lesion which confers a state of regenerative competence to the central (spinal) branch when consecutively injured. This transient boost in cAMP levels is sufficient activate DRG ability to in vitro overcome myelin associated proteins even when cAMP levels have returned to normality, what suggest the induction of a transcription-dependent mechanism [33, 34]. Moreover, injecting a cAMP analog (db-cAMP) into the DRG before the spinal lesion completely simulates the conditioning lesion effect and promotes dorsal column axon regeneration to a comparable extent of what is achieved with a conditioning injury. These findings suggest that the cAMP increase derived from conditioning lesion allows the of the acquisition of a growth-competent state after the peripheral injury [34]. However, cAMP does not naturally increase in central neurons after a CNS injury; whitin 1-day post-SCI cAMP levels sustainably dropped by 64.3%, 69.7% and 68.1% in the spinal cord, sensorimotor cortex and brainstem, respectively [35]. Thus, we propose artificial cAMP inductions in corticospinal neurons to mimic the conditioning lesion effect and trigger regeneration after SCI.

In the past decades, cAMP therapies have made use of intraspinal or intrathecal infusion of analogs [36], adenylate cyclases activators [37], or phosphodiesterase inhibitors [38], providing limited and off-target effects but still yielding promising results in terms of functional recovery [35, 39]. Recent advances in molecular biology have enabled the applicability of powerful tools to increase cAMP levels in vivo, including the photoactivatable adenylate cyclase (PAC). PAC (extracted from the soil bacterium *Beggiatoa*, bPAC) is a homodimeric protein containing a BLUF domain, which display sensitivity to blue light stimulation, linked to an adenylate cyclase domain [40]. Compared to other proteins of its family, its small size, low dark activity and high efficiency light activity (yielding a ~300-fold increase upon illumination) make bPAC the preferred option [40, 41]. However, bPAC's residual dark activity might raise resting cAMP levels [42], an essential consideration for the designing appropriate negative controls. In CNS damage research, Xiao et al. previously applied bPAC in vivo in Zebrafish model revealing that afferent neurons displayed significantly enhanced axonal regeneration following axotomy, which reinnervated their original target area, upon bPAC

stimulation [43]. This discovery serves as a solid basis for our willingness to implement bPAC into mammalian SCI models

Here, we hypothesized that the cAMP-mediated stimulation of corticospinal projecting neurons would trigger a regeneration, facilitating neuroplastic changes of the CST and ultimately leading to improvements in locomotor function. Therefore, we developed an optogenetic inducible system for on-demand cAMP induction in vivo, studied the functional effects of daily cortical bPAC-stimulated cAMP induction on locomotor outcomes in SCI rats (subjected to dorsal hemisection injuries that ultimately damage the dorsal aspect of the CST), and investigated the anatomical basis of bPAC-mediated functional recovery. Overall, our study revealed the effectiveness of using bPAC to induce cAMP in corticospinal neurons for the purpose of restoring locomotor function after SCI through the serotonergic descending pathway.

RESULTS

bPAC stimulation increased cAMP in vitro and induced P-CREB and c-FOS in vivo.

To validate the CAMKII-bPAC-mCherry adenoviral construct used to deliver the expression of bPAC protein, we first measured cAMP levels in cultured cortical neurons extracted from E14.5 fetal rats transduced with either CAMKII-bPAC-mCherry (bPAC) or CAMKII-mCherry (Control). Saturating blue light exposure (480 nm, 90 s, 20 mW/cm²) [41] successfully prompted a 14-fold increase of cAMP levels measured in total extracts of bPAC neurons compare to control (**Figure 1A**).

To implement the bPAC optogenetic system in vivo, bPAC expression was delivered into corticospinal neurons by stereotaxic injection of the AVV construct in the layer V of primary motor cortex. Control animals were likewise injected with the AVV control. One week after, a wireless stimulation device was implanted (**Figure 1B**) and the dorsal hemisection was induced. Considering that cAMP increases lead to CREB phosphorylation, we assessed P-CREB after ten days of optogenetic stimulation (30 min/day, 1 s ON- 4 s OFF). As expected, bPAC animals displayed widespread P-CREB staining within the primary motor cortex, significantly induced compare to control, indicating the suitability of the optogenetic system for inducing cAMP signaling in vivo within the cortex (**Figure 1C**). cAMP elevations have been largely related to increased neuronal activation, with previous studies reporting transient neuronal hyperactivation after bPAC-mediated cAMP elevation in the hippocampus at the CA1 region [43]. In agreement, we detected a significant increase in c-Fos (marker of neuronal activity) in bPAC stimulated animals specifically in layer IV and V of the motor cortex (**Figure 1D**).

These results indicate that the daily in vivo bPAC-stimulated cAMP induction in the motor cortex of SCI rats results in induced CREB phosphorylation and neuronal activation of corticospinal neurons.

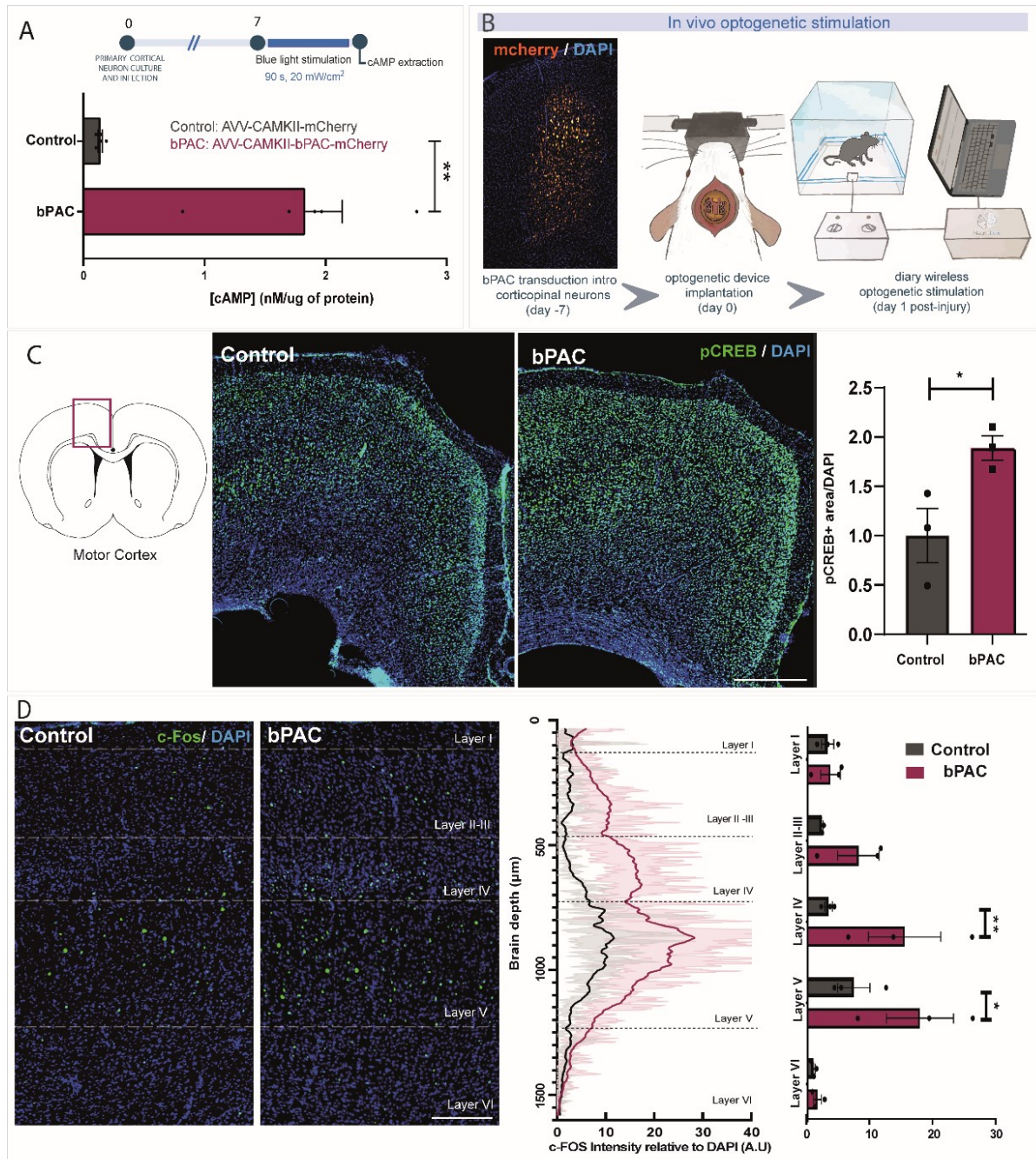


Figure 1: bPAC stimulation increased cAMP in primary cultures of cortical neurons and induced P-CREB and c-FOS in SCI rats motor cortex. (A) cAMP measurements by high-performance liquid chromatography -chromatography in control (grey) or bPAC (magenta) cultured cortical neurons after saturating blue light exposure (90 s, 20 mW/cm²) relativized to total protein contents. (B) Experimental schema describing the in vivo application of the bPAC strategy. (C) representative images (left) and analysis (right) of the effect of bPAC stimulation on CREB phosphorylation in the motor cortex, 10 days after dorsal hemisection. Scale bar: 500 μm (D)

representative images of the c-fos immunostaining across cortical layers and its quantification (right). Scale bar:200µm

bPAC stimulation in the corticospinal neurons improved locomotor recovery after SCI

Given that cAMP is a well-established inducer of CNS regeneration [44] we hypothesized that daily cAMP elevations in corticospinal neurons could drive locomotor improvements after SCI.

The locomotor recovery of rats after receiving a thoracic dorsal hemisection was evaluated for 35 days after injury (**Figure 2A-F**). All animals gradually recovered a certain degree of locomotion during the period under study; however, bPAC animals achieved higher Basso, Beattie and Bresnahan (BBB) scores starting at day 6 and sustained through the entire period (**Figure 2B**). Specifically, bPAC rats elicited a pronounced early recovery compared to control; by day 10 after injury 100% of bPAC animals had recovered the ability to support their weight with the hind paws and perform frequent plantar stepping (BBB score ≥ 11), while only 55.5% of the control exhibited weight-bearing capacity at that time (**Figure 2B-C**) also validated by the measurement of the height of the iliac crest (**Figure 2D**)

Once the animals regained certain function, we further interrogate more skilled locomotion by evaluation of the score of injured rats when crossing through a horizontal ladder or narrow beam. bPAC animals outperformed Control rats throughout the time period under study in both tests (**Figure 2E**) being the differences statistically significant at day 6 and 10 for ladder beam and day 17, 29 and 35 for narrow beam. For finer locomotor evaluation at the end point (day 35) we assessed hindlimb joints kinematics by TSE Motorater. bPAC stimulated animals showed hip, knee and ankle angle range curves along the step cycle more similar to intact animals than control (**Figure 2F**). The computation of collected locomotor parameters in a principal component analysis revealed a clear segregation between bPAC and Control rats, which provides robust evidence of bPAC's efficacy in recovering different locomotory behaviors (**Figure 2G**).

Importantly, post-mortem injury evaluation by histological study of GFAP negative and cyst area showed no differences between control and bPAC demonstrating injury consistency among experimental groups (**supplementary Figure 1**).

To evaluate whether bPAC stimulation causes alterations in thermal hyperalgesia (as an indicator of neuropathic pain), we have performed thermal test of hind limb paws (**Figure**

2H). Our result displayed no significant difference between bPAC and Control animals, demonstrating the absence of unintended effects over nociceptive perception.

This data demonstrates that dialy optogenetic cAMP induction in corticospinal neurons after SCI results in early functional recovery and improvements in fine locomotor skills without affecting nociception.

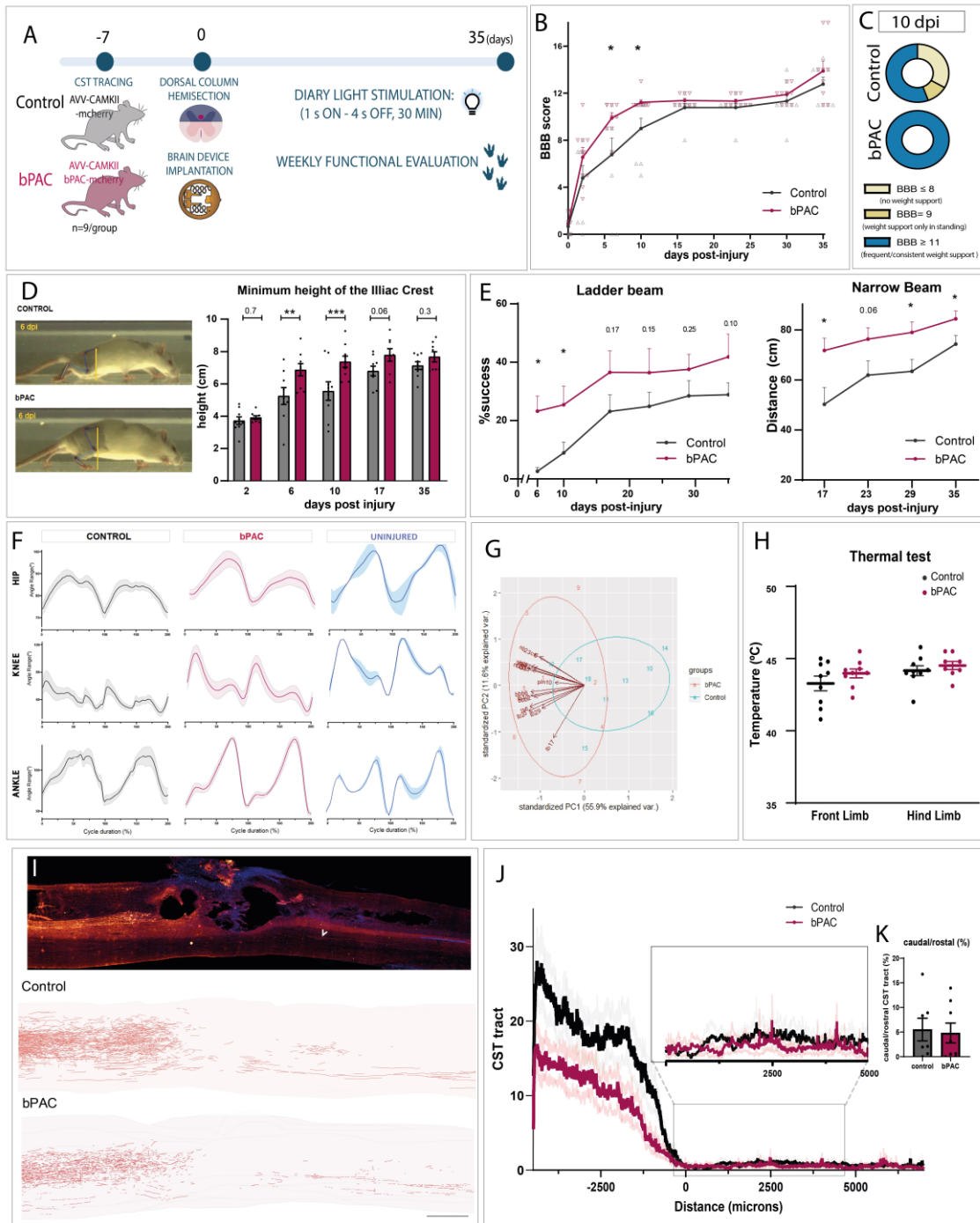


Figure 2: bPAC stimulation promotes early and sustained locomotor recovery after SCI. (A) Experimental design for a long-term (35 days) functional evaluation in control and bPAC animals after dorsal hemisection (n=9 rats/group). (B) Evaluation of the BBB scores. Multiple t-

test analysis (*, $p \leq 0.05$). (C) Pie-charts of the percentage of animals with or without weight support and plantar stepping capacity at 10 dpi (D) Measurements of the height of the iliac crest indicative of their weight-bearing capacity. Fisher's LSD comparison test (**, $p \leq 0.01$; ***, $p \leq 0.001$). (E) Performance of bPAC and control animals in ladder (left) and narrow (right) beam tests. Fisher's LSD comparison test. (*, $p \leq 0.05$). (F) hindlimb kinematics at the end point of the experiment (35 days) of bPAC and control animals compared to uninjured as shown by the hip (top), knee (middle) and ankle (bottom) angle range. (G) Principal component analysis of the locomotor parameters showing a clear segregation between experimental groups at the end point (35 dpi) (H) Thermal test of the front paws (as an internal control) and hind paws indicating the temperature at which animals removed the paw from the thermal plate. (I) Histological analysis of the CST tract by anterograde tracing. Original images (top) and camera lucida reconstructions (bottom) of serial sagittal spinal cord slices. Scale bar: 1000 μm . (J) CST profile along the spinal cord from rostral (left side of the graph) to caudal (right). Injury epicenter is indicated by 0. (K) ratio caudal to rostral CST tract indicating that approximately 5% of the rostral tract is maintained in the caudal region without differences between experimental groups.

bPAC stimulated animals display higher numbers of labeled neurons in the motor cortex by spinal retrograde tracing.

Next, we sought to study the anatomical basis for the improvement in locomotion in bPAC animals. For that aim, CST state after SCI was evaluated by anterograde tracing by AVV1-CAMKII-mcherry (Control) or AVV9-CAMKII-bPAC-mCherry (bPAC).

Sparse CST fibers were detected caudal to the injury site in 60% of bPAC and Control animals, arising mainly from the ventral side of the CST (uninjured by the dorsal hemisection; **Figure 2H**). The other 40% of the rats showed barely detectable CST labelling caudal to the injury (**Supplementary Figure 1**), not even in the ventral tracts, possibly due to inefficient anterograde tracing or to the effect of secondary injury also damaging the ventral CST tract. The proportion of CST fibers able to cross the injury accounted only for a 5.14 ± 5.69 % of the total rostral tracts.

However, we noticed an important difference in the tracing capacities of the vectors used for anterograde CST detection in control or bPAC (**Figure 2J**, rostral side of the graph), which could be biasing the results. The fluorescent reporter (mCherry) contained in the control adenoviral vector resulted to be brighter than that used in bPAC animals, most likely due to the fusion bPAC to the mCherry protein. Furthermore, anterograde tracing techniques for CST include an important limitation since it only allows the labelling of a small fraction ($\sim 1\%$) of all CST fibers [46].

Therefore, we decided to further explore CST regeneration across the injury by retrograde tracing using injections of the retrograde AAV2-Syn1-eGFP in the lumbar

spinal cord segment (**Figure 3A**). First, we analyzed retrogradely labelled corticospinal neurons of the primary motor cortex (bregma from +2 to -3), the origin of the CST. In uninjured animals GFP+ corticospinal neurons were nicely labelled in the layer V of the motor cortex (91.6 ± 2 neurons/brain slice; **Figure 3B**). As expected, thoracic dorsal hemisection dramatically reduced the number of GFP+ corticospinal neurons due to the transection of the CST descending tracts rostral to the retrograde injection site (lumbar) (** $p \leq 0.01$ for uninjured vs bPAC, *** $p \leq 0.01$ for uninjured vs control, Fisher's LSD). Of note, while sparse GFP+ cells were found in control animals (1.3 ± 1.2 neurons/brain slice), bPAC stimulated animals showed increased number of retrogradely labelled corticospinal neurons (30.7 ± 20.7 neurons/brain slice) in the primary motor cortex (* $p \leq 0.05$ for control vs bPAC, Fisher's LSD; **Figure 3B**).

Unexpectedly while almost 100% of retrogradely labeled corticospinal neurons in uninjured Control animals located in the Layer V, injured Control and bPAC rats also showed GFP+ in other cortical layers. Frequencies of GFP+ counts in each layer were as follows: 54.8 ± 18.7 in Layer V, 30.8 ± 20.9 in Layer II-III, 8.4 ± 6.14 in Layer IV, 3.7 ± 4.9 in Layer VI and 1.3 ± 1.8 in Layer I. Layered distribution analysis revealed no significant difference between bPAC and control indicating that this observation is injury-dependent and bPAC-independent effect (**Supplementary Figure 2A**). In agreement with the aforesaid layered total counts analysis revealed that bPAC rats have higher GFP+ neurons in all the layers being statistically significant for layer II-III and V (**Supplementary Figure 2B**). This result suggests that bPAC stimulation may improve the CST tract regeneration/preservation to the lumbar segments of the spinal cord.

bPAC stimulation increases the number of supraspinal neurons projecting to the lumbar spinal segment from the raphe-reticular formation, but not the red nuclei.

Taking advantage of the retrograde labelling to trace all descending tracts that reach the injection area, we explored additional supraspinal motor nuclei which can account for a certain degree of functional locomotor recovery such as the red nuclei, caudal raphe nuclei and the reticular formation

The red nuclei, located in the rostro-ventral midbrain, is the niche of rubrospinal neurons projecting a bundle of axons as the rubrospinal tract (RST) into the dorsolateral funiculus of the spinal cord [46]. As the RST results completely transected after dorsal hemisection, injured rats displayed very few retrogradely traced neurons compared to uninjured Control rats (**Figure 3C**). The inspection of retrogradely labelled neurons in the red nuclei showed no significant differences between bPAC or control animals (**Figure**

3C), suggesting that the rubrospinal pathway is not actively involved in the functional recovery exerted by bPAC stimulation.

Caudal to the red nucleus, other important motor centers reside within the brainstem. The medullary reticular formation represents a complex network of motor nuclei including the gigantocellular reticular nuclei and the caudal raphe nuclei, which project caudally to the ventrolateral funiculus of the spinal cord as the reticulospinal and raphespinal pathways, respectively [10]. The diffuse boundaries between these regions difficult their separated study; therefore here they are referred together as raphe-reticular formation. Dorsal hemisection partially transects the medullary ReST and RpST, leaving undamaged tracts. In agreement to that, 6.9 ± 7.9 neurons/slice were retrogradely labelled after injury compared to uninjured controls. Interestingly, bPAC animals showed higher number of retrogradely traced neurons in the raphe-reticular formation compared to injured controls (5.0 ± 5.7 versus 20.3 ± 7.3 neurons/brain slice, p value=0.05, Fisher LSD, **Figure 3D**).

To explore the functional relevance of each brain region in our model, the number of retrogradely neurons counted in each area was correlated to BBB scores at several time points after injury. GFP+ counts in motor cortex or red nuclei did not compute significant correlation with the BBB. However, the number of retrogradely labelled neurons within the raphe-reticular region significantly directly correlates with the BBB scores after 7 and 10 dpi (the time points when the functional difference between bPAC and control are the greatest; **Figure 3E**).

Overall, these results unveil the functional relevance of the reticulospinal and raphespinal pathways in bPAC-mediated functional recovery after SCI.

bPAC stimulation induced serotonergic tract regeneration which correlates with functional recovery after SCI

Is important to consider that serotonergic neurons (the mayor cellular component of the raphe nuclei) are not effectively transduced by AVV2 retro due to serotype-dependent tropism, as previously described [48]. In our hands less than 10% of serotonergic cells were retrogradely traced in uninjured controls, and barely any in injured animals (data not shown). As serotonergic innervation caudal to the injury site has proven to be crucial for motor recovery [49], we decided to further study serotonergic tract by direct serotonin (or 5-hidroxitriptamine, 5-HT) immunohistochemistry in the spinal cord.

5-HT immunostaining allowed the visualization of serotonergic tracts in the intermediolateral cell column and in the ventral horns of the spinal cord (**Figure 4A**). As

expected, the detection of 5-HT positive fiber caudal to the lesion was much more frequent than that previously observed for CST fibers both in control or bPAC (Figure 4A). Of note, the amount of caudal 5-HT positive signal (relativized to rostral) was increased in bPAC animals compared to control (p value= 0.029, unpaired t-test, Figure 4B) suggesting better preservation/regeneration of the serotonergic tracts in bPAC rats.

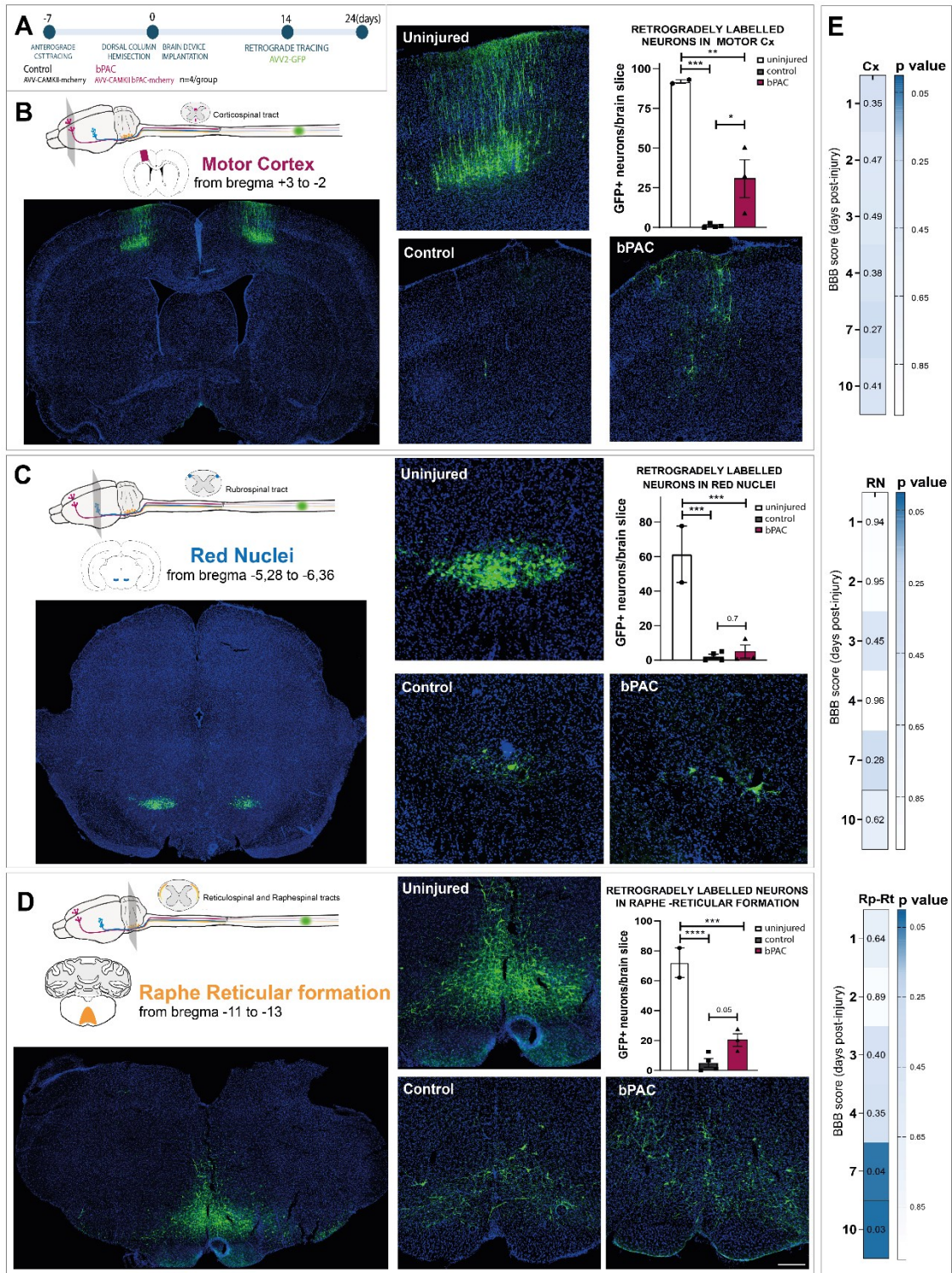


Figure 3. bPAC stimulation increased the number of retrogradely traced neurons in the motor cortex and raphe-reticular formation but not in the red nucleus. (A) experimental design for the analysis of the supraspinal descending tracts by retrograde tracing using AVV2-Syp-eGFP injections in the lumbar spinal cords. (B) Representative images (left) of retrogradely labelled neurons (GFP+) encountered in motor cortex, (C) red nuclei and (D) raphe-reticular formation and their respective quantifications (right). Lower magnification images from uninjured animals (left) and higher magnification images of uninjured, control or bPAC are shown. (E) Pearson correlations between the counts of retrogradely labelled neurons in motor cortex (cx, top), red nuclei (RN, middle) and raphe reticular formation (Rp-Rt, bottom) and the BBB scores at 2,3,4,7 and 10 dpi. Graph show the p-values for the correlations, the intensity of the color being indicative of the statistical significance

Moreover, the amount of caudal 5-HT staining significantly positively correlated with better performance in several locomotor tests (BBB scores: $p \leq 0.001$, Narrow beam: $p \leq 0.05$, Ladder beam: $p \leq 0.05$ and inclined plane: $p \leq 0.0001$) while it did not correlate with thermal test measurements or the GFAP negative area (**Figure 4C, left**). The implication of serotonergic tract in motor recovery might be accounted by the innervation of 5HT+ axons into choline acetyltransferase (ChAT) spinal motor neurons of the ventral horns (**Figure 4C, right**).

Altogether, this data conveys the active implication of serotonergic tracts in the locomotor recovery after dorsal hemisection and highlights the functional importance of their induction by bPAC.

bPAC stimulation increases the density of corticobulbar projections into the brainstem and induced CREB phosphorylation

Next, we aimed to explain how the initial stimulation of bPAC in the motor cortex might affect serotonergic neurons. Given that projections from the pyramidal tracts (py, **Figure 4D**) innervate raphe and reticular areas, what is known as the corticobulbar pathway, we hypothesize that bPAC stimulation might become transmitted to other descending tracts at the brainstem level.

We detected numerous corticobulbar projections arising from the pyramidal tract (py) by anterograde tracing from the motor cortex (**Figure 4D, bottom left**). To study the distribution of corticobulbar projections in the brainstem original images were transformed into heatmaps for each animal, normalized to the tracing efficiency (as given by the signal in the py) and then computed to obtain one density heat map per group (**Figure 4D, right**). Heatmaps showed that while some areas as the medial lemniscus (ml) remained poorly innervated, the raphe and gigantocellular nuclei were nicely delineated in the density heatmaps. Of note, bPAC stimulated animals showed higher

density of corticobulbar projections in the raphe-reticular region specially in the medial zone (**Figure 4D, right**). To study whether primary cAMP signaling activation in cortical neurons (**Figure 1C**) can be transduced to brainstem areas we studied CREB phosphorylation by immunostaining (**Figure 4E**). bPAC stimulated animals showed a discrete but significant PCREB induction at the raphe magnus nuclei; the same tendency to the increase, though not significant, was observed in the lateral and medial gigantocellular nuclei (LPGi and GiA, **Figure 4F**). Moreover, higher CREB phosphorylation in the brainstem correlates with higher CREB phosphorylation in the motor cortex (**Figure 4G**). Overall, this result suggests that bPAC stimulation may induce corticobulbar plasticity after SCI what could mediate an injury bypass trough cortico-brainstem pathways.

The corticospinal tract is synaptically integrated with motor nuclei of the brain stem

Next, in order to probe a synaptic cortico-reticular interaction we coinjected WGA (a transsynaptic neuronal tracer) with either AVV bPAC or control in the motor cortex (**Figure 4H**). WGA was effectively capted by pyramidal neurons in the injection zone (**Figure 4I**). Interestingly WGA dotted-like staining was detected in cells of the raphe-reticular formation demonstrating that the brainstem is synaptically integrated with the cortex (**Figure 4J**).

Counts of WGA+ neurons were analyzed in the brainstem showing no significant differences between bPAC and control (**Figure 4K** and **Supplementary Figure 3**). Contrary to expected, 5-HT immunostaining revealed that serotonergic neurons were not WGA+, but were distributed in closed proximity to them. This result discards a direct cortico-serotonergic synaptic interactions and revealed the existence of a tripartite partner.

Serotonergic neurons of subcortical regions from bPAC rats exhibited similar burst AP firing to uninjured rats

Subsequently, our objective was to investigate whether bPAC stimulation induced electrophysiological alterations in subcortical serotonergic neurons. To address this, we employed the dorsal raphe nucleus (DRN) as a standardized region due to its significance as the primary source of serotonergic neurons in the brain and its well-documented electrophysiological protocols [50]. Serotonergic neurons were differentiated from astrocytes based on their morphology, resting membrane potential and their response to a depolarizing pulse (Em, **Figure 5A-B**). Astrocytes do not generate action potentials in response to depolarizing current (**Figure 5A**). As expected,

there was no difference in astrocytic Em, membrane capacitance (Cm), membrane time constant (τ), and membrane resistance (Rm) between the three groups (Supplementary figure 4).

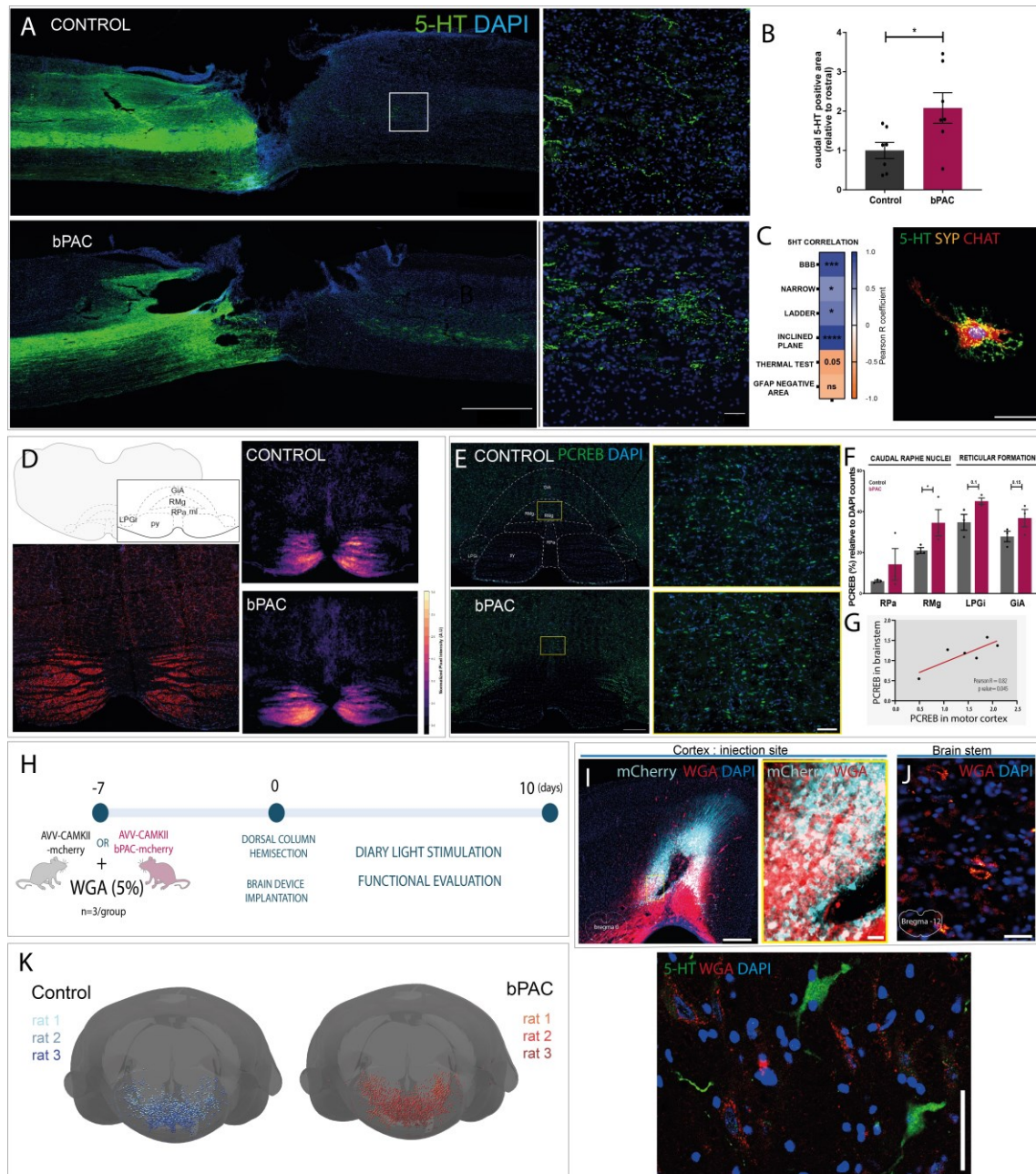


Figure 4. bPAC stimulation induce serotonergic tract regeneration/preservation across the injury area due to the transduction of bPAC stimulus form the cortex to the brainstem level by corticobulbar innervation. (A) representative images of 5-HT immunostaining in sagittal sections of the spinal cords (lower: right and higher: left magnifications; Scales bar = 1000 and 50 μ m, respectively) and (B) its quantification (two-tailed t-test). (C, right) Pearson correlations between several locomotor measurements and the amount of caudal 5HT. Color code indicate the Pearson R coefficient as shown in the legend and p-values are indicated inside each cell. * $p \leq 0.05$, ** $p \leq 0.01$, *** $p \leq 0.001$, **** $p \leq 0.0001$. (C, left) ChAT+ spinal motor neurons synaptically

innervated by serotonergic axons. Scale bar = 50 μ m (D) Example of an original (left) image and computed heat maps showing the density of corticobulbar projections into the brainstem for control and bPAC animals (n=4 animals/group). (E) Representative images of PCREB staining in brainstem slices at higher (left) and lower (right) magnifications. Scale bars=500 and 100 μ m, respectively. (F) Quantification of PCREB% relative to DAPI in each of the indicated regions n=3 animals/group). (G) Correlation between CREB phosphorylation state in motor cortex and brainstem. (H) Experimental design for the study of synaptic connections between motor cortex and brainstem. (I) Images of the injection site of WGA and AVV at low (left) and high (right) magnifications. Scale bars=500 and 50 μ m, respectively (J) Images of brainstem region showing WGA+ cells indicating synaptic input from the motor cortex Scale bar=.50 μ m (K) 3D reconstructions of the WGA+ cell counts and distribution in the brainstem region. Each brain representation includes 3 animals. (L) 5HT immunostaining in the raphe magnus nuclei showing no colocalization with WGA labelling. Scale bar= 50 μ m

In turn, putative serotonergic neurons from the DRN of uninjured rats fired AP in response to protocols of depolarizing step (**Figure 5B**, left) or ramp (**Figure 5B**, right) currents (5 out of 9 cells; **Figure, 5B** top), in contrast with DRN neurons from control rats that failed to fire APs (0 out of 8 cells; **Figure 5B**, middle) in response to both protocols. Interestingly, neurons recorded in the DRN from bPAC rats exhibited burst AP firing similar to those observed in uninjured rats (bPAC, 2 out of 3 cells, Figure 5B bottom).

While C_m and R_m were similar between the groups (**Figure 5C** and F), τ was larger in the DRN neurons from control injured rats (**Figure 5E**) compared to bPAC and control, though not significantly. Intriguingly, at a similar R_m in resting state, this could denote larger cell indicating that lesion could be altering the somatodendritic volume/surface of DRN neurons, an alteration that is not observed in uninjured rats and is counteracted by bPAC stimulation. Such finding deserves future study. In addition, serotonergic neurons of the DRN of injured control rats showed depolarized E_m compared with bPAC-treated rats (**Figure 5D**). This could indicate that putative serotonergic DRN neurons from injured rats are less functional as observed in the loss of the ability to generate APs and that the treatment restores such functionality to the levels of uninjured rats.

Serotonergic depletion by DHT treatment abrogates bPAC-induced functional recovery

Finally, we sought to interrogate the relevance of serotonergic descending tracts for the observed functional recovery in bPAC animals. To selectively deplete serotonergic system 5,7-dihydroxytryptamine (DHT) was administered via intraventricular injections once the animals reached a steadier state in their recovery (22 days after SCI) (**Figure 6A**). Post-mortem analysis revealed that DHT efficiently depleted serotonergic inputs

caudal to the lesion as shown by the reduced 5-HT staining in lumbar spinal cord slices of DHT treated animals (DHT+) compared to SHAM controls (DHT-, **Figure 6B**).

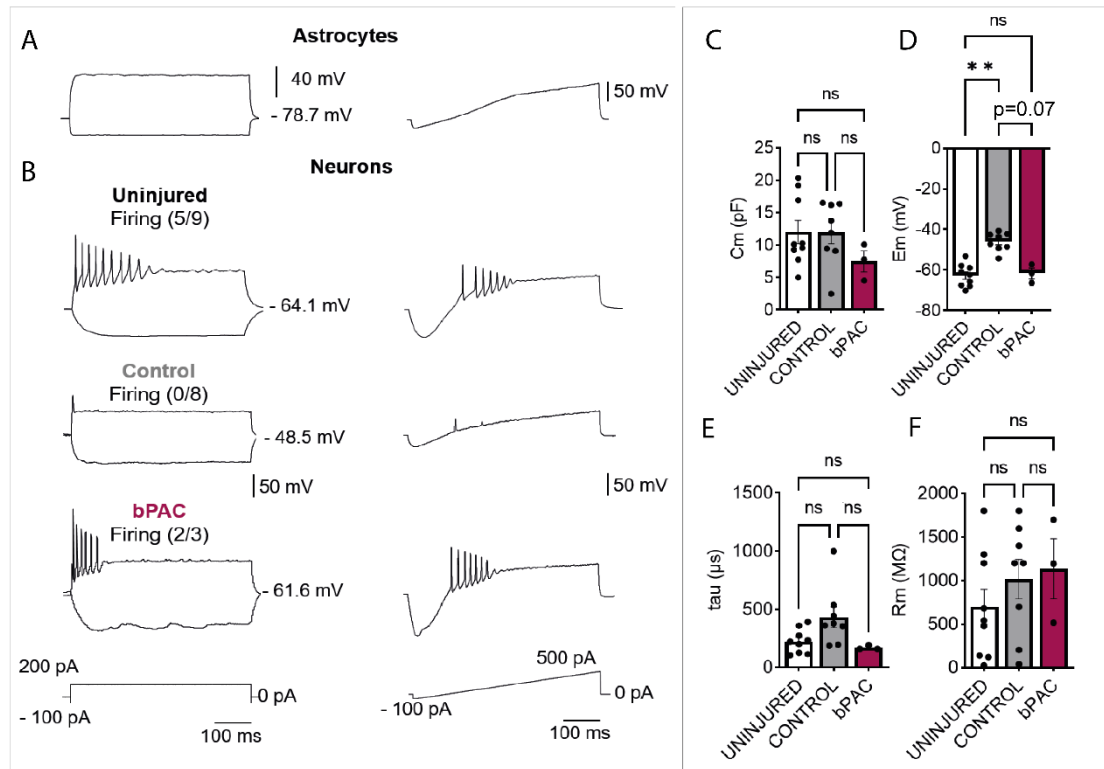


Figure 5: Electrical responses of astrocytes and neurons from DRN in response to hyperpolarizing pulses and depolarizing ramp stimulation and passive electrophysiological membrane properties of putative serotonergic neurons. (A) Representative example traces of the responses of an astrocyte recorded from DRN of control rat. Left: Typically, the astrocyte does not show AP firing in response to 500 ms, 200 pA depolarizing current step and no hyperpolarizing sag is observed in response to -100 pA (left) neither to increasing 500 pA ramp pulse (right). **(B)** Representative examples trace of the neuronal responses to the protocols described at the bottom showing that DRN neurons from uninjured rats (top) fire APs in response to depolarization similarly to neurons recorded from bPAC-treated rats (bottom) while DRN neurons from control rats fail to fire APs in response to either 100 pA pulse step (left) or increasing 500 pA ramp pulse (right). **(C)** Graph showing that the Cm of DRN neurons recorded is similar in the three experimental groups. **(D)** Graph showing that serotonergic neurons of control rats are more depolarized than the uninjured group, and that bPAC restores the neuronal Em to uninjured levels. **(E)** Quantification of DRN neurons tau showing that control rats exhibit increased membrane time constant. **(F)** Histogram showing that the DRN neurons have similar Rm irrespective of the condition. Data is presented as a mean \pm SEM with statistically significance set as * $p < 0.005$ performing Kruskal-Wallis (K-W) test due to the relatively small sample size (bPAC group) followed by Dunn's multiple comparisons test.

Functional evaluation by ladder beam test was assessed prior and 6 days after DHT administration. Of note, while bPAC animals elicited significantly higher scores than control pre-DHT treatment, after DHT treatment bPAC scores decline while controls continued improving, dampening the initial differences (**Figure 6C**, left graph). When expressed in terms of increment, as the difference in the score pre- and the score post-DHT treatment for each rat, all bPAC animal yield negative values (indicative of functional worsening) while controls rendered positive values (indicative of functional improvements, **Figure 6C**, right graph).

Overall, this result strongly suggests the bPAC-mediated locomotor improvements are mediated, at least in part, by the serotonergic descending pathway.

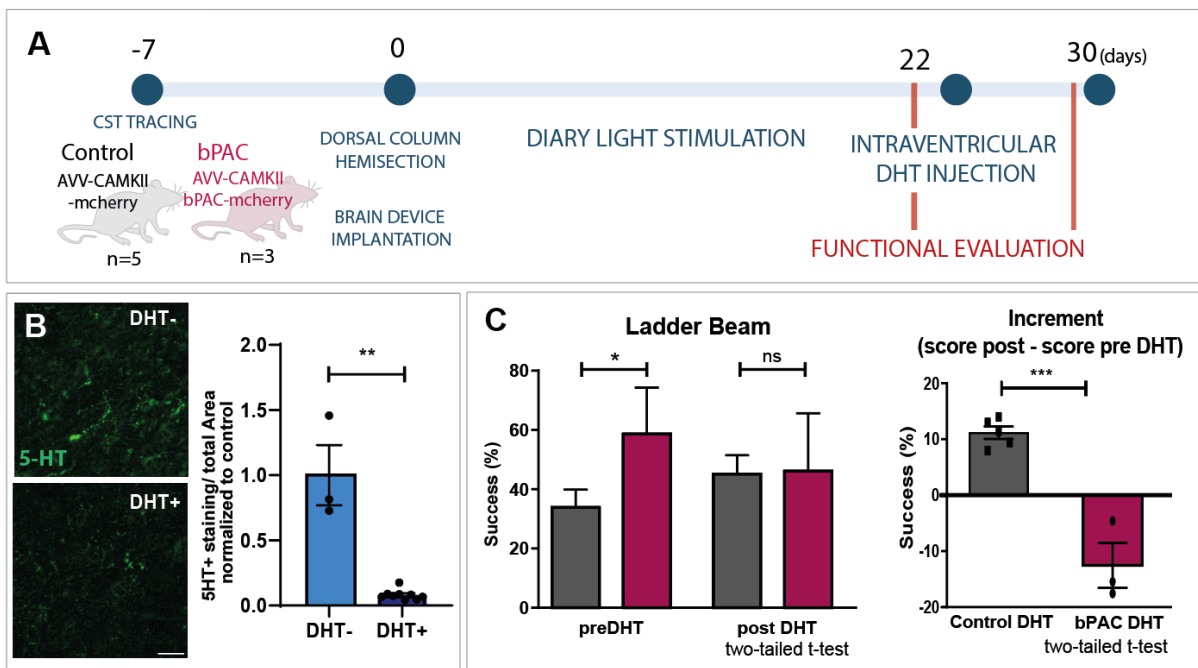


Figure 6. Serotonergic depletion by DHT treatment abrogates bPAC-induced functional recovery. (A) Experimental design to study serotonergic involvement in the observed functional recovery. DHT treatment was applied to bPAC and control animals 22 days after receiving a dorsal hemisection and their locomotor skills were evaluated prior and 6 days post-treatment. (B) 5-HT immunostaining in lumbar spinal cord slices of SHAM controls (DHT-) and DHT-treated (both bPAC and control, DHT+) rats (scale bar:50 μ m) and its quantification. (C) Functional evaluation pre and 6 days post- DHT expressed as the absolute achieved score in ladder beam test (left) or the increment post to pre-DHT treatment (right). Two-tailed t-test; * $p \leq 0.05$, ** $p \leq 0.01$, *** $p \leq 0.001$)

DISCUSSION

Spinal cord injury occurs in an instant, dramatically disrupting brain-to-muscle neuronal circuits that will not be recovered in a lifetime. Despite, in the majority of the cases a

significant portion of the tracts remain uninjured, leading the door open for certain extend of functional recovery [51]. Locomotor improvement can derive from either structural or functional injury-induced neuronal plasticity that may take place at different levels of the CNS including the cortex, brainstem and the spinal cord [52]. Deciphering how the neuronal circuitry at all these levels reorganize to take over the function of damaged pathways is a daunting challenge, yet essential for the development of new neuromodulatory therapies that could better direct the reorganization process. In the past years, efforts have been mainly focused in understanding plastic reorganization of CST at the spinal level [16, 53], while supraspinal plasticity mechanism still remained more elusive.

This study characterized the effects of specific neuromodulation of corticospinal upper motor neurons by dialy optogenetic cAMP inductions via bPAC stimulation after a T8 dorsal hemisection. Conversely to traditional pharmacological interventions for cAMP augmentations [39, 54], bPAC enabled on-demand minimally-invasive high-scale cAMP inductions avoiding the need of injections or surgical intervention which allow repetitive rather than punctual treatment.

As expected, bPAC stimulation induced CREB phosphorylation in the primary motor cortex of injured rats. Given that PCREB is a transcription factor controlling hundreds of regenerative associated genes, this result suggests that bPAC could mediate a transcriptional reprogramming of corticospinal neurons [55] towards a more regenerative state, which deserves future further exploration. Of note, Caracciolo et al. reported that overexpression of CREB in motor neurons promoted motor recovery after stroke by inducing cortical re-mapping, while CREB inactivation turned off functional recovery [56], evidencing that CREB phosphorylation in the motor cortex is sufficient to drive motor recovery. Moreover, we showed that cAMP inductions by bPAC led to increased c-fos immunostaining in Layers IV and V of the motor cortex, possibly by generating calcium waves through cAMP-gated calcium channel [57], indicating that bPAC maintained neuronal activity of corticospinal neurons after SCI.

When we inspected locomotor outcomes of injured rats, we noticed that the greatest differences in BBB score between bPAC and control animals occurred surprisingly earlier than expected, compared with the timing of other SCI therapies [58]. At 6 and 10 dpi the significant differences in BBB scores and height of the iliac crest can be explained due to bPAC induced weight-bearing ability of the rats. Both observations pointed out to serotonergic tract implication since previous reports have demonstrated the implication of 5-HT tracts in hindlimb weight-support after SCI [11, 59, 60] and previous SCI

therapies acting through raphespinal tract regeneration also reported very early functional recovery [58]. Despite the earliness of bPAC mediated functional recovery, the locomotor differences between bPAC and control animals were sustained through the experiment as shown by more challenging tests (ladder, narrow) which require more advanced postural control, FL-HL coordination, and muscular tone.

Of note, alongside the functional benefits of bPAC stimulation, we did observe deleterious effect resulted from bPAC stimulation; 52% (11/21) of the bPAC animals included in this study developed seizure episodes during stimulation. In long-term experiments, by day 30 of diary stimulation, 3 out of 9 rats developed seizures episodes several minutes after the beginning of the stimulation routine. By day 35 of the experiment all animals, 9 out of 9, developed seizures during the first 5 min of stimulation. Considering all the experiments included in this study only 2/21 rats developed seizures at earlier time points (7 days post-injury). Detailed report of seizures apparition can be found at **supplementary table 1**. Seizures were stopped shortly after the animals were removed from the stimulation cage and no spontaneous seizures were detected in the elapsed time between stimulations, nor in bPAC lacking controls, indicating that seizures are dependent on bPAC hyperexcitability. Similarly, phosphatase and tensin homolog (PTEN) deletion, the first therapy to efficiently induce CST regeneration and motor improvement after SCI [61,62], also reported spontaneous epileptic seizures in 82% of animals [61]. Further refinement of the temporal windows of bPAC stimulation, may prevent the development of seizures while retaining the functional benefits, casting some optimism for this therapy.

We next aimed to unveil the underlying mechanism for functional recovery in bPAC-stimulated animals. While anterograde evaluation of CST failed to display significant differences between bPAC or control (possibly due to differential AVV bPAC or control tracing capacity, biasing the results), retrograde tracing from lumbar spinal cord segment showed that bPAC increased the number of retrogradely labelled neurons in the motor cortex compared to control. This finding may be of great relevance since it opens up the possibility of cortical inputs reaching sublesional regions of the spinal cord, were they could influence the Central Pattern Generator (CPG) [63]. Thus, CPG might be susceptible to bPAC mediated neuronal firing which may have functional relevance [64]. However, our data remained inconclusive in this regard since we didn't find significant correlation between the number of retrogradely labelled neurons in the motor cortex and the BBB scores. The influence of bPAC stimulation over CPG neuromodulation is an attractive issue for further studies.

Retrograde tracing studies allow the study of other descending tracts with supraspinal origins, an advantage that is not included in anterograde tracing which only allow the study of one tract at a time. While we found no significant differences in the red nuclei, bPAC treatment increased the number of retrogradely labelled neurons found in the raphe-reticular formation which nicely correlated with BBB scores at days 7 and 10, remarking its locomotor implication. This finding suggests that bPAC promoted the regeneration of transected or the preservation of non-transected RpST and RtST, since increased sprouting would not explain the difference in retrogradely labelled neurons (although sprouting cannot be excluded). Accordingly serotonergic descending tract, originating at the raphe-reticular formation, displayed increased caudal/rostral ratio immunostaining in bPAC stimulated animals compare to control.

The effects of bPAC stimulation over serotonergic tracts raised an open question: How does primary bPAC stimulation in corticospinal neurons trigger functional effects mediated by a secondary non-originally-targeted tract? In this regard, Leibinger et al. reported that transneuronal delivery of Hyper interleukin 6 (hIL6) and JAK/STAT activation of raphespinal neurons after AVV delivery of hIL6 into motor cortex, resulting in raphespinal regeneration and functional recovery [65]. Similarly, we have reported moderate P-CREB induction in the raphe Magnus nuclei of bPAC animals correlating with CREB phosphorylation state of the primary motor cortex, suggesting transneuronal cAMP induction.

Cortico-brainstem projections (also denominated corticobulbar or corticofugal) is an ancient evolutionary mechanism of the cortex that have been reported in multiple species including rodents[11], cats [66], pigs [67] and primates [68]. For instance, Del Cerro et al. demonstrated that the porcine CST only reached T6 spinal cord level and seem to relay on cortico-brainstem interaction to drive inputs to lumbar segment even in naïve conditions [67]. Moreover, Courtine et al. have reported that silencing of reticulospinal neurons of the vGi during channelrodopsin 2 (ChR2) cortical stimulation abolished evoked leg muscle potentials in contusion rodent models, indicating that these neurons relayed the cortical command to hindlimb motor neurons [11]. These two facts highlight the relevance of cortico-brainstem interaction both in injured or uninjured scenarios.

Here we have reported copious cortical projections arising from the pyramidal tract and innervating the raphe-reticular formation. bPAC stimulation slightly altered the distribution of corticobulbar projection showing higher densities at the raphe magnus and GiA nucleus. However, the number of neurons in the raphe reticular formation synaptically integrated with the motor cortex (as shown by the WGA+ counts) didn't show

significant difference between groups. Importantly bPAC stimulation triggered functional plasticity over serotonergic neurons of the DRN of the midbrain as shown by their differential electrophysiological properties. Further studies are required to evaluate bPAC stimulation effect specifically in serotonergic neurons of the caudal raphe nuclei of the brainstem.

Last but not least serotonergic tract implication in bPAC-mediated functional recovery was evaluated in loss-of-function experiments by DHT, a neurotoxin that successfully demonstrated serotonergic role on therapy-mediated motor outputs in previous report [65, 69]. Interestingly DHT administration worsened the performance of bPAC rat in ladder beam test rendering the scores to control levels. This finding strongly supports the involvement of serotonergic descending pathways in bPAC -induced locomotor recovery. However, serotonergic depletion at this stage of recovery (22 days-post-injury) only resulted in modest motor impairment, trackable in skilled motor tests, but no detectable motor deficits in open field walking. This observation suggests the implication spontaneous plasticity of other tracts on progressive recovery in bPAC or control rats.

Is important to remark that our data do not exclude the implication of additional supraspinal or propriospinal pathways in bPAC-mediated mechanism of action. In fact, here we showed certain insight of bPAC effect over corticospinal and reticulospinal tract which has not been fully studied and deserve exploration. These sets of experiments opened the path for future refinement of bPAC therapy and further exploration of other still veiled mechanisms.

Taken together these results strongly suggest that the brainstem is an important transshipment station for rerouting cortical inputs into intact descending RpST/ReST. The cortico-serotonergic tract may provide a more-regenerative descending pathway parallel to the more sophisticated but less-regenerative corticospinal tract. Overall, this study allowed us to discover the relevance of cortico-brainstem plasticity for functional recovery after spinal cord injury. Importantly, raphespinal and reticulospinal tracts are likely to remain partially intact in human SCI [70] due to their ventral anatomical location and their function is well conserved across mammals [71, 72]. In the light of that premise, future therapies targeted to reroute cortical commands into spare brainstem descending circuits might be more clinically relevant than those attempting to promote vague CST regeneration at the injury level.

METHODS AND MATERIALS

Primary cortical neuron culture and cAMP determination

Cortical neurons were harvested from E14.5 fetal Sprague Dawley rats. Briefly, the cortices were dissected from the brains and enzymatically dissociated using trypsin-EDTA (0.05%, 25300-054, Gibco). Next, neurons were counted and seeded over polylysine pre-coated plate on plating medium (containing DMEM High Glucose (SH30243.01, Cytiva), 10% Fetal Bovin Serum and P/S 1x). After 2 hours plating medium was changed to neuronal medium containing Neurobasal (21103-049, Gibco), B27 (17504-044, Gibco), Glutamax 200 mM (35050061, Gibco) and P/S 1x. Then, to transduce neurons with our protein of interest, either AVV1-CAMKII-mcherry or AAV2/9-CAMKII-bPAC-mcherry were added to control or bPAC conditions at a multiplicity of infection (MOI) of 10^9 . Cells were incubated at 37°C, 5% CO₂ at dark conditions.

One week after, to induce bPAC activity, neurons were exposed to blue light (480 nm, 90 s of 20 mW/cm²) using an Optogenetic Stimulator for In-vitro Experimentation (OSIVE) [73]. This stimulation parameters were selected to achieve a saturating effect over cAMP levels according to previous reports showing that cAMP levels reached a plateau after bPAC exposure to 60s of 6 mW/cm² blue light [41] .

Immediately after stimulation the reactions were quench by removal of the culture medium and addition of 0.4 M of perchloric acid (HClO₄). Next, cells were scrapped off from the surface of the wells, homogenized by sonication and centrifuged at 20000 rpm at 4°C for 10 min. Supernatants (containing cAMP extracts) were stored at -80°C until used. Pellets (containing total protein contents) were resuspended in 1M NaOH and protein concentrations were measured using BCA assay kit (23227, Pierce™ BCA Protein Assay Kit, Thermo Scientific). Chromatographic parameters were optimized to XBridge C18 2.1x75 2.5 um (BEH Technology. Cat 186005626 Waters) based on previous reports [74]. The mobile phase composition was as follows: 0.1% formic acid in water, 100% acetonitrile. The conditions for chromatographic run were: flow rate 0.4 ml/min, gradient: 0.5 min-100 %A; 1 min-10% A; 2.2 min-10% A, 2.3 min-100% A; 3.5 min-100 % A. Volume injected was 25 µl. Obtained cAMP concentrations were normalized to the total ug of protein in each experimental replicate. Three different experiments were performed (2 replicates/experiment). Two outliers were identified by ROUT method (Q = 1%). Group comparisons were made by Welch t-test.

Animal care

Only female Sprague Dawley rats were used in this study given the ease of manual bladder drainage which reduces the prevalence of urinary infections and more stable body weight after SCI compared to male rats. Animals were bred and housed with littermates under standard conditions with ad libitum access to food and water at Animal Experimentation Unit of the Research Institute Príncipe Felipe (Valencia, Spain) in accordance with the guidelines of the European Communities Council Directive (86/609/ECC) and the Spanish Royal Decree 53/2013. Experimental procedures were approved by the Animal Care and Use Committee of the Research Institute Prince Felipe (2021/VSC/PEA/0032).

For surgical interventions, animals were subcutaneously treated with morphine (2.5 mg/kg) and anesthetized with 2% isoflurane. After interventions, animals received post-surgical care consisting in subcutaneous injections of 5 mg/kg of Enrofloxacin (Baytril) for seven days, 0.1 mg /kg of Buprenorphine twice a day for four days and manual drainage of bladders twice a day until vesical reflex is recovered. Rats' well-being was monitored and end point criteria was applied if major signs of distress were observed.

CST tracing and dorsal hemisection

One week prior to SCI excitatory corticospinal neurons were transduce to express bPAC by AAV9-CAMKII-bPAC-mcherry injections of into the Layer V of the motor cortex (coordinates from bregma: AP: 0, 2; ML: ± 1.5 ; DV: -1.4, 6e12 VG/injection site). Control animals were likewise injected with a bPAC-deficient vector (AVV1-CAMKII-mcherry, 114469, Addgene, Massachusetts, USA). Both vectors contained a red fluorescent reporter to allow the tracing of the descending corticospinal tracts. No significant differences in AVV1 and AVV9 serotype tropism have been previously reported when used in CAMKII construct in macaques, marmoset and mice [75].

For inducing SCI, a laminectomy was performed to expose the spinal cord at the thoracic segment 8. Bilateral dorsal column hemisection was performed by causing an incision of 1.1 mm in depth from the dorsal surface, leading to the total transection of the dorsal half of the spinal cord.

Light stimulation

On the same day of the injury bilateral brain devices were implanted in all the rats to allow the stimulation with blue light at 470 nm (Neurolux; Northfield, USA). Devices were mounted sub-dermally on top of the animal's skull and the μ LEDs were placed beneath the skull and over each hemisphere of the motor cortex (**Figure 1B**). The stimulation

routine started 1 day after the SCI and was applied once a day until the end point consisting in 1 s on - 4 s off for 30 min at 8W, adapted from [76]. During the stimulation the animals were placed in a cage connected to a power distribution control box (NeuroLux; Northfield, EE. UU) responsible for delivering wireless power to the implants.

Functional tests

To assess open-field locomotion animals were recorded for 5 min once a week throughout the experiment while freely walking in an open space. BBB scores were analyzed by a blinded evaluator by using the 21-point BBB locomotion scale [77].

To analyse motor gait, we used the high-speed video system TSE MotoRater (TSE Systems, Bad Homburg, Germany) which records animal locomotion while crossing to a transparent corridor simultaneously from 3 different perspectives (ventral, left and right) in two different modalities: ladder skilled walking or overground walking. Animals were previously acclimatized to the set up prior to the test day. For the ladder walking animals were allowed to partially regain the ability to support their weight (for 6 days after injury) and then tested once a week throughout the experiment. The rate of success of each animal was scored by using the scale previously defined by Gerlinde A et al [78].

Once the animals have recovered the trunk stability, they were tested to pass through an elevated narrow beam weekly from the day 17 post-injury until the end of the experiment. Narrow beam test measures the longer distance that a rat can walk forward without making any paw slips in at least 3 consecutive runs.

At the end point of the experiment rats were passed through a transparent corridor (TSE MotoRater) for the analysis of finer motor kinematics. To track hind paw movement during locomotion, corporal landmarks of the hindlimb joints were marked on the shaved skin. SIMI Motion (SIMI Reality Motion Systems, Germany) software was used to acquire two-dimensional coordinates of each joint for each run. We have manually defined the step cycles for both paws in each run, defined as the transition between two ground contacts. Angle ranges for each joint have been calculated as defined in **Figure 2F** and averaged across the two paws for two different step cycles.

Thermal test

Neuropathic pain is a usual side effect after CNS damage. A common indicator of the presence of neuropathic pain in animal models of SCI is the thermal hyperalgesia. Thermal test studies the behavior of an animal upon a thermal stimulus by observation of the hind paw withdrawal from a heat radiant surface [79] (Ugo Basile Hot/Cold Plate, 35150). Thermal ramp starts at 25°C and increases at a rate of 0.07 °C/s. Animals were

instead to maintain a quadrupedal position being their behavior monitored along the test. The test concluded when the animals removed their paws from the plate as a reaction to the thermal stimulus, registering at that moment the temperature reached.

Retrograde tracing

Fourteen days after dorsal hemisection animals were retrogradely traced from the lumbar spinal cord. In brief laminectomy was performed at the lumbar segments to expose the spinal cord. Four μ l at 1:2 dilution of pAAV-Syn1-eGFP; addgene#50465 were injected in 8 different points (4 points/hemisphere) at 1 mm of depth in the dorsoventral axis using the PV850 microinjector (World Precision Instruments, USA)

Sample processing and Immunostaining

At the end of the experiment, the animals were overdosed with 100mg/kg sodium pentobarbital and transcardially perfused with 4% paraformaldehyde (PFA) solution. Brains and spinal cords were carefully removed, fixed in 4% PFA and stored in 0.1M phosphate buffer (PB). Samples were cryopreserved in 30% sucrose in PB for at least 7 days. Spinal segments 1.8 cm in length, including the lesion epicenter, were cut into 35-microm thick slices in the sagittal plane using the Cryostat Microm HM550 (Thermofisher, Germany). Brains were cut into 40-micron thick in the coronal plane.

Standard immunofluorescence staining was performed by incubation at 4°C in the primary antibody solution in TBS+ 5% donkey serum + 0,25% Triton for at least two nights and 1 night in the secondary antibody solution. mCherry/c-FOS/P-CREB/spinal 5-HT signals were amplified using the tyramide signal amplification (TSA) protocol [80]. Primary antibodies used were anti-GFAP (α -Rb, 1:800, Z0334, DAKO, Denmark), anti-5-HT (α -Gt, 1:1000, AB_572262, Immunostar, Wisconsin, USA), anti-5-HT (α -Rb, 1:400, S5545, Merck Millipore, Massachusetts, USA), anti-c-FOS (α -Rb, 1:100, ab190289, Abcam, Cambridge, United Kingdom), anti-P-CREB (α -Rb, 1:100, 06-519, Merck Millipore, Massachusetts, USA) Anti-Choline Acetyltransferase, ChAT (α -Gt, 1:200, AB144P, Merck Millipore, Massachusetts, USA), anti-RFP/mCherry (α -Gp, 1:1000, 390 004 Synaptic systems, Göttingen, Germany). Secondary antibodies used for standard immunohistochemistry used were either Alexa Fluor-488, -555, or -647 conjugated antibodies (1:400, Invitrogen, Massachusetts, USA). Secondary antibodies used in TSA amplification immunohistochemistry were either Biotinylated Donkey anti-Rb or anti-Gp (706-065, Jackson ImmunoResearch, Cambridgeshire, United Kingdom) and either 555 (S21381, Thermofischer, Massachusetts, United States) or 488 streptavidin (016-540-084 Jackson ImmunoResearch, Cambridgeshire, United Kingdom). Cell nuclei were

counterstained with DAPI (1:1000, Sigma, Missouri, USA). Sections were mounted in Mowiol and imaged using an Aperio Versa scanner (Leica Biosystems, Germany). Images were visualized and analyzed with the Image Scope software or ImageJ software.

5-HT quantification

The 5-HT positive area was quantified separately in the rostral and caudal regions of the injured spinal cords. To reduce the possible deviation of the cutting angle, 5-HT absolute data was then normalized to the amount of ChAT positive area (as the zones putative for having 5-HT innervation). Next, the ratios from caudal to rostral were calculated for each slice (n= 1-3 slices/animal). The correlation of 5-HT measurements with locomotor parameters were studied by calculating Pearson coefficients for each pair of variables.

c-fos and P-CREB quantification

To quantify the amount of c-fos along the cortical layers first we selected regions within the primary motor cortex in brain slices approximately at bregma -1. For each animal 3 to 5 independent images were analyzed. All images were thresholded using the same parameters and the histogram of mean grey value along the layers was displayed using plot profile plugin of ImageJ both for DAPI and c-fos. Then, c-fos histogram profiles were relativized to DAPI and the all the images for each animal averaged to a single profile. Finally, we calculated the mean grey value of c-fos encountered in each layer (two-way ANOVA fisher's test)

For P-CREB quantification in the motor cortex we selected regions comprising the primary motor cortex as defined by Paxinos and Watson atlas, in brain slices at bregma -1.5 and measured the area positive for P-CREB staining which was then relativized to the total DAPI counts (**Figure 1C**, t-test). To quantify CREB phosphorylation in the brain stem brain slices at bregma -11.88 were immunostained and imaged. Several regions of the raphe nuclei and the reticular formation were manually defined (according to Paxinos and Watson atlas) and the number of P-CREB+ nuclei and DAPI quantified for each region. The average of P-CREB+ relative to DAPI was calculated (3 animals/group; 2 slices/animal) (**Figure 4E**).

Ex vivo electrophysiological recordings.

Coronal brain slices containing the DRN were obtained from 3-5 months old female rats as previously reported [81]. In brief, rats were deeply anesthetized with isoflurane (2%), decapitated, and the brain was quickly removed and placed in an ice-cold artificial cerebrospinal fluid (ACSF) containing (in mM): NaCl, 126; KCl, 3; NaH₂PO₄, 1.25;

MgSO₄, 2; CaCl₂, 2; NaHCO₃, 26; and glucose, 10 (pH 7.2, 300 mOsm/L). Coronal slices (200- μ m thick) were obtained with a vibratome Leica VT1000S and maintained oxygenated (95% O₂/5% CO₂) in ACSF for at least 1 h before use at room temperature. Recordings were carried out at 32–34 °C and the slices were continuously superfused with oxygenated ACSF during the experiments.

Astrocytes and putative serotonergic neurons were identified visually by their characteristic morphology, location, and their distinctive electrophysiological responses to different stimulation protocols. These protocols were also used for the identification of GABAergic interneurons [81-83] that were discarded from the study. Identification protocols consisted of 2 steps protocol (-100 hyperpolarizing pA and 300 depolarizing pA) and depolarizing ramp current injection (500 pA). Whole-cell patch clamp recordings of astrocytes and serotonergic cells located in the caudal DRN were obtained under visual guidance by IR-DIC microscopy (Axio Examiner, Zeiss; Germany). Patch electrodes were pulled from borosilicate glass tubes having a resistance of 4–7M Ω when filled with (in mM): potassium gluconate, 110; HEPES, 40; NaCl, 4; ATP-Mg, 4; and GTP, 0.3 (pH 7.2–7.3, 290 mOsm/L). Passive membrane electrophysiological properties and the ability to fire action potentials were acquired immediately after getting access to the cell with a patch-clamp amplifier (Multiclamp 700B) using pCLAMP 10.4 software (Molecular Devices). Raw signals were low pass filtered at 3 kHz, acquired at 10 kHz, digitized, and stored using Digidata 1550A and pCLAMP 10.4 software (Molecular Devices).

WGA tracing

Wheat germ agglutinin (WGA) is commonly used as a neuronal tracer given its ability to travel both anterogradely or retrogradely as well as to jump transsynaptically [85]. Injecting WGA into Layer V of the motor cortex allows the tracing of the synaptic connectome of corticospinal neurons. For that, we co-injected 5% WGA Alexa Fluor 647 conjugated (W32466, Thermo Fisher, Massachusetts, USA) in saline solution along with either control or bPAC adenoviral vectors (**Figure 4H-K**).

5,7-DHT treatments

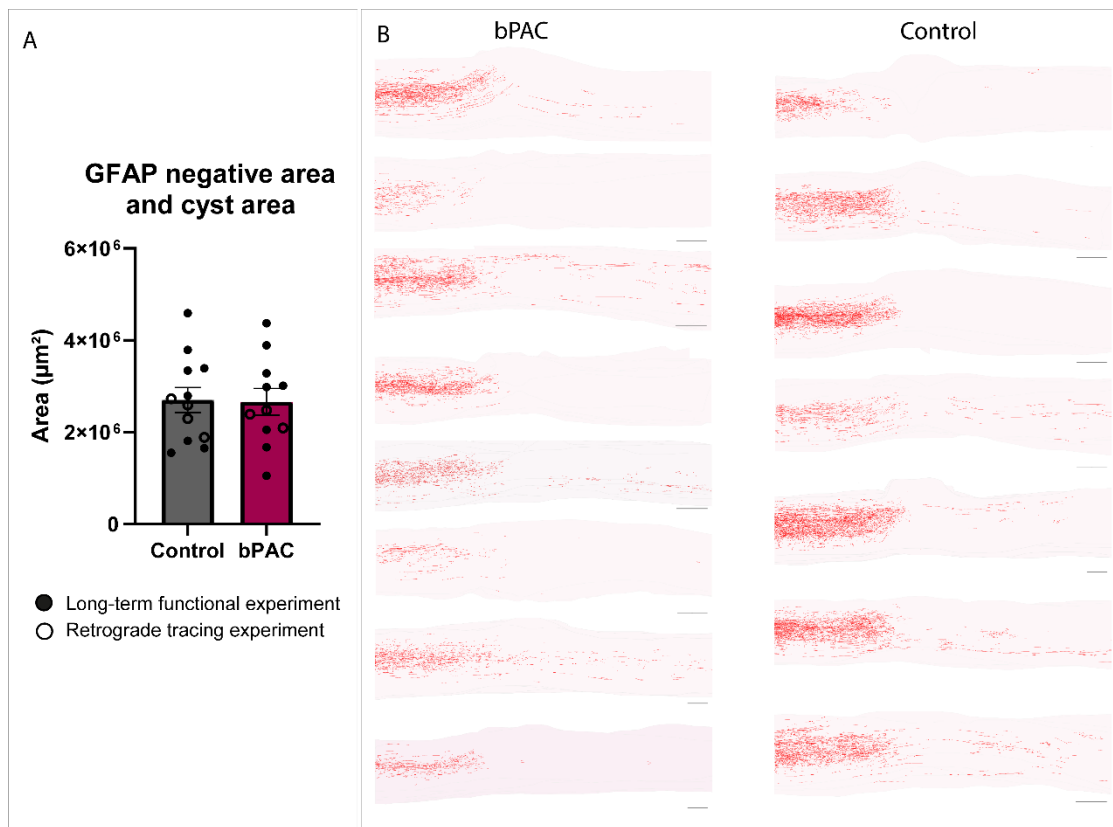
To induce the depletion in the serotonergic system, rats were treated with a serotonergic neurotoxin: 5,7-Dihydroxytryptamine hydrobromide (DHT; CDX-H0026-M010, Labclinics, Barcelona, Spain), 22 days after SCI (Figure 6). Briefly, 20 μ l of 7.5 μ g/ml 5,7-DHT in 0.02% ascorbate saline solution was intraventricularly infused bilaterally (coordinates from bregma: AP: -0.8; ML: \pm 1.5; DV: -4.6; 10 μ l per side; infusion rate: 1 μ l/min) both to bPAC (bPAC DHT) and control (control DHT) rats. The accessibility to

the injection area required the removal of the optogenetic device. Injured sham controls (DHT-) were likewise injected with 0.02% ascorbate saline solution. The noradrenergic system was protected by intraperitoneal premedication (25 mg/kg) with desipramine hydrochloride (D3900, Merk Millipore Massachusetts, USA) 30 min before 5,7-DHT injections [86].

Supplementary Material

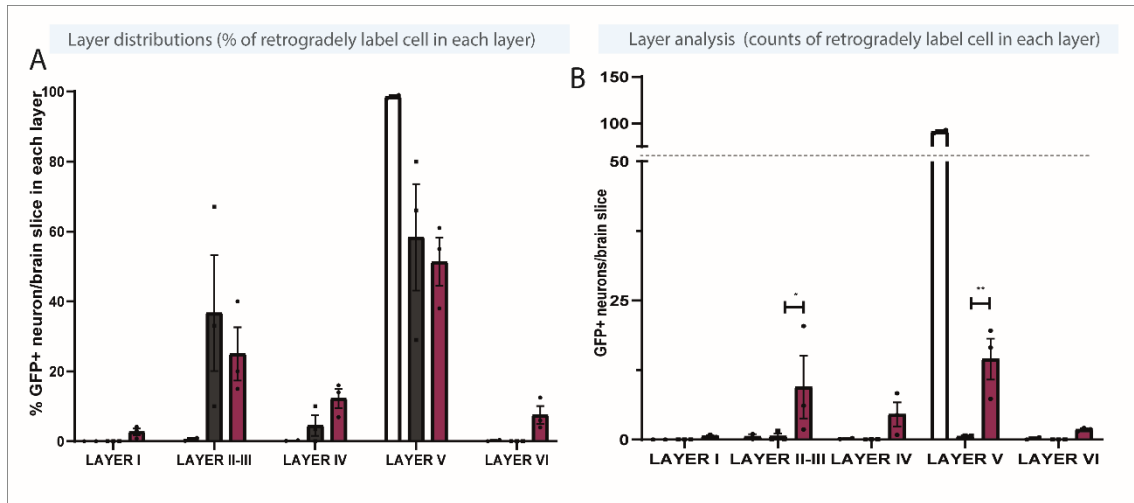
Experiment	N (bPAC animals)	Optogenetic Stimulation	Seizures
Long term experiment for functional evaluation	9	From 1 to 35 dpi	3/9 animals developed seizures at 30 dpi 9/9 animals developed seizures at 35 dpi within the first 5 minutes of stimulation (end point of the experiment).
Retrograde tracing experiment	3	From 1 to 17 dpi	2/3 animals developed seizures at 7 dpi within the first 5 minutes of stimulation. Diary stimulation was stopped at 7 dpi in the animals that develop seizures. The animal that did not developed seizures was stimulated until day 17
WGA experiment	3	From 1 to 10 dpi	none
DHT experiment	3	From 1 to 22 dpi	none
Ex vivo electrophysiological recordings	3	From 1 to	none

Table 1: Report of the apparition of seizures episodes in all the experiments included in this study

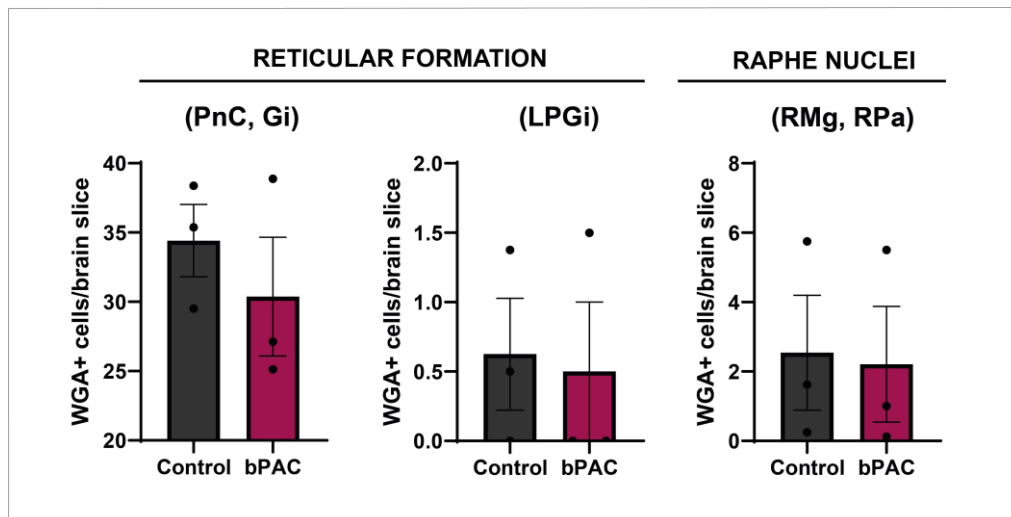


Supplementary Figure 1: Injury areas and CST anterograde tracing panels. (A) Injury areas measured as the area negative for GFAP staining+ cyst cavity areas in sagittal sections of the spinal cord showing injury homogeneity between experimental groups in two experiments of this study. **(B)** Panels of camera lucida reconstruction of

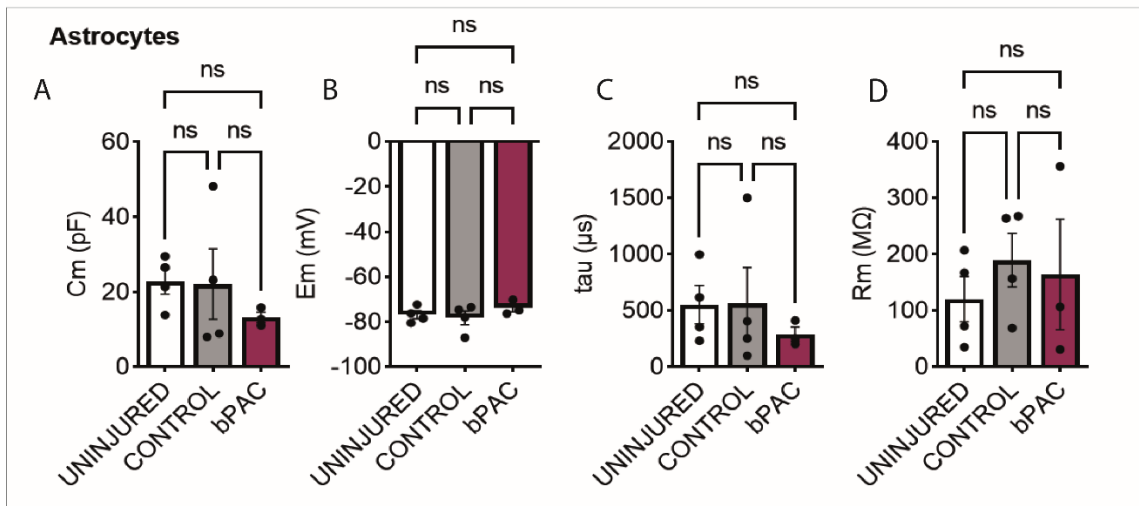
CST tract by anterograde tracing from animals of the long-term experiments. Scale bar: 1000 μ m



Supplementary Figure 2. Layered analysis of retrogradely labeled neurons in the motor cortex. (A) Distributions of retrogradely labeled cells in each layer of the motor cortex expressed as the % of the total count encountered in each layer. (B) Layered analysis of the counts of retrogradely labeled neurons encountered in each layer. Multiple t-test Holm Sidak analysis * $p \leq 0.05$, ** $p \leq 0.01$, *** $p \leq 0.001$).



Supplementary Figure 3. WGA+ cell counts in different anatomical regions. Bar graphs representing the WGA counts encountered in different regions of the brainstem including the medial aspect (including the caudal pontine nuclei and the gigantocellular nuclei, PnC and Gi respectively) and the lateral aspect (LPGi) of the reticular formation and the caudal raphe nuclei (including raphe magnus and palidus nuclei, RMg and RPa respectively)



Supplementary figure 4. Passive electrophysiological membrane properties of astrocytes. A) Quantification of the membrane capacitance (Cm), B) resting membrane potential (Em), C) membrane time constant (tau), and D) membrane resistance (Rm) of astrocytes in uninjured (white), injured control (grey) and bPAC (magenta) rats. Data is presented as a mean \pm SEM; Kruskal-Wallis (K-W) and Dunn's multiple comparisons test.

Acknowledgments

The authors thank Dr Xavier Navarro Acebes, Pietro Fazzari and Juan Aguilar for his scientific discussion and suggestions, Marta Llansona for her technical support in chromatographic measurements, and Stuart P. Atkinson for English editing. This research was funded by FEDER/Ministerio de Ciencia e Innovación – Agencia Estatal de Investigación [RTI2018-095872-B-C21/ERDF]. Part of the equipment employed in this work was funded by Generalitat Valenciana and cofinanced with ERDF funds (OP ERDF of Comunitat Valenciana 2014–2020) and the UE; Fondo Europeo de Desarrollo Regional (FEDER) 2014-2020. B. Martinez-Rojas was supported by a grant from the Conselleria de Educació, Investigació, Cultura y Deporte de la Generalitat Valenciana and the European Social Fundation ACIF/2019/120.

Competing Interests

The authors have no relevant financial or non-financial interests to disclose.

Author Contributions:

B. Martinez-Rojas: CHA

E. Giraldo: Data curation; Writing - review & editing; Supervision

López-Mocholi E, Alastrue-Agudo A, Paniagua G, Pedraza M, Sonia Hingorani Jai Prakash, Benjamin R Rost: Methodology; Technical assistance, Data curation; Formal analysis.

Javier Monreal Trigo, Alcaniz Filloi M: engineering of the in vitro stimulation Array OSIVE.

V. Moreno-Manzano: Conceptualization; Data curation; Formal analysis; Writing - original draft; Writing - review & editing; Funding acquisition; Supervision; Project administration

Data Availability

The data that support the findings of this study are available on request from the corresponding author.

Ethics approval

The maintenance and use of all animals were in accordance with guidelines established by the European Communities Council Directive (86/609/ECC) and the Spanish Royal Decree 53/2013. All experimental procedures were approved by the Animal Care and Use Committee of the Research Institute Prince Felipe (2021/VSC/PEA/0032).

Consent to participate

Informed consent was obtained from all individual participants included in the study.

References:

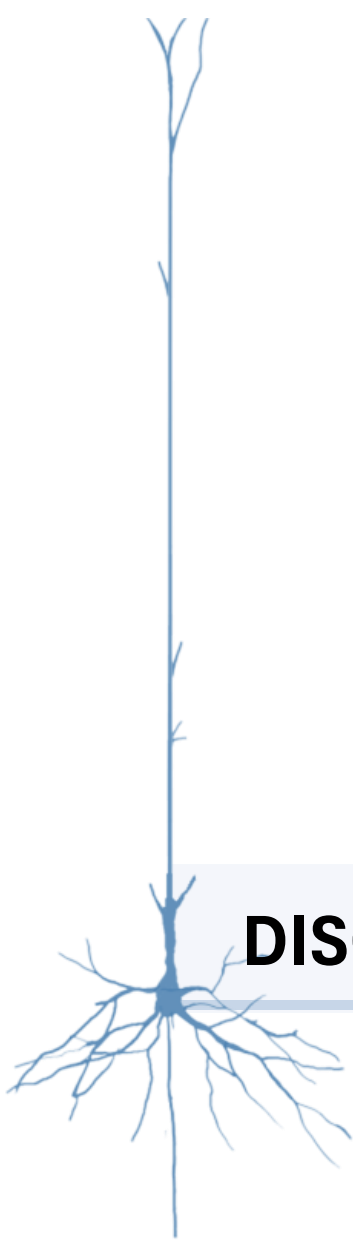
1. Arber, S. and R.M.J.S. Costa, *Connecting neuronal circuits for movement*. 2018. **360**(6396): p. 1403-1404.
2. Dietz, V.J.N.R.N., *Behavior of spinal neurons deprived of supraspinal input*. 2010. **6**(3): p. 167-174.
3. de la Torre-Valdovinos, B., L.P. Osuna-Carrasco, and C.A.C. Ramos, *The Role of Supraspinal Structures for Recovery after SCI: From Motor Dysfunction to Mental Health*, in *Paraplegia*. 2021, IntechOpen.
4. Welniarz, Q., I. Dusart, and E.J.D.n. Roze, *The corticospinal tract: Evolution, development, and human disorders*. 2017. **77**(7): p. 810-829.
5. Van Wittenberghe, I.C. and D.C. Peterson, *Corticospinal tract lesion*. 2019.
6. Joosten, E.A., et al., *Postnatal development of the ipsilateral corticospinal component in rat spinal cord: a light and electron microscopic anterograde HRP study*. 1992. **326**(1): p. 133-146.
7. Isa, T., T. Tohyama, and M.J.C.R.i.N. Kinoshita, *Phylogenetic view of the compensatory mechanisms in motor and sensory systems after neuronal injury*. 2022: p. 100058.
8. Liang, H., et al., *Terminations of reticulospinal fibers originating from the gigantocellular reticular formation in the mouse spinal cord*. 2016. **221**: p. 1623-1633.

9. Brownstone, R.M. and J.W.J.F.i.n.c. Chopek, *Reticulospinal systems for tuning motor commands*. 2018. **12**: p. 30.
10. Mangold, S.A. and J.M. Das, *Neuroanatomy, reticular formation*, in *StatPearls [Internet]*. 2022, StatPearls Publishing.
11. Asboth, L., et al., *Cortico-reticulo-spinal circuit reorganization enables functional recovery after severe spinal cord contusion*. *Nat Neurosci*, 2018. **21**(4): p. 576-588.
12. Perreault, M.-C. and A.J.C.o.i.p. Giorgi, *Diversity of reticulospinal systems in mammals*. 2019. **8**: p. 161-169.
13. Sengul, G. and C. Watson, *Ascending and descending pathways in the spinal cord*, in *The rat nervous system*. 2015, Elsevier. p. 115-130.
14. Antal, M.J.J.f.H., *Termination areas of corticobulbar and corticospinal fibres in the rat*. 1984. **25**(6): p. 647-659.
15. Keizer, K. and H.J.E.B.R. Kuypers, *Distribution of corticospinal neurons with collaterals to the lower brain stem reticular formation in monkey (Macaca fascicularis)*. 1989. **74**: p. 311-318.
16. Oudega, M. and M.A.J.T.J.o.p. Perez, *Corticospinal reorganization after spinal cord injury*. 2012. **590**(16): p. 3647-3663.
17. Hill, C.E., M.S. Beattie, and J.C.J.E.n. Bresnahan, *Degeneration and sprouting of identified descending supraspinal axons after contusive spinal cord injury in the rat*. 2001. **171**(1): p. 153-169.
18. Álvarez, Z., et al., *Bioactive scaffolds with enhanced supramolecular motion promote recovery from spinal cord injury*. 2021. **374**(6569): p. 848-856.
19. Bradbury, E.J., et al., *Chondroitinase ABC promotes functional recovery after spinal cord injury*. 2002. **416**(6881): p. 636-640.
20. Rao, J.-S., et al., *NT3-chitosan enables de novo regeneration and functional recovery in monkeys after spinal cord injury*. 2018. **115**(24): p. E5595-E5604.
21. Fischer, I., J.N. Dulin, and M.A.J.N.R.N. Lane, *Transplanting neural progenitor cells to restore connectivity after spinal cord injury*. 2020. **21**(7): p. 366-383.
22. Lu, P., et al., *Rehabilitation combined with neural progenitor cell grafts enables functional recovery in chronic spinal cord injury*. *JCI Insight*, 2022. **7**(16).
23. Asboth, L., et al., *Cortico-reticulo-spinal circuit reorganization enables functional recovery after severe spinal cord contusion*. 2018. **21**(4): p. 576-588.
24. Fink, K.L. and W.B. Cafferty, *Reorganization of Intact Descending Motor Circuits to Replace Lost Connections After Injury*. *Neurotherapeutics*, 2016. **13**(2): p. 370-81.
25. Bareyre, F.M., et al., *The injured spinal cord spontaneously forms a new intraspinal circuit in adult rats*. 2004. **7**(3): p. 269-277.
26. Ishida, A., et al., *Dynamic Interaction between Cortico-Brainstem Pathways during Training-Induced Recovery in Stroke Model Rats*. *J Neurosci*, 2019. **39**(37): p. 7306-7320.
27. Alam, M., et al., *Electrical neuromodulation of the cervical spinal cord facilitates forelimb skilled function recovery in spinal cord injured rats*. 2017. **291**: p. 141-150.
28. Deng, W.-w., et al., *Optogenetic neuronal stimulation promotes functional recovery after spinal cord injury*. 2021. **15**: p. 640255.
29. Gao, Z., et al., *Chemogenetic stimulation of proprioceptors remodels lumbar interneuron excitability and promotes motor recovery after SCI*. 2021. **29**(8): p. 2483-2498.
30. Marufa, S.A., et al., *Neuromodulatory effects of repetitive transcranial magnetic stimulation on neural plasticity and motor functions in rats with an incomplete spinal cord injury: A preliminary study*. 2021. **16**(6): p. e0252965.
31. Kathe, C., et al., *The neurons that restore walking after paralysis*. 2022. **611**(7936): p. 540-547.
32. Lorach, H., et al., *Walking naturally after spinal cord injury using a brain-spine interface*. *Nature*, 2023. **618**(7963): p. 126-133.

33. Qiu, J., et al., *Spinal axon regeneration induced by elevation of cyclic AMP*. *Neuron*, 2002. **34**(6): p. 895-903.
34. Neumann, S., et al., *Regeneration of sensory axons within the injured spinal cord induced by intraganglionic cAMP elevation*. *Neuron*, 2002. **34**(6): p. 885-93.
35. Pearse, D.D., et al., *cAMP and Schwann cells promote axonal growth and functional recovery after spinal cord injury*. *Nat Med*, 2004. **10**(6): p. 610-6.
36. Xia, T., et al., *The combination of db-cAMP and ChABC with poly(propylene carbonate) microfibers promote axonal regenerative sprouting and functional recovery after spinal cord hemisection injury*. *Biomed Pharmacother*, 2017. **86**: p. 354-362.
37. Meng, Q.-q., et al., *Combined rosiglitazone and Forskolin have neuroprotective effects in SD rats after spinal cord injury*. 2018. **2018**.
38. Schaal, S.M., et al., *The therapeutic profile of rolipram, PDE target and mechanism of action as a neuroprotectant following spinal cord injury*. 2012.
39. Costa, L.M., et al., *Rolipram promotes functional recovery after contusive thoracic spinal cord injury in rats*. *Behav Brain Res*, 2013. **243**: p. 66-73.
40. Lindner, R., et al., *Photoactivation Mechanism of a Bacterial Light-Regulated Adenylyl Cyclase*. *J Mol Biol*, 2017. **429**(9): p. 1336-1351.
41. Stierl, M., et al., *Light modulation of cellular cAMP by a small bacterial photoactivated adenylyl cyclase, bPAC, of the soil bacterium Beggiatoa*. *J Biol Chem*, 2011. **286**(2): p. 1181-8.
42. Yang, S., et al., *PACmn for improved optogenetic control of intracellular cAMP*. *BMC Biol*, 2021. **19**(1): p. 227.
43. Xiao, Y., W. Tian, and H. Lopez-Schier, *Optogenetic stimulation of neuronal repair*. *Curr Biol*, 2015. **25**(22): p. R1068-9.
44. Kleis, P., et al., *Long-term in vivo application of a potassium channel-based optogenetic silencer in the healthy and epileptic mouse hippocampus*. *BMC Biol*, 2022. **20**(1): p. 18.
45. Spencer, T. and M.T.J.J.o.a. Filbin, *A role for cAMP in regeneration of the adult mammalian CNS*. 2004. **204**(1): p. 49-55.
46. Brösamle, C. and M.E.J.J.o.c.n. Schwab, *Cells of origin, course, and termination patterns of the ventral, uncrossed component of the mature rat corticospinal tract*. 1997. **386**(2): p. 293-303.
47. Basile, G.A., et al., *Red nucleus structure and function: from anatomy to clinical neurosciences*. *Brain Struct Funct*, 2021. **226**(1): p. 69-91.
48. Wang, Z., et al., *Global Connectivity and Function of Descending Spinal Input Revealed by 3D Microscopy and Retrograde Transduction*. *J Neurosci*, 2018. **38**(49): p. 10566-10581.
49. Mullner, A., et al., *Lamina-specific restoration of serotonergic projections after Nogo-A antibody treatment of spinal cord injury in rats*. *Eur J Neurosci*, 2008. **27**(2): p. 326-33.
50. Gartside, S., et al., *Neurochemical and electrophysiological studies on the functional significance of burst firing in serotonergic neurons*. 2000. **98**(2): p. 295-300.
51. Anderson, M.A., et al., *Natural and targeted circuit reorganization after spinal cord injury*. *Nat Neurosci*, 2022. **25**(12): p. 1584-1596.
52. Lynskey, J.V., A. Belanger, and R. Jung, *Activity-dependent plasticity in spinal cord injury*. *J Rehabil Res Dev*, 2008. **45**(2): p. 229-40.
53. Nakagawa, H., et al., *Reorganization of corticospinal tract fibers after spinal cord injury in adult macaques*. *Sci Rep*, 2015. **5**: p. 11986.
54. Lau, B.Y., et al., *Cyclic AMP promotes axon regeneration, lesion repair and neuronal survival in lampreys after spinal cord injury*. *Exp Neurol*, 2013. **250**: p. 31-42.
55. Gascon, S., F. Ortega, and M. Gotz, *Transient CREB-mediated transcription is key in direct neuronal reprogramming*. *Neurogenesis (Austin)*, 2017. **4**(1): p. e1285383.
56. Caracciolo, L., et al., *CREB controls cortical circuit plasticity and functional recovery after stroke*. 2018. **9**(1): p. 2250.

57. Halls, M.L. and D.M. Cooper, *Regulation by Ca²⁺-signaling pathways of adenylyl cyclases*. Cold Spring Harb Perspect Biol, 2011. **3**(1): p. a004143.
58. Kadoya, K., et al., *Spinal cord reconstitution with homologous neural grafts enables robust corticospinal regeneration*. Nat Med, 2016. **22**(5): p. 479-87.
59. Kim, J.E., et al., *Nogo-66 receptor prevents raphespinal and rubrospinal axon regeneration and limits functional recovery from spinal cord injury*. Neuron, 2004. **44**(3): p. 439-51.
60. Courtine, G., et al., *Transformation of nonfunctional spinal circuits into functional states after the loss of brain input*. Nat Neurosci, 2009. **12**(10): p. 1333-42.
61. Liu, K., et al., *PTEN deletion enhances the regenerative ability of adult corticospinal neurons*. Nat Neurosci, 2010. **13**(9): p. 1075-81.
62. Pun, R.Y., et al., *Excessive activation of mTOR in postnatally generated granule cells is sufficient to cause epilepsy*. Neuron, 2012. **75**(6): p. 1022-34.
63. Guertin, P.A., *Preclinical evidence supporting the clinical development of central pattern generator-modulating therapies for chronic spinal cord-injured patients*. Front Hum Neurosci, 2014. **8**: p. 272.
64. Golowasch, J., *Neuromodulation of central pattern generators and its role in the functional recovery of central pattern generator activity*. J Neurophysiol, 2019. **122**(1): p. 300-315.
65. Leibinger, M., et al., *Transneuronal delivery of hyper-interleukin-6 enables functional recovery after severe spinal cord injury in mice*. Nat Commun, 2021. **12**(1): p. 391.
66. Pilyavskii, A.J.N., *Corticofugal influences on reticulospinal neurons of the gigantocellular nucleus in cats*. 1976. **8**(3): p. 192-199.
67. Del Cerro, P., A. Rodriguez-De-Lope, and J.E. Collazos-Castro, *The Cortical Motor System in the Domestic Pig: Origin and Termination of the Corticospinal Tract and Cortico-Brainstem Projections*. Front Neuroanat, 2021. **15**: p. 748050.
68. Fisher, K.M., et al., *Extensive Cortical Convergence to Primate Reticulospinal Pathways*. J Neurosci, 2021. **41**(5): p. 1005-1018.
69. Ruschel, J., et al., *Axonal regeneration. Systemic administration of epothilone B promotes axon regeneration after spinal cord injury*. Science, 2015. **348**(6232): p. 347-52.
70. Nathan, P., M. Smith, and P.J.B. Deacon, *Vestibulospinal, reticulospinal and descending propriospinal nerve fibres in man*. 1996. **119**(6): p. 1809-1833.
71. Nudo, R. and R.J.J.o.C.N. Masterton, *Descending pathways to the spinal cord: a comparative study of 22 mammals*. 1988. **277**(1): p. 53-79.
72. Perrin, F.E., et al., *Anatomical study of serotonergic innervation and 5-HT(1A) receptor in the human spinal cord*. Cell Death Dis, 2011. **2**(10): p. e218.
73. Monreal-Trigo, J., et al., *Optogenetic Stimulation Array for Confocal Microscopy Fast Transient Monitoring*. 2022. **16**(6): p. 1397-1405.
74. Joshi, A., et al., *Handling considerations for the mass spectrometry of reactive organometallic compounds*. 2022. **57**(3): p. e4807.
75. Watakabe, A., et al., *Comparative analyses of adeno-associated viral vector serotypes 1, 2, 5, 8 and 9 in marmoset, mouse and macaque cerebral cortex*. Neurosci Res, 2015. **93**: p. 144-57.
76. Chen, M., et al., *Corticospinal circuit neuroplasticity may involve silent synapses: Implications for functional recovery facilitated by neuromodulation after spinal cord injury*. IBRO Neurosci Rep, 2023. **14**: p. 185-194.
77. Basso, D.M., M.S. Beattie, and J.C.J.J.o.n. Bresnahan, *A sensitive and reliable locomotor rating scale for open field testing in rats*. 1995. **12**(1): p. 1-21.
78. Metz, G.A. and I.Q.J.J.o.n.m. Whishaw, *Cortical and subcortical lesions impair skilled walking in the ladder rung walking test: a new task to evaluate fore-and hindlimb stepping, placing, and co-ordination*. 2002. **115**(2): p. 169-179.

79. Allen, J.W., T.L.J.P.r.M. Yaksh, and protocols, *Assessment of acute thermal nociception in laboratory animals*. 2004: p. 11-23.
80. Gijlswijk, R.P.v., et al., *Fluorochrome-labeled tyramides: use in immunocytochemistry and fluorescence in situ hybridization*. 1997. **45**(3): p. 375-382.
81. Hernández-González, O., et al., *Mechanisms of stimulatory effects of mecamylamine on the dorsal raphe neurons*. 2020. **164**: p. 289-298.
82. Morton, R.A., Y. Yanagawa, and C.F.J.e. Valenzuela, *Electrophysiological assessment of serotonin and GABA neuron function in the dorsal raphe during the third trimester equivalent developmental period in mice*. 2015. **2**(6).
83. Andrade-Talavera, Y., et al., *Ablation of p75NTR signaling strengthens gamma–theta rhythm interaction and counteracts A β -induced degradation of neuronal dynamics in mouse hippocampus in vitro*. 2021. **11**(1): p. 212.
84. Pérez-Rodríguez, M., et al., *Adenosine receptor-mediated developmental loss of spike timing-dependent depression in the hippocampus*. 2019. **29**(8): p. 3266-3281.
85. Levy, S.L., et al., *WGA-Alexa Conjugates for Axonal Tracing*. *Curr Protoc Neurosci*, 2017. **79**: p. 1 28 1-1 28 24.
86. Bjömorklnd, A., H. Baumgarten, and A.J.J.o.n. Rensch, *5, 7-Dihydroxytryptamine: improvement of its selectivity for serotonin neurons in the CNS by pretreatment with desipramine*. 1975. **24**(4): p. 833-835.



DISCUSSION

DISCUSSION

Over the 4-year period (2019-2023) of the development of this doctoral thesis ~18,900 articles have been published containing the keywords 'spinal cord injury' (see figure XX, red square). This fact depicts that the scientific SCI community is working unceasingly and increasingly toward a common goal: overcoming the failure of CNS regeneration after injury. This overwhelming scientific production in basic research is the best guarantee for clinic progress in the times to come. The work gathered in this thesis represents only a small contribution to the global SCI knowledge, however every tiny research effort is meaningful.

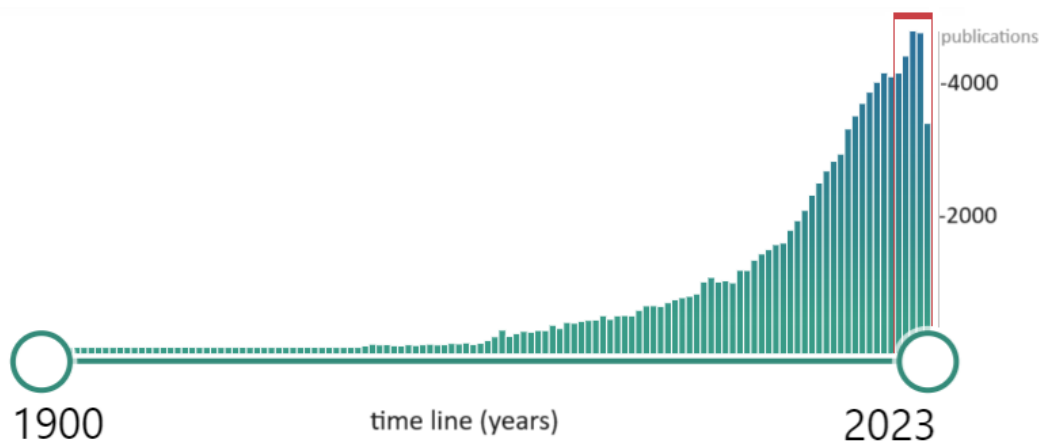


Figure 5: Timeline of publications in PubMed under the search query 'spinal cord injury' (from 1900 up to September 2023). Available at the following [hyperlink](#).

Chapter 1 represents a significant contribution to the not yet fully described pathological mechanisms involved in the concatenated processes that unfold over time after SCI. Here we presented, first, a transcriptional characterization of the expression profile of a wide-temporal period after SCI. It is important to highlight our contribution to the transcriptional assessment specifically at chronic phase, the least represented time points transcriptional studies in the current literature, despite the high prevalence of chronic SCI patients.

Second, we have provided new data regarding the impact of NPCs transplantation over whole spinal cord transcriptional profile, describing its modulatory effect over ~1200 SCI-altered genes. The exploration of this gene set may serve to remark the NPCs' therapeutical strengths as well as to uncover the weak points of this cell therapy, which could be further addressed through specific signaling pathways modulation over the engrafted cells.

Navigating through the vast amount of transcriptional data has not been a trivial task due to its 'omics' nature. Nonetheless we have managed to successfully identify a signaling pathway that opened a new intriguingly research line, having proved so far to be remarkably interesting based on our following results.

Yet, one of the most powerful contributions derived from this study is that the resulting large amount of data has been systematically arranged and deposited in public repositories with free access for any researcher (www.ncbi.nlm.nih.gov/geo/query/acc.cgi?acc=GSE183591, accession code GSE183591). Indeed, the generated data set has already served to provide effortless insights about gene expression levels (throughout SCI progression and in response to NPCs therapy) of other proteins of interest of on-going research lines of our team. Likewise, we hope that other fellow researchers of this field will find this transcriptional tool as valuable for their specific objectives as we do.

Moreover, as a continuation of the present work, the Bioestatistic and Bioinformatic Unit is currently conducting a systematic metanalysis compiling the transcriptional data of our study and 12 other datasets gathered from transcriptional repositories. This bioinformatics endeavor aims to identify gene markers that govern each temporal stage following SCI, along with markers of injury severity, with a particular focus on transcription factors.

The transcriptional studies offer a potent tool for delving into the molecular processes of complex pathologies. Traditional transcriptional studies from total tissue homogenates, as is the case of our approach, hold certain limitations such as the lack of cellular resolution. In the current study, we have addressed this limitation by conducting subsequent immunohistochemical studies to unveil the cellular expression of our protein of interest in the spinal tissue. It is important to note that in the recent years, innovative transcriptional strategies have gained increasing popularity in the virtue of their advanced potential to provide much more detailed information. It's worth to highlight single-cell sequencing and spatial transcriptomics, as they hold tremendous potential particularly in the SCI context [1, 2].

Moreover, the *in-silico* study has been validated *ex silico* by qPCR over a new experimental batch of samples and further complemented with experimental research focusing on cAMP signaling. Through the generation of new findings as well as the compilation of prior ones, our work in Chapter 1 remarks the pivotal role of EPAC2 in CNS function, whose importance had been previously overshadowed by its well-known counterpart, the PKA. Formerly, studies using ubiquitous methods to activate cAMP have

attributed cAMP-derived molecular outcomes directly to PKA, the only known cAMP effector at that time. It was not until the discovery of EPAC2 and the development of tools to specifically manipulate EPAC2/PKA activity that we began to unveil specific roles of both targets. For instance, one recent study using small interference RNA (siRNA) knockdown and specific pharmacological inhibitors of PKA or EPAC2 has shown that while PKA promotes axonal branching, EPAC2 governs axonal elongation [3]. Similarly, in our experimental design, the use of the specific EPAC2 inhibitor (ESI-05) for the first time in a SCI context allowed to describe the specific contribution of EPAC2 over microglial polarization leading to more neuro-permissive after SCI.

Nonetheless, given that both EPAC2 and PKA exert relevant neuroregenerative roles, we believe that for the sake of therapeutic strategies, the targeting of an upstream activator of both EPAC and PKA could yield more benefits by providing synergistic function of both effector proteins (despite hampering the distinction of their individual contributions). Thus, for the following chapter (Chapter 2) we decided to directly manipulate endogenous levels of cAMP in corticospinal neurons with temporal and cellular precision by the implementation of bPAC protein, a very potent tool to enable efficient cAMP elevations.

The stimulation of bPAC in corticospinal projecting neurons has demonstrated a considerable effect over locomotor function recovery, especially noticeable at early stages. In this study, we have provided evidence that suggests that the functional improvement may be attributed to enhanced corticospinal tract neuroplasticity, in addition to the stimulation transduction at the brainstem level for better preservation/regeneration of serotonergic tracts. One of the most noteworthy aspects of this work is the establishment of significant correlations between 5-HT histological immunolabeling and locomotor output, indicating that we have encountered tangible evidence of locomotor behavior.

As the relevance of this findings has been extensively discussed in the Chapter 2, in this section, I ought to focus on the current limitations of our study. In this regard, it is important to emphasize that bPAC does not represent a clinically translatable option for SCI treatment. bPAC strategy involves the use of a viral vector for the delivery of a transgene of bacterial origin into the motor cortex. Currently this may represent an impediment to human treatment due to biosafety-related concerns and limited popular acceptance. Still, viral-based gene therapies have already been successfully applied into the clinics, particularly for monogenic diseases, so it is very likely that this therapeutical landscape will be better embraced in the next years [4]. Moreover, bPAC application

requires the implantation of light device and, on the top of that, the electrophysiological changes derived from bPAC stimulation are associated with a predisposition to epileptic episodes. All these factors make the path toward the clinical feasibility of bPAC still a long way off. Although being discussed here, it is important to mention as well that the original conceptualization of bPAC application in animal SCI models has never been intended for future clinical translation. Instead of that, bPAC has served as a valuable tool to better understand the anatomical basis of neuronal plasticity and recovery, serving as a paradigm of central regeneration in analogy to the so-called conditioning lesion effect.

Derived from the limited time for the research development and its high complexity, some issues have remained opened in the second section of this thesis project and deserve further research continuation. In the light of this, in the next paragraphs I would like to propose a few ideas for the project's future endeavors.

First, our results showing an increased number of retrogradely-labelled neurons in the reticular formation of bPAC animals suggests that the reticulospinal tract probably contributes to bPAC recovery-response. This represents a really attractive research direction that will require the anterograde labelling of the reticulospinal tract for its visualization in the spinal cord. This experimental setting includes two time-consuming technical limitations which have impeded its assessment in the present study: 1) the requirement of the use of a viral vector with the reporter protein under specific promoter (VGlut2) and 2) the complications of the dorsal intervention for stereotaxic injection to target the reticular formation, that may damage other brain areas, possibly dampening the recovery after SCI.

Second, we hypothesize that diary bPAC stimulation could drive a transcriptional-dependent mechanism of pro-regenerative reprogramming of the corticospinal neurons, presumably mediated by P-CREB. Thus, the transcriptional profiling of bPAC stimulated corticospinal projecting neurons could give us relevant notes about the gene expression patterns that underlie regenerative-mechanisms. Their comparison to adult control CST neurons and embryonic neurons may also indicate if bPAC mediates a regression to early-developmental state of the CST, a theory that has been extensively proposed. Moreover, the transcriptional study of bPAC cortical stimulation over other types of neurons (i.e., serotonergic or reticulospinal) could help to define the molecular basis of their interaction. Importantly, these comprehensive transcriptional studies may pave the way to the proposal of new translational therapies by the in-silico search of clinically approved drugs that faithfully resemble the transcriptional profiles induced by bPAC.

On a different note, in this study we have set a stimulation program starting the day after the injury and continued daily until the end point for two main reasons: 1) we hypothesize that the immediacy of the onset of the optogenetic stimulation is crucial to face a still responsive scenario and 2) the stimulation of the animals right before sample collection enables the exploration of transient biological mechanisms (i.e., c-fos or PCREB expression). That being said, we also consider that testing bPAC stimulation at chronic stage of SCI could also constitute an interesting avenue for future experiments. This approach would illustrate whether bPAC is able to promote regeneration over already degenerated axons, or if still responsive tracts are required to mediate functional recovery. Moreover, the refinement of the stimulation protocol, by shortening the application period or modulating the light parameters, is an essential task in order to impede the apparition of seizures.

Additionally, our retrograde study suggested that bPAC increased the number of supraspinal neurons reaching the central pattern generator (CPG) region, and thus, that bPAC might influence CPG activity. From an ambitious perspective, the characterization of the electrophysiological outputs of CPG activity in living animals during bPAC stimulation on the motor cortex would be of great interest and huge functional relevance. There are many other aspects to further investigate in bPAC experiments (i.e., bPAC dark inactive controls, multi- transsynaptic tracing or live imaging of Calcium/cAMP dynamics) but, to make a long story short, I just want to conclude stating that we are eager to further delving into these unexplored issues and excited about new insights that lie ahead.

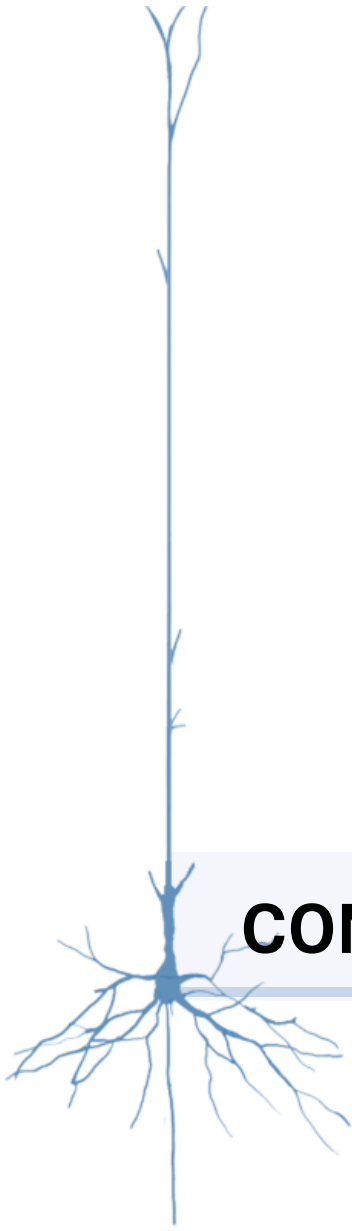
On a personal perspective, my experience throughout the study of this thesis project has shaped my scientific impetus, leading me to the conviction that strategies focused on neuromodulating spared tracts after injury are more feasible than those attempting to regenerate injured tracts. This perspective is in consensus with conclusions of reference authors of this field, whose works have served me as enormous source of inspiration.

In fact, the timeframe of this thesis period has been exceptionally encouraging for a first-stage SCI researcher. This year we have witnessed a unprecedented event: a man with chronic tetraplegia regained the ability to stand and walk autonomously. While this quote may sound as a passage from the Bible, indeed it has become reality thanks to the pioneering advances of Gregoire Courtine, Jocelyn Bloch and their research team. Their breakthrough consisted in the implantation of a brain-spinal digital bridge which decodes cortical signals of the individual's executive intentions into epidural electrical stimulation of the spinal cord, further supported by neurorehabilitation training [5]. The patient has

claimed that the brain-spine interface enabled him to naturally control his leg movements to stand, walk and climb stairs. Moreover, even when the interface was turned off the patient was able to walk assisted by crutches.

Those researchers have previously described that a propriospinal population of neurons essential for walking recovery after SCI [6]. This neuronal population which expresses the marker *Vsx2* has no detectable impact on locomotion in uninjured rodents [7, 8] but that become essential to motor recovery after incomplete SCI as demonstrated by experiments designed for their optogenetic ablation [7]. They show that these neurons are innervated by reticulospinal projecting neurons of the VGI and innervate walking execution centers of the lumbar spinal cord. Importantly, treatments that simply prompted *Vsx2* axonal growth across lesions were ineffective in the recovery of walking, while refined strategies of graded chemoattraction and guidance of regenerating axons to their natural target of the lumbar cord resulted in substantial recovery [9].

Courtine's lab is at the forefront of SCI research; his group underscore the importance of compelling multidisciplinary cooperation of molecular biologists, bioinformaticians, software engineers, electrophysiologists, electronic engineers, neurosurgeons, etc., for efficient workflow. A multidisciplinary approach is pivotal in many fields but it is particularly required in SCI research. However, it is important to note as well that Courtine's work represents the just tip of an iceberg, sustained by myriad of authors whose contributions are undoubtedly valuable, which have all together forged the most optimistic landscape we have lived so far on the path towards spinal cord injury cure.



CONCLUSIONS

CONCLUSIONS

In this final section we bring together the key findings from our research along the two chapters that comprise this work. Although each chapter has delved into independent research scopes, they were inherently interconnected. Thus, the conjunction of the conclusions from the two chapters overall provides a holistic view understanding on how SCI impact over cAMP signaling and how cAMP manipulations by either NPCs transplantation or bPAC provide therapeutical outcomes after SCI.

The conclusions have been concisely summarized as follows:

Chapter 1

1. **Severe spinal cord contusion in rats led to a pronounced transcriptional dysregulation.** Up to 15,655 genes were altered at the first week post-injury compared to uninjured animals. This dysregulation persisted over time, as shown by the similar number of DEGs for all evaluated time points (2, 4 and 8 weeks) what evidenced the lack of an effective transcriptional resolution throughout the injury progression.
2. **Functional analysis of this dysregulated transcriptome revealed the downregulation of cAMP signalling components.** EPAC2, PKA, BDNF, and CAMKK2 were found under-expressed immediately after SCI and their downregulation persisted over time. Of those, EPAC2 suffered a more dramatic downregulation at all evaluated time points.
3. **The ectopic transplantation of NPCs was able to exert a substantial transcriptional modulation in total spinal cord extracts.** Acute and subacute NPC transplantation transcriptionally modulated 4227 and 3364 genes; of those 1032 and 1281 genes, respectively, were genes directly-affected by SCI. Interestingly, the differentially-expressed genes (DEGs) modulated by NPCs included relevant functional blocks for CNS regeneration, such as neural function, ionic homeostasis or immune response, among others.
4. **The transcriptional modulatory effect elicited by NPC transplantation entailed the up-regulation of cAMP-related genes (including EPAC2).** Moreover, NPC transplantation in injured rats increased cAMP levels rostral to the injury site, as measured by ELISA immunoassay.
5. **EPAC2 underlies the NPC-mediated mechanism in SCI treatment, mitigating the microglial inflammation and providing a more neuro-permissive environment.** Sustained in vivo inhibition of EPAC2 for one week via the intrathecal administration of ESI-05 along with NPCs transplantation (NPCs+ESI-05) compared

to NPCs alone in injured animals resulted in increased GFAP positive area, microglial polarization towards an inflammatory phenotype and widened the gap distance between preserved neurons cells across the lesion.

Chapter 2:

1. **bPAC is a valuable tool for on-demand optogenetic inductions of cAMP signalling in CST neurons.** In vitro validation into cortical neuron cultures demonstrated that bPAC efficiently induced a ~14-fold increase of cAMP levels upon saturating blue light exposure. Moreover, in vivo bPAC stimulation into CAMKII CST neurons induced CREB phosphorylation and c-Fos in primary motor cortex compared to control animals.
2. **Of note, daily bPAC stimulation in CST neurons promoted a substantial locomotor recovery in rats with dorsal hemisection injuries.** Animals receiving bPAC stimulation displayed higher scores in BBB, ladder and narrow beam tests, with differences being more pronounced at the early stage but sustained along the study. Moreover, at the end-point (35 days) bPAC animals showed more similarities to uninjured-like hindlimb kinematics than control. In summary, the locomotor evaluation revealed that bPAC stimulation induced improved functional recovery after SCI.
3. **bPAC stimulation increased the number of retrogradely labelled neurons the lumbar spinal cord in the primary motor cortex and in the raphe-reticular formation but not in the red nuclei.** This suggests that cAMP inductions may promote the preservation/regeneration of CST and RtST/RpST. Furthermore, the number of retrogradely labelled neurons in the raphe-reticular region significantly correlated with the BBB scores, what unveils its functional relevance in bPAC-mediated functional recovery.
4. **The immunostaining of the serotonergic tract (the major component of raphespinal tract) in the spinal cord revealed that bPAC stimulation increased the amount of serotonergic axons caudal to the injury (relativized to rostral) when compared to control, correlating with better performance** in several locomotor tests. Moreover, 5-HT coimmunostaining with ChAT (choline acetyltransferase) showed that serotonergic tracts innervate ventral spinal motor neurons.
5. **Brainstem motor centres may play a pivotal role in rerouting cortical commands caudal to the injury through other descending tracts.** bPAC stimulation modulated the density pattern of CST collateral projections into brainstem motor centres and resulted in a moderate but significant PCREB induction at the raphe magnus nuclei correlating with higher CREB phosphorylation in the motor

cortex. Additionally, transsynaptic tracing by WGA confirmed that the primary motor cortex is synaptically integrated with the caudal raphe nuclei of the brainstem. Although, serotonergic neurons were not WGA+, they were distributed in close proximity to them, revealing the existence of a tripartite partner.

6. **Ultimately, the depletion of serotonergic system by DHT treatment abolished bPAC-mediated recovery** rendering bPAC group ladder beam scores to control levels what conveys the role of this tract in bPAC mechanism. However, our results have also shown insights in the RtST implication what deserved further exploration in future research.

References

1. Alizadeh, A., S.M. Dyck, and S. Karimi-Abdolrezaee, *Traumatic Spinal Cord Injury: An Overview of Pathophysiology, Models and Acute Injury Mechanisms*. Front Neurol, 2019. **10**: p. 282.
2. Gascon, S., F. Ortega, and M. Gotz, *Transient CREB-mediated transcription is key in direct neuronal reprogramming*. Neurogenesis (Austin), 2017. **4**(1): p. e1285383.
3. Roberts, T.T., G.R. Leonard, and D.J. Cepela, *Classifications In Brief: American Spinal Injury Association (ASIA) Impairment Scale*. Clin Orthop Relat Res, 2017. **475**(5): p. 1499-1504.
4. Chen, Y., et al., *Causes of spinal cord injury*. Top Spinal Cord Inj Rehabil, 2013. **19**(1): p. 1-8.
5. Stahel, P.F., *Essentials of Spinal Cord Injury: Basic Research to Clinical Practice*. 2013, LWW.
6. Popa, C., et al., *Vascular dysfunctions following spinal cord injury*. J Med Life, 2010. **3**(3): p. 275-85.
7. Ohry, A. and G.J.S.C. Zeilig, *Traumatic spinal cord injury followed by cerebrospinal fluid complications*. 1990. **28**(3): p. 208-211.
8. Oyinbo, C., <Secondary_injury_mechanisms_in_traumatic_spinal_co.pdf>. Acta Neurobiologiae Experimentalis, 2012. **71**.
9. Li, S. and P.K. Stys, *Mechanisms of ionotropic glutamate receptor-mediated excitotoxicity in isolated spinal cord white matter*. J Neurosci, 2000. **20**(3): p. 1190-8.
10. Quadri, S.A., et al., *Recent update on basic mechanisms of spinal cord injury*. Neurosurg Rev, 2020. **43**(2): p. 425-441.
11. Silver, J., M.A. Edwards, and P.J.J.o.C.N. Levitt, *Immunocytochemical demonstration of early appearing astroglial structures that form boundaries and pathways along axon tracts in the fetal brain*. 1993. **328**(3): p. 415-436.
12. Anderson, M.A., et al., *Astrocyte scar formation aids central nervous system axon regeneration*. 2016. **532**(7598): p. 195-200.
13. Sofroniew, M.V. and H.V.J.A.n. Vinters, *Astrocytes: biology and pathology*. 2010. **119**: p. 7-35.
14. Sofroniew, M.V.J.N.R.N., *Astrocyte barriers to neurotoxic inflammation*. 2015. **16**(5): p. 249-263.
15. David, S., A.D. Greenhalgh, and A. Kroner, *Macrophage and microglial plasticity in the injured spinal cord*. Neuroscience, 2015. **307**: p. 311-8.
16. David, S. and A. Kroner, *Repertoire of microglial and macrophage responses after spinal cord injury*. Nat Rev Neurosci, 2011. **12**(7): p. 388-99.
17. Kai Zhang, M.J.a.Y.F., *The drama of Wallerian degeneration: the cast, crew, and script*. Annual Review of Genetics, 2021.
18. Schwab, J.M., et al., *The paradox of chronic neuroinflammation, systemic immune suppression, autoimmunity after traumatic chronic spinal cord injury*. Exp Neurol, 2014. **258**: p. 121-129.
19. Batchelor, P.E., et al., *Meta-analysis of pre-clinical studies of early decompression in acute spinal cord injury: a battle of time and pressure*. PLoS One, 2013. **8**(8): p. e72659.
20. Dimar, J.R., 2nd, et al., *The influence of spinal canal narrowing and timing of decompression on neurologic recovery after spinal cord contusion in a rat model*. Spine (Phila Pa 1976), 1999. **24**(16): p. 1623-33.
21. Ahuja, C.S., J.H. Badhiwala, and M.G. Fehlings, *"Time is spine": the importance of early intervention for traumatic spinal cord injury*. Spinal Cord, 2020. **58**(9): p. 1037-1039.
22. Flack, J.A., K.D. Sharma, and J.Y.J.N.r.r. Xie, *Delving into the recent advancements of spinal cord injury treatment: a review of recent progress*. 2022. **17**(2): p. 283.

23. Loh, E., et al., *The CanPain SCI clinical practice guidelines for rehabilitation management of neuropathic pain after spinal cord injury: 2021 update*. 2022. **60**(6): p. 548-566.
24. Fehlings, M.G., et al., *A clinical practice guideline for the management of patients with acute spinal cord injury: recommendations on the type and timing of rehabilitation*. 2017. **7**(3_suppl): p. 231S-238S.
25. Lorach, H., et al., *Walking naturally after spinal cord injury using a brain-spine interface*. Nature, 2023. **618**(7963): p. 126-133.
26. Sharif-Alhoseini, M., et al., *Animal models of spinal cord injury: a systematic review*. 2017. **55**(8): p. 714-721.
27. Berni, J., *The motor system*.
28. Stifani, N., *Motor neurons and the generation of spinal motor neuron diversity*. Front Cell Neurosci, 2014. **8**: p. 293.
29. Cote, M.P., L.M. Murray, and M. Knikou, *Spinal Control of Locomotion: Individual Neurons, Their Circuits and Functions*. Front Physiol, 2018. **9**: p. 784.
30. Harrow-Mortelliti, M., V. Reddy, and G. Jimsheleishvili, *Physiology, spinal cord*, in *StatPearls [Internet]*. 2023, StatPearls Publishing.
31. Kardong, K.V., *Vertebrates: comparative anatomy, function, evolution*. 1997: Heinle and Heinle Publishers.
32. M. V. PankivYe, V.P.Z., MasnaZoriana Z. Masna, *Structural components of the normal thoracic and lumbar vertebrae in rats*. Journal of Education Health and Sport, 2021.
33. Bican, O., A. Minagar, and A.A.J.N.c. Pruitt, *The spinal cord: a review of functional neuroanatomy*. 2013. **31**(1): p. 1-18.
34. Craven, J.J.A. and I.C. Medicine, *Major ascending and descending tracts in the spinal cord*. 2011. **12**(1): p. 26-27.
35. Nudo, R. and R.J.J.o.C.N. Masterton, *Descending pathways to the spinal cord: a comparative study of 22 mammals*. 1988. **277**(1): p. 53-79.
36. Nathan, P., M. Smith, and P.J.B. Deacon, *Vestibulospinal, reticulospinal and descending propriospinal nerve fibres in man*. 1996. **119**(6): p. 1809-1833.
37. Vartak, A., D. Goyal, and H.J.N. Kumar, *Role of Axon Guidance Molecules in Ascending and Descending paths in Spinal Cord Regeneration*. 2023.
38. Wang, L.H., W.Q. Ding, and Y.G. Sun, *Spinal ascending pathways for somatosensory information processing*. Trends Neurosci, 2022. **45**(8): p. 594-607.
39. Sengul, G. and C. Watson, *Ascending and descending pathways in the spinal cord*, in *The rat nervous system*. 2015, Elsevier. p. 115-130.
40. Welniarz, Q., I. Dusart, and E.J.D.n. Roze, *The corticospinal tract: Evolution, development, and human disorders*. 2017. **77**(7): p. 810-829.
41. Jang, S.H.J.J.o.r.m., *The corticospinal tract from the viewpoint of brain rehabilitation*. 2014. **46**(3): p. 193-199.
42. Joosten, E.A., et al., *Postnatal development of the ipsilateral corticospinal component in rat spinal cord: a light and electron microscopic anterograde HRP study*. 1992. **326**(1): p. 133-146.
43. Nathan, P., M.C. SMITH, and P.J.B. Deacon, *The corticospinal tracts in man: course and location of fibres at different segmental levels*. 1990. **113**(2): p. 303-324.
44. Liang, H., et al., *Distribution of raphespinal fibers in the mouse spinal cord*. 2015. **11**: p. s12990-015-0046-x.
45. Courtine, G., et al., *Can experiments in nonhuman primates expedite the translation of treatments for spinal cord injury in humans?* 2007. **13**(5): p. 561-566.
46. Darian-Smith, C.J.T.N., *Synaptic plasticity, neurogenesis, and functional recovery after spinal cord injury*. 2009. **15**(2): p. 149-165.
47. Del Cerro, P., Á. Rodríguez-De-Lope, and J.E.J.F.i.n. Collazos-Castro, *The Cortical Motor System in the Domestic Pig: Origin and Termination of the Corticospinal Tract and Cortico-Brainstem Projections*. 2021. **15**: p. 748050.

48. Ittyachen, A.M.J.C.M.I., *Paradox of the cranial nerves: Does the description of the facial nerve need a reinterpretation?* 2021. **19**(4): p. 282-283.
49. Antal, M.J.J.f.H., *Termination areas of corticobulbar and corticospinal fibres in the rat.* 1984. **25**(6): p. 647-659.
50. Liang, H., et al., *Terminations of reticulospinal fibers originating from the gigantocellular reticular formation in the mouse spinal cord.* 2016. **221**: p. 1623-1633.
51. Brownstone, R.M. and J.W.J.F.i.n.c. Chopek, *Reticulospinal systems for tuning motor commands.* 2018. **12**: p. 30.
52. Perreault, M.-C. and A.J.C.o.i.p. Giorgi, *Diversity of reticulospinal systems in mammals.* 2019. **8**: p. 161-169.
53. Peterson, B., et al., *Patterns of projection and branching of reticulospinal neurons.* 1975. **23**(4): p. 333-351.
54. Kachidian, P., et al., *Immunohistochemical evidence for the coexistence of substance P, thyrotropin-releasing hormone, GABA, methionin-enkephalin, and leucin-enkephalin in the serotonergic neurons of the caudal raphe nuclei: A dual labeling in the rat.* 1991. **30**(3): p. 521-530.
55. Stamp, J.A. and K.J.B.r. Semba, *Extent of colocalization of serotonin and GABA in the neurons of the rat raphe nuclei.* 1995. **677**(1): p. 39-49.
56. Lee, J. and M.R. Muzio, *Neuroanatomy, extrapyramidal system.* 2020.
57. Filipp, M.E., et al., *Differences in neuroplasticity after spinal cord injury in varying animal models and humans.* 2019. **14**(1): p. 7.
58. Leibinger, M., et al., *Transneuronal delivery of hyper-interleukin-6 enables functional recovery after severe spinal cord injury in mice.* *Nat Commun*, 2021. **12**(1): p. 391.
59. Ishida, A., et al., *Dynamic interaction between cortico-brainstem pathways during training-induced recovery in stroke model rats.* 2019. **39**(37): p. 7306-7320.
60. Asboth, L., et al., *Cortico-reticulo-spinal circuit reorganization enables functional recovery after severe spinal cord contusion.* 2018. **21**(4): p. 576-588.
61. Jang, S.H., et al., *Functional role of the corticoreticular pathway in chronic stroke patients.* 2013. **44**(4): p. 1099-1104.
62. Jang, S.H., et al., *Postural instability in patients with injury of corticoreticular pathway following mild traumatic brain injury.* 2016. **95**(8): p. 580-587.
63. Ramón y Cajal, S., *Degeneration and regeneration of the nervous system.* 1928.
64. Anderson, M.A., et al., *Natural and targeted circuit reorganization after spinal cord injury.* *Nat Neurosci*, 2022. **25**(12): p. 1584-1596.
65. Cortes, M., et al., *The corticomotor projection to liminally-contractable forearm muscles in chronic spinal cord injury: a transcranial magnetic stimulation study.* *Spinal Cord*, 2017. **55**(4): p. 362-366.
66. Kleim, J.A., S. Barbay, and R.J.J.J.o.n. Nudo, *Functional reorganization of the rat motor cortex following motor skill learning.* 1998. **80**(6): p. 3321-3325.
67. Brown, A.R. and M. Martinez, *From cortex to cord: motor circuit plasticity after spinal cord injury.* *Neural Regen Res*, 2019. **14**(12): p. 2054-2062.
68. Raineteau, O. and M.E.J.N.R.N. Schwab, *Plasticity of motor systems after incomplete spinal cord injury.* 2001. **2**(4): p. 263-273.
69. Brown, A.R. and M. Martinez, *Ipsilesional Motor Cortex Plasticity Participates in Spontaneous Hindlimb Recovery after Lateral Hemisection of the Thoracic Spinal Cord in the Rat.* *J Neurosci*, 2018. **38**(46): p. 9977-9988.
70. Rioult-Pedotti, M.-S., et al., *Strengthening of horizontal cortical connections following skill learning.* 1998. **1**(3): p. 230-234.
71. Monfils, M.-H. and G.J.N. Teskey, *Skilled-learning-induced potentiation in rat sensorimotor cortex: a transient form of behavioural long-term potentiation.* 2004. **125**(2): p. 329-336.

72. Xu, T., et al., *Rapid formation and selective stabilization of synapses for enduring motor memories*. 2009. **462**(7275): p. 915-919.
73. Asboth, L., et al., *Cortico-reticulo-spinal circuit reorganization enables functional recovery after severe spinal cord contusion*. *Nat Neurosci*, 2018. **21**(4): p. 576-588.
74. Siegel, C.S., et al., *Plasticity of intact rubral projections mediates spontaneous recovery of function after corticospinal tract injury*. *J Neurosci*, 2015. **35**(4): p. 1443-57.
75. Stampanoni Bassi, M., et al., *Synaptic Plasticity Shapes Brain Connectivity: Implications for Network Topology*. *Int J Mol Sci*, 2019. **20**(24).
76. Chen, M., et al., *Corticospinal circuit neuroplasticity may involve silent synapses: Implications for functional recovery facilitated by neuromodulation after spinal cord injury*. *IBRO Neurosci Rep*, 2023. **14**: p. 185-194.
77. Darian-Smith, C., et al., *Corticospinal sprouting differs according to spinal injury location and cortical origin in macaque monkeys*. 2014. **34**(37): p. 12267-12279.
78. Schnell, L. and M.J.E.J.o.N. Schwab, *Sprouting and regeneration of lesioned corticospinal tract fibres in the adult rat spinal cord*. 1993. **5**(9): p. 1156-1171.
79. Oudega, M. and M.A.J.T.J.o.p. Perez, *Corticospinal reorganization after spinal cord injury*. 2012. **590**(16): p. 3647-3663.
80. Bareyre, F.M., et al., *The injured spinal cord spontaneously forms a new intraspinal circuit in adult rats*. 2004. **7**(3): p. 269-277.
81. Filli, L. and M.E.J.N.r.r. Schwab, *Structural and functional reorganization of propriospinal connections promotes functional recovery after spinal cord injury*. 2015. **10**(4): p. 509.
82. Beauparlant, J., et al., *Undirected compensatory plasticity contributes to neuronal dysfunction after severe spinal cord injury*. *Brain*, 2013. **136**(Pt 11): p. 3347-61.
83. Müllner, A., et al., *Lamina-specific restoration of serotonergic projections after Nogo-A antibody treatment of spinal cord injury in rats*. 2008. **27**(2): p. 326-333.
84. Fitzcharles, M.A., et al., *Nociplastic pain: towards an understanding of prevalent pain conditions*. *Lancet*, 2021. **397**(10289): p. 2098-2110.
85. Fouad, K., A. Krajacic, and W.J.B.r.b. Tetzlaff, *Spinal cord injury and plasticity: opportunities and challenges*. 2011. **84**(4-5): p. 337-342.
86. Fawcett, J.W.J.N.r., *The struggle to make CNS axons regenerate: why has it been so difficult?* 2020. **45**(1): p. 144-158.
87. Bradbury, E.J. and E.R.J.N.c. Burnside, *Moving beyond the glial scar for spinal cord repair*. 2019. **10**(1): p. 3879.
88. Pinelli, F., et al., *Biomaterial-mediated factor delivery for spinal cord injury treatment*. 2022. **10**(7): p. 1673.
89. Tsintou, M., K. Dalamagkas, and A.M.J.N.r.r. Seifalian, *Advances in regenerative therapies for spinal cord injury: a biomaterials approach*. 2015. **10**(5): p. 726.
90. Bradbury, E.J. and L.M.J.B.r.b. Carter, *Manipulating the glial scar: chondroitinase ABC as a therapy for spinal cord injury*. 2011. **84**(4-5): p. 306-316.
91. Jin, Y., et al., *Transplantation of neural progenitor cells in chronic spinal cord injury*. *Neuroscience*, 2016. **320**: p. 69-82.
92. Garraway, S.M. and J.R. Huie, *Spinal Plasticity and Behavior: BDNF-Induced Neuromodulation in Uninjured and Injured Spinal Cord*. *Neural Plast*, 2016. **2016**: p. 9857201.
93. Álvarez, Z., et al., *Bioactive scaffolds with enhanced supramolecular motion promote recovery from spinal cord injury*. 2021. **374**(6569): p. 848-856.
94. Liu, K., et al., *PTEN deletion enhances the regenerative ability of adult corticospinal neurons*. *Nat Neurosci*, 2010. **13**(9): p. 1075-81.
95. Assinck, P., et al., *Cell transplantation therapy for spinal cord injury*. *Nat Neurosci*, 2017. **20**(5): p. 637-647.
96. Shao, M., et al., *Exosomes from long noncoding RNA-Gm37494-ADSCs repair spinal cord injury via shifting microglial M1/M2 polarization*. 2020. **43**: p. 1536-1547.

97. Bonner, J.F., et al., *Preparation of neural stem cells and progenitors: neuronal production and grafting applications*. 2013: p. 65-88.
98. Fischer, I., J.N. Dulin, and M.A.J.N.R.N. Lane, *Transplanting neural progenitor cells to restore connectivity after spinal cord injury*. 2020. **21**(7): p. 366-383.
99. Lane, M.A., A.C. Lepore, and I. Fischer, *Improving the therapeutic efficacy of neural progenitor cell transplantation following spinal cord injury*. *Expert Rev Neurother*, 2017. **17**(5): p. 433-440.
100. Willerth, S.M. and S.E.J.A.d.d.r. Sakiyama-Elbert, *Cell therapy for spinal cord regeneration*. 2008. **60**(2): p. 263-276.
101. Brock, J.H., et al., *Rodent neural progenitor cells support functional recovery after cervical spinal cord contusion*. 2018. **35**(9): p. 1069-1078.
102. Rosenzweig, E.S., et al., *Restorative effects of human neural stem cell grafts on the primate spinal cord*. 2018. **24**(4): p. 484-490.
103. Garbossa, D., et al., *Recent therapeutic strategies for spinal cord injury treatment: possible role of stem cells*. 2012. **35**: p. 293-311.
104. Zipser, C.M., et al., *Cell-based and stem-cell-based treatments for spinal cord injury: evidence from clinical trials*. 2022. **21**(7): p. 659-670.
105. Qiu, J., D. Cai, and M.T.J.P.i.b.r. Filbin, *A role for cAMP in regeneration during development and after injury*. 2002. **137**: p. 381-387.
106. Spencer, T. and M.T.J.J.o.a. Filbin, *A role for cAMP in regeneration of the adult mammalian CNS*. 2004. **204**(1): p. 49-55.
107. Zhou, G., et al., *Multifaceted roles of cAMP signaling in the repair process of spinal cord injury and related combination treatments*. 2022. **15**: p. 808510.
108. Cai, D., et al., *Neuronal cyclic AMP controls the developmental loss in ability of axons to regenerate*. *J Neurosci*, 2001. **21**(13): p. 4731-9.
109. Cai, D., et al., *Prior exposure to neurotrophins blocks inhibition of axonal regeneration by MAG and myelin via a cAMP-dependent mechanism*. 1999. **22**(1): p. 89-101.
110. Qiu, J., et al., *Spinal axon regeneration induced by elevation of cyclic AMP*. *Neuron*, 2002. **34**(6): p. 895-903.
111. Neumann, S., et al., *Regeneration of sensory axons within the injured spinal cord induced by intraganglionic cAMP elevation*. *Neuron*, 2002. **34**(6): p. 885-93.
112. Bos, J.L.J.T.i.b.s., *Epac proteins: multi-purpose cAMP targets*. 2006. **31**(12): p. 680-686.
113. Cheng, X., et al., *Epac and PKA: a tale of two intracellular cAMP receptors*. 2008. **40**(7): p. 651-662.
114. Kim, S.-S., et al., *cAMP induces neuronal differentiation of mesenchymal stem cells via activation of extracellular signal-regulated kinase/MAPK*. 2005. **16**(12): p. 1357-1361.
115. Hannila, S.S. and M.T. Filbin, *The role of cyclic AMP signaling in promoting axonal regeneration after spinal cord injury*. *Exp Neurol*, 2008. **209**(2): p. 321-32.
116. Li, M., et al., *Cyclic AMP promotes neuronal survival by phosphorylation of glycogen synthase kinase 3 β* . 2000. **20**(24): p. 9356-9363.
117. Malone, M., et al., *Neuronal activity promotes myelination via a cAMP pathway*. 2013. **61**(6): p. 843-854.
118. Kajana, S. and H.J.B.r. Goshgarian, *Spinal activation of the cAMP-PKA pathway induces respiratory motor recovery following high cervical spinal cord injury*. 2008. **1232**: p. 206-213.
119. Schaal, S.M., et al., *The therapeutic profile of rolipram, PDE target and mechanism of action as a neuroprotectant following spinal cord injury*. 2012.
120. Xia, T., et al., *The combination of db-cAMP and ChABC with poly(propylene carbonate) microfibers promote axonal regenerative sprouting and functional recovery after spinal cord hemisection injury*. *Biomed Pharmacother*, 2017. **86**: p. 354-362.
121. Macks, C., et al., *Rolipram-Loaded Polymeric Micelle Nanoparticle Reduces Secondary Injury after Rat Compression Spinal Cord Injury*. *J Neurotrauma*, 2018. **35**(3): p. 582-592.

122. Moradi, K., et al., *Inhibition of phosphodiesterase IV enzyme improves locomotor and sensory complications of spinal cord injury via altering microglial activity: Introduction of Roflumilast as an alternative therapy*. *Int Immunopharmacol*, 2020. **86**: p. 106743.
123. Sousa, C.S., et al., *Pre-Clinical Assessment of Roflumilast Therapy in a Thoracic Model of Spinal Cord Injury*. 2023. **15**(5): p. 1556.
124. Mussen, F., et al., *Unleashing Spinal Cord Repair: The Role of cAMP-Specific PDE Inhibition in Attenuating Neuroinflammation and Boosting Regeneration after Traumatic Spinal Cord Injury*. 2023. **24**(9): p. 8135.
125. Costa, L.M., et al., *Rolipram promotes functional recovery after contusive thoracic spinal cord injury in rats*. 2013. **243**: p. 66-73.
126. Schaal, S.M., et al., *The therapeutic profile of rolipram, PDE target and mechanism of action as a neuroprotectant following spinal cord injury*. *PLoS One*, 2012. **7**(9): p. e43634.
127. Yin, Y., et al., *Effects of combining methylprednisolone with rolipram on functional recovery in adult rats following spinal cord injury*. *Neurochem Int*, 2013. **62**(7): p. 903-12.
128. Richard J. Heaslip, D.Y.E., *<Emetic, central nervous system and pulmonary activities of rolipram in the dog.pdf>*. *European Journal of Pharmacology*, 1995. **286**: p. 281-290.
129. Deisseroth, K. and P.J.S. Hegemann, *The form and function of channelrhodopsin*. 2017. **357**(6356): p. eaan5544.
130. Farrell, M.S., et al., *A Gas DREADD mouse for selective modulation of cAMP production in striatopallidal neurons*. 2013. **38**(5): p. 854-862.
131. Patel, N. and M.G.J.F.i.P. Gold, *The genetically encoded tool set for investigating cAMP: more than the sum of its parts*. 2015. **6**: p. 164.
132. Iseki, M., et al., *A blue-light-activated adenylyl cyclase mediates photoavoidance in Euglena gracilis*. 2002. **415**(6875): p. 1047-1051.
133. Ryu, M.-H., et al., *Natural and engineered photoactivated nucleotidyl cyclases for optogenetic applications*. 2010. **285**(53): p. 41501-41508.
134. Lindner, R., et al., *Photoactivation Mechanism of a Bacterial Light-Regulated Adenylyl Cyclase*. *J Mol Biol*, 2017. **429**(9): p. 1336-1351.
135. Yang, S., et al., *PACmn for improved optogenetic control of intracellular cAMP*. *BMC Biol*, 2021. **19**(1): p. 227.
136. Oldani, S., et al., *SynaptoPAC, an optogenetic tool for induction of presynaptic plasticity*. 2021. **156**(3): p. 324-336.
137. Zhou, Z., et al., *Astrocytic cAMP modulates memory via synaptic plasticity*. *Proc Natl Acad Sci U S A*, 2021. **118**(3).
138. Xiao, Y., W. Tian, and H.J.C.B. López-Schier, *Optogenetic stimulation of neuronal repair*. 2015. **25**(22): p. R1068-R1069.
139. Wang, Y. and N.E. Navin, *Advances and applications of single-cell sequencing technologies*. *Mol Cell*, 2015. **58**(4): p. 598-609.
140. Lein, E., L.E. Borm, and S.J.S. Linnarsson, *The promise of spatial transcriptomics for neuroscience in the era of molecular cell typing*. 2017. **358**(6359): p. 64-69.
141. Zhou, Z., et al., *Photoactivated adenylyl cyclase (PAC) reveals novel mechanisms underlying cAMP-dependent axonal morphogenesis*. *Sci Rep*, 2016. **5**: p. 19679.
142. Bulcha, J.T., et al., *Viral vector platforms within the gene therapy landscape*. 2021. **6**(1): p. 53.
143. Kathe, C., et al., *The neurons that restore walking after paralysis*. 2022. **611**(7936): p. 540-547.
144. Courtine, G., et al., *Recovery of supraspinal control of stepping via indirect propriospinal relay connections after spinal cord injury*. 2008. **14**(1): p. 69-74.
145. Van den Brand, R., et al., *Restoring voluntary control of locomotion after paralyzing spinal cord injury*. 2012. **336**(6085): p. 1182-1185.

146. Squair, J.W., et al., *Recovery of walking after paralysis by regenerating characterized neurons to their natural target region*. 2023. **381**(6664): p. 1338-1345.